

HYDROGEN, CARBON MONOXIDE, AND METHANE  
IN THE MARINE ENVIRONMENT

A Thesis

by

JOHN LOGAN BULLISTER

Submitted to the Graduate College of  
Texas A&M University  
in partial fulfillment of the requirement for the degree of  
MASTER OF SCIENCE

August 1980

Major Subject: Oceanography

HYDROGEN, CARBON MONOXIDE, AND METHANE  
IN THE MARINE ENVIRONMENT

A Thesis

by

JOHN LOGAN BULLISTER

Submitted to the Graduate College of  
Texas A&M University  
in partial fulfillment of the requirement for the degree of  
MASTER OF SCIENCE

---

August 1980

Major Subject: Oceanography

HYDROGEN, CARBON MONOXIDE, AND METHANE  
IN THE MARINE ENVIRONMENT

A Thesis

by

JOHN LOGAN BULLISTER

Approved as to style and content by:

W.R. Schindler  
(Chairman of Committee)

Yvonne A. Fyfe  
(Member)

Gerard A. O'Donovan  
(Member)

S.K. Sandwell  
(Head of Department)

August 1980

## ABSTRACT

Hydrogen, Carbon Monoxide, and Methane  
in the Marine Environment. (August 1980)

John Logan Bullister, B.S., University of Pittsburgh  
Chairman of Advisory Committee: Dr. David R. Schink

The horizontal and vertical distribution of three dissolved trace gases, namely molecular hydrogen ( $H_2$ ), carbon monoxide (CO), and methane ( $CH_4$ ), was measured in coastal and oceanic areas. Atmospheric concentrations of these gases were measured both at locations influenced by nearby human activity, and in areas far removed from these inputs.

Analytical equipment was constructed to perform measurements on discrete water samples, and for the automated analysis of dissolved gases in a pumped seawater stream. Closely spaced sampling of a seawater stream pumped from a depth of a few meters allowed small-scale variations of these gases to be detected while underway on a research vessel.

Continual surface sampling on Cruise 79-G-6 in the Central Pacific revealed diurnal fluctuations in dissolved CO concentration, with highest levels seen in the afternoon. In contrast, dissolved  $H_2$  at the surface was more uniform both temporally and spatially in the open ocean along the cruise track.  $H_2$  concentration was higher and more variable in near-shore areas, where biological activity (indicated by chlorophyll-a concentration) was also greater.

Vertical profiles were obtained using discrete water samples at hydro-stations along the cruise track. Highest levels of the three gases were seen in the upper 200 m. When compared to atmospheric concentrations, dissolved CO was seen to be highly supersaturated

during daylight hours, while  $H_2$  and  $CH_4$  were only slightly supersaturated in this upper layer. For all three gases, concentrations decreased to below equilibrium levels at greater depths.

A detailed study of these dissolved gases in the near-shore environment was made over a period of six weeks at the CEPEX site, in Saanich Inlet, B.C., Canada. The upper 20 m of the water column at this location, although high in dissolved oxygen, contained these reduced gases at concentrations that were significantly supersaturated with respect to atmospheric equilibrium values.  $H_2$  and CO were generally highest in the upper 4 m, while  $CH_4$  generally showed one or more mid-water maxima. No excess of  $H_2$  or CO was found in the methane-rich deeper water of Saanich Inlet.

Diurnal cycles of CO concentrations in the CEPEX enclosures and in the water outside the enclosures were observed. A similar, but less pronounced,  $H_2$  cycle was seen only in the CEPEX enclosures.

Sea water samples collected at the site and incubated in dark containers, at *in situ* temperature, showed rapid decreases of CO and  $H_2$  levels to below air equilibrium. CO reached subequilibrium levels within periods of 12 hrs. Shallow and deep water samples, exposed briefly to sunlight during daytime sample handling, subsequently showed higher levels of dissolved CO than those samples shielded from outside light.

Laboratory experiments with bacteria and phytoplankton cultures demonstrated that biological processes can significantly alter trace gas content in seawater media.

Under conditions present at the CEPEX site (low turbulence and high biological productivity) concentrations of  $H_2$ , CO, and  $CH_4$  were controlled by *in situ* production and consumption. In the less productive open ocean environment, where horizontal and vertical mixing and atmospheric exchange rates are greater, physical processes play a larger role in determining overall trace gas concentration in the upper layer of the ocean.

## ACKNOWLEDGEMENTS

I would like to thank Dr. David R. Schink, chairman of my advisory committee, and the other committee members, Dr. Greta Fryxell and Dr. Gerard O'Donovan.

I also am grateful to Denis Wiesenburg, Norman Guinasso, Robert Key, Patrick Setser, and John Stockwell for their help in developing and deploying the analytical equipment. Their experience and many valuable suggestions greatly aided in the completion of this work.

Special thanks to Catherine Livingston for much patience and understanding throughout.

This work was supported in part by NSF Grant OCE77-27222 and ONR Contract N00014-C-75-0537 to Texas A&M University through the Texas A&M Research Foundation.

## TABLE OF CONTENTS

CHAPTER		PAGE
I	INTRODUCTION AND REVIEW.....	1
	Objectives.....	1
	Studies of Trace Gases in the Atmosphere.....	2
	Studies of Dissolved Trace Gases.....	3
	Carbon Monoxide.....	3
	Hydrogen.....	4
	Methane.....	5
II	ANALYTICAL TECHNIQUES.....	8
	Introduction.....	8
	Description of H <sub>2</sub> and CO Instrument.....	8
	Electronics.....	8
	Absorbance Cell.....	10
	Mercuric Oxide.....	12
	Carrier Gas.....	15
	Description of the Methane Instrument.....	17
	Atmospheric Sampling.....	17
	Water Sampling.....	19
	Gas Extraction.....	19
	Equilibration.....	21
	Sample Processing.....	22
	Continual Water Analysis.....	23
	Standards.....	29
	Microbiological Techniques.....	37
III	FIELD WORK AT CEPEX.....	39
	Measurements.....	39
	The CEPEX Site.....	39
	Sampling Methods.....	40
	Atmospheric Measurements.....	41
	Water Measurements.....	43
	Incubation Experiments.....	54
	Discussion - CEPEX.....	57
IV	MEASUREMENTS IN OPEN OCEAN ENVIRONMENTS.....	66
	Observations Made Aboard <i>USNS Desteiguer</i> .....	66
	Cruise 79-G-6.....	68
	Atmospheric Measurements.....	68
	Water Profiles.....	68
	Underway Measurements.....	73

## TABLE OF CONTENTS (continued)

CHAPTER	PAGE
	Discussion - Cruise 79-G-6 ..... 76
	Air Measurements..... 76
	Dissolved Gas Measurements..... 80
	Water Profiles..... 81
V	SUMMARY AND CONCLUSIONS..... 84
	REFERENCES..... 88
	APPENDIX ..... 93
	VITA..... 95



## LIST OF TABLES

TABLE	PAGE
1. Reproducibility of Determinations.....	13
2. Sensitivity to $H_2$ as Catalyst Temperature Varies.....	14
3. Retention Times.....	16
4. Efficiency of Extraction with 30-Minute Equilibration.	24
5. Comparison of Commercially Prepared Gas Standards Held in High Pressure Steel or Aluminum Cylinders.....	35
6. CO Sampling in Clear and Dark Bottles.....	41
7. Vertical Cast, Saanich Inlet 16 Aug. (Day 39).....	53
8. Open Water Surface Values.....	54
9a. Effect of Light on Trace Gases in Seawater.....	55
9b. Effect of Dark Storage on Trace Gas Concentration in Seawater.....	56
10. Samples from 10 m.....	66
11. Samples from 100 m.....	67
12. Comparison of Direct and Pumped Samples.....	73
13. Comparison of Two Types of Surface Samples.....	75
14. Comparison of Near-Shore Surface Samples.....	76

## LIST OF FIGURES

FIGURE	PAGE
1a. Schematic diagram of $H_2$ and CO analyzer.....	9
1b. Electronic amplifier for $H_2$ and CO analyzer.....	9
2. Continuous extractor of dissolved gases in surface water.....	26
3. Extractor response to changes in gas concentration....	28
4. Peak height response to samples of known concentration passing through the extractor.....	30
5. Dilutions of 2.78ppm CO standard with purified air....	32
6. Dilutions of 2.78ppm $H_2$ standard with purified air....	33
7. Dilutions of $CH_4$ -spiked CO standard.....	34
8. Techniques used for the calibration of a working standard for $H_2$ .....	36
9. Average daily atmospheric concentration of $H_2$ , CO, and $CH_4$ at the CEPEX site (1978).....	42
10. Vertical profiles of gases in Bag 4 at 11 AM on Day 12 (July 20, 1978).....	44
11a. Dissolved gases in Bag 4 on Day 18 (July 26, 1978)....	45
11b. Dissolved $O_2$ , bacteria numbers, and bacterial activity in Bag 4 on Day 18 (July 26, 1978).....	45
12. Silicate profiles from Bag 4.....	47
13. Chlorophyll-a concentrations in Bag 4.....	48
14. Hydrogen concentrations in Bag 4.....	49
15. Methane concentrations in Bag 4.....	50
16a. $H_2$ , $CH_4$ , and bacteria cell numbers in Bag 3 on Day 13.	51
16b. $H_2$ , $CH_4$ , and bacteria cell numbers in Bag 3 on Day 45.	51
17. Shallow hydrocast in Saanich Inlet on Day 16.....	52

## LIST OF FIGURES (continued)

FIGURE	PAGE
18. Diurnal variations in $H_2$ and CO in surface waters of Bag 4 on Days 32 and 33.....	53
19. Incubations of phytoplankton cultures in light and dark bottles (March, 1979).....	58
20. Daily averages of atmospheric $H_2$ and CO along cruise track 79-G-6.....	69
21. Measurements of atmospheric $H_2$ and CO while approaching Papeete, Tahiti, Day 226J 1979.....	70
22. Typical $H_2$ and CO concentrations in the upper 200 m.....	71
23. $H_2$ and CO concentration profiles in full water column hydrocasts.....	72
24. Decrease of CO at sunset in surface water, Day 253J 1979.....	74
25. $H_2$ concentrations approaching the coast of California.	77
26. Surface water CO concentrations approaching the coast of California.....	78

## CHAPTER I

### INTRODUCTION AND REVIEW

#### Objectives

There has been considerable interest recently in measuring the background levels of trace substances now being released by man into the environment. Much attention has been given to the importance of man's input of materials to the atmosphere and oceans.

Studies have demonstrated that some compounds, although naturally present in a system, can produce significant changes in the system when their normal concentrations are altered by human activity.

Using field and laboratory measurements, this study attempts to relate the observed distributions of hydrogen ( $H_2$ ), carbon monoxide (CO), and methane ( $CH_4$ ) to potential sources and sinks of these gases. In addition to the consideration of trace gases as pollutants, a study of these substances in the ocean can yield important information on natural processes occurring in the marine environment.

The upper layer of the ocean is far from homogeneous. Rather, it is a heterogenous region of rapid reactions - mostly of biological origin - coupled with rapid vertical mixing, air-sea exchange, and lateral mixing. Biological activity is not homogeneously distributed, but clusters in patterns still poorly understood. To understand the nature of such distributions may require very detailed sampling of biological parameters. Such repetitive sampling is often tedious and difficult to perform within close intervals. As an alternative, "indicator" measurements have been sought (*e.g.* chlorophyll, ATP) to provide easier insights into these biological activities. These indicators have had limited success; the search continues for better measurements to show biological and physical processes in the mixed layer. Biogenous gas concentrations may be an indicator of certain chemical, biological, and physical processes. If such gas measurements

---

Format from *Journal of Geophysical Research*.

can be combined with a knowledge of the factors that determine distributions, we may have a valuable monitor of processes in the upper ocean.

### Studies of Trace Gases in the Atmosphere

Since trace gases can cross the air-sea interface, a knowledge of atmospheric levels, along with dissolved concentrations, is important. At the present time, on a global scale, only a limited amount of information is available on atmospheric levels.

Early measurements of  $H_2$  concentrations were made by *Glueckauf and Kitt* [1957]. Their technique was based on the liquefaction of a large volume of air, followed by fractional distillation of the  $H_2$ , and its subsequent oxidation at high temperature by copper oxide ( $CuO$ ) to produce water. This method yields fairly reliable results, but sample processing is complex and time consuming. More extensive atmospheric measurements have been made by *Schmidt* [1978] on a cruise between West Germany and the Dominican Republic, and on a flight between Germany and Chile. An air value of 0.582 parts per million by volume (ppmv)  $H_2$  was reported. The instrument used [*Schmidt and Seiler*, 1970] allowed continuous sampling and analysis to be performed.

Using a high resolution spectrometer, *Migeotte* [1949] detected CO in the atmosphere. Another instrument, described by *McCullough et al.* [1947] and later used by *Robbins et al.* [1968], allowed quantitative measurements of atmospheric CO to be made on a routine basis. CO is one of the most abundant pollutants released into the atmosphere, second only to carbon dioxide in total amount being generated by man's activities [*Jaffe*, 1973]. Along with industrial activities, there are natural sources of CO in the atmosphere. *McConnell et al.* [1971] examined reactions occurring in the atmosphere that convert  $CH_4$  to CO via a hydroxyl (OH) radical reaction.

Atmospheric  $CH_4$  was initially detected by *Migeotte* [1948]. Later, *Fink et al.* [1965] reported an atmospheric average of 1.4 ppmv.

On a cruise in June, 1968, *Swinerton et al.* [1969] reported  $\text{CH}_4$  concentrations greater than 3 ppmv over the Potomac River near Washington, D.C. In the atmosphere above the Atlantic, average  $\text{CH}_4$  concentration was reported as 1.24 ppmv.

### Studies of Dissolved Trace Gases

#### Carbon Monoxide

Studies of dissolved trace gases have, for the most part, lagged behind similar studies in the atmosphere. Recently, however, increased attention has been focused upon the unstable gases in seawater. These studies show we have much yet to learn. For example, high concentrations of CO have been found in unexpected areas. Raindrops have been shown to contain CO concentrations far above atmospheric equilibrium [*Swinerton et al.*, 1971]. CO is found in the floats of the Portuguese man-of-war [*Wittenburg*, 1960] and in marine algae [*Loewus and Delwiche*, 1963; *Chapman and Tocher*, 1966]. *Pickwell et al.* [1964] found that species of siphonophores produce and release CO bubbles in the water column. *Wilson et al.* [1970] observed CO, ethylene, and propylene production in illuminated cell-free seawater containing dissolved organic carbon (DOC). However, much lower production of CO was seen in darkened containers.

The important role that microorganisms may play in CO production and consumption has been examined [*Schlegel*, 1974]. Soil has been found to absorb quantities of CO from the atmosphere [*Ingersoll et al.*, 1974]. The CO removing capability varied with soil type, and was consistently high for roadside soils exposed to high CO levels. *Kluyver and Schnellen* [1947] found that anaerobic bacteria could oxidize CO to  $\text{CO}_2$ , or reduce CO to  $\text{CH}_4$  in the presence of  $\text{H}_2$ .

Numerous other potential sources and sinks for CO have been identified [*Jaffe*, 1973]. CO has been found in the surface waters of the ocean at concentrations far higher than equilibrium solubility would predict [*Swinerton et al.*, 1968], making the ocean a potential

source of the gas to the atmosphere. *Swinerton et al.* [1969] observed that CO levels fluctuated diurnally, with the highest values found about mid-day. These findings were later confirmed by *Seiler and Junge* [1970], who examined vertical profiles in the Atlantic and found CO values in excess of 10 to 40 times that predicted from atmospheric concentrations and experimentally determined solubilities. The maxima in these variations correlate with sunlight in both amplitude and phase, with CO excess extending as deep as 100 m [*Seiler and Schmidt*, 1974]. The daily build-up of CO would appear to result from biological activity. Both plants and animals may be sources of gas.

The diurnal cycles of CO extend too deep for the daily declines to be explained in terms of air-sea exchange. Much CO must be consumed in the ocean by biological or chemical processes.

### Hydrogen

The earliest measurements of dissolved  $H_2$  in seawater were made by *Williams and Bainbridge* [1973] using a gas chromatograph with a low-pressure, direct-current glow discharge tube detector. Approximate values of  $H_2$  ranging from 10 to 250 times atmospheric equilibrium were reported in surface water, probably representing the effects of contamination. *Borgerson* [1978] showed that samples can be very badly contaminated with  $H_2$  produced from the contact of seawater with several metals. *Seiler and Schmidt* [1974] reported values of  $H_2$  taken in vertical profiles from 0 to 600 m in the North Atlantic. They found values from 0.8 to 5.4 times atmospheric saturation, with a distinct maximum at about 500 m. *Herr and Barger* [1978], using a similar instrument, made measurements of atmospheric and dissolved  $H_2$  in the tropical North Atlantic region. Their average air concentration (0.65 ppm) was slightly higher than that reported eight years earlier by *Schmidt and Seiler* [1970], possibly due to calibration differences or to an actual increase in atmospheric levels during the intervening period. Their mid-water samples (100 to 4000 m) showed significantly less variation in  $H_2$  content

than did *Seiler and Schmidt* [1974], even when taken at similar locations and depths. They observed significant variations in the surface water (e.g. 4-71 nl/l) in their study. The sources of these variations are not completely understood. None of these studies reported a regular diurnal pattern in  $H_2$  concentrations. In general, the vertical distribution pattern of  $H_2$  in the water column resembles that of CO.  $H_2$  is more abundant than CO in clean marine air, but slightly less soluble in seawater [*Douglas*, 1967; *Crozier and Yamamoto*, 1974; *Gordon et al.*, 1977].

There are several proposed methods by which molecular  $H_2$  can be added and removed from the environment. Known sources include man's activities, such as the use of automobiles [*Jones et al.*, 1971], along with atmospheric reactions involving  $CH_4$  and CO [*Levy*, 1972]. *Gray and Gest* [1965] reviewed the biological formation of hydrogen by a wide variety of microorganisms. Such production also occurs in the gut of many animals. *Mitsui and Kumazawa* [1977] have studied hydrogen production in marine microorganisms. Molecular hydrogen plays an important role in the biological production and consumption of trace gases. *Wolfe* [1971] describes  $H_2$  as a major product of sugar degradation in anaerobic environments. *Schlegel* [1974] discusses the role  $H_2$  plays in reactions removing CO. These reactions occur in both aerobic and anaerobic environments.  $H_2$  is an important intermediate in some microbial respiration processes, and is a major substrate in the formation of methane.

Much of the  $H_2$  produced is quickly consumed by other microorganisms in the same micro-environment [*Schlegel*, 1974], thus preventing its escape into the atmosphere. *Junge et al.* [1972] noted similar production rates of CO and of  $H_2$  by *Pseudomonas* (= *Alginomonas*) bacteria isolated from seawater. This might suggest identical sources and sinks, but the dramatic diurnal cycle in CO concentration is not so evident in  $H_2$ , and this requires that sources and/or sinks must differ in character.

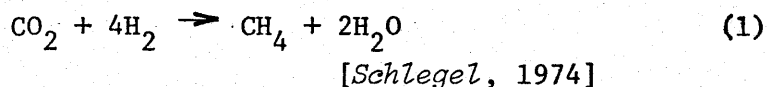
### Methane

Dissolved  $CH_4$  in seawater has been studied in detail. *Swinerton and Linnenbom* [1967], using a gas chromatograph with a flame ionization



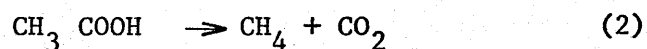
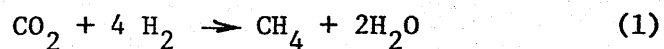
detector, measured dissolved  $\text{CH}_4$  in the Atlantic. They found surface water to be supersaturated by a factor of about 1.3X. *Lamontagne et al.* [1973] reported highly supersaturated concentrations in near-shore areas. The concentration of  $\text{CH}_4$  was found to decrease to near equilibrium levels in the open ocean. *Atkinson and Richards* [1967] measured  $\text{CH}_4$  and hydrogen sulfide ( $\text{H}_2\text{S}$ ) in anoxic waters from several locations. *Brooks and Sackett* [1973] measured light hydrocarbons, including  $\text{CH}_4$  in the surface water of the Gulf of Mexico. High concentrations were found in locations near ports, an indication of anthropogenic input. *Deuser et al.* [1973] considered bacterial action on abiotically produced  $\text{CO}_2$  and  $\text{H}_2$  as a possible source of the methane found in the deep water of Lake Kivu. The  $\text{CO}_2$  and  $\text{H}_2$  in this African rift lake may be supplied by volcanic emanations. *Brooks* [1979] reported a deep water methane maximum in the Caribbean, possibly resulting from methane seepage along the sea floor. Using measurements made in the open ocean, *Scranton and Brewer* [1977] discuss possible sources for the maximum in methane observed at 100 meters. They suggest that *in situ* production of  $\text{CH}_4$ , rather than simply horizontal advection, is important in producing the distribution they report.

Sources of methane include industrial processes and anaerobic decay of organic material [*Wolfe*, 1971]. Anaerobic processes can occur on land, in aquatic environments, and in the intestines of animals. The conversion to  $\text{CH}_4$  is performed by strictly anaerobic bacteria, and involves the reduction of  $\text{CO}_2$  by hydrogen.



Methane formation in marine and fresh water sediments has received considerable attention [*Cappenberg*, 1974; *Martens and Berner*, 1974; *Reeburgh*, 1976; *Barnes and Goldberg*, 1976]. Although highest methane concentrations are found in areas where 90% or more of sulfate has been reduced [*Martens and Berner*, 1977], *Bernard* [1978] observed

apparent  $\text{CH}_4$  production in Gulf of Mexico sediments containing high sulfate concentrations. Production of  $\text{CH}_4$  in such areas could take place in sulfate-free micro-environments in the sediment. *Mechalas* [1974] describes  $\text{CH}_4$  production as a two-stage process. A heterogeneous group of microorganisms first degrade complex organic molecules into short-chain alcohols, fatty acids, acetates, formates,  $\text{H}_2\text{O}$  and  $\text{CO}_2$ . Methanogenic bacteria then use these products to form  $\text{CH}_4$  in reactions such as



## CHAPTER II

### ANALYTICAL TECHNIQUES

#### Introduction

In order to examine the distribution and potential sources and sinks of these gases in the environment, analytical instruments were constructed. Sampling techniques were designed for both atmospheric and seawater analysis. Several techniques exist for the measurement of trace quantities of  $H_2$ , CO, and  $CH_4$ . Methane was measured using a Flame Ionization Detector in a gas chromatographic system. The measurement of  $H_2$  and CO was based on a technique involving the reduction of mercuric oxide (HgO). At high temperatures, both  $H_2$  and CO reduce HgO to elemental mercury vapor. The reaction of HgO is described by *McCullough et al.* [1947] and has been further developed by *Schmidt and Seiler* [1970]. The mercury vapor generated from this reaction was swept into a quartz optical cell, and changes in absorbance of ultraviolet light at the 254 nm line measured. After amplification, this signal was recorded. A gas chromatographic column was added to the system to allow separation of  $H_2$ , CO, and other gases before they entered the heated chamber and passed across the HgO (Figure 1a).

#### Description of $H_2$ and CO Instrument

##### Electronics

The mercury vapor analyzer utilized the principle of atomic absorption at 254 nm to measure mercury produced from  $H_2$  and CO in the HgO column. Light at the mercury wavelength was generated by a Hamamatsu L927 mercury lamp powered by a Hamamatsu power supply. One beam was directed into a flow-through cell, and then onto a quartz photodiode. Another beam was projected directly onto a reference photodiode. A potential of approximately 185 volts DC was applied

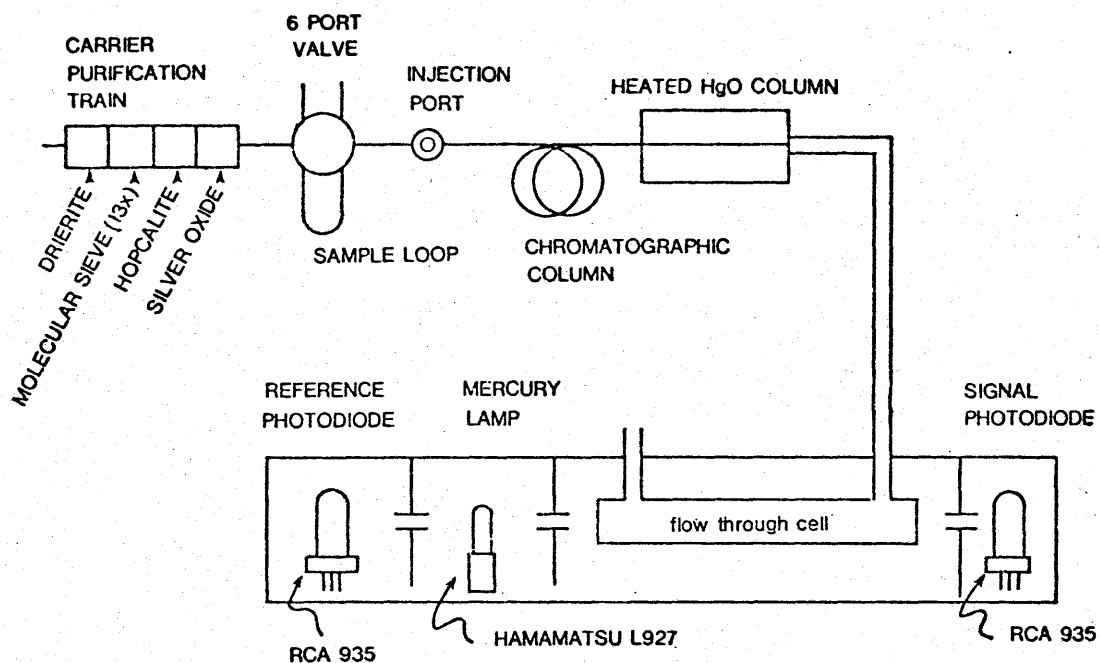


Fig. 1a. Schematic diagram of  $H_2$  and CO analyzer.

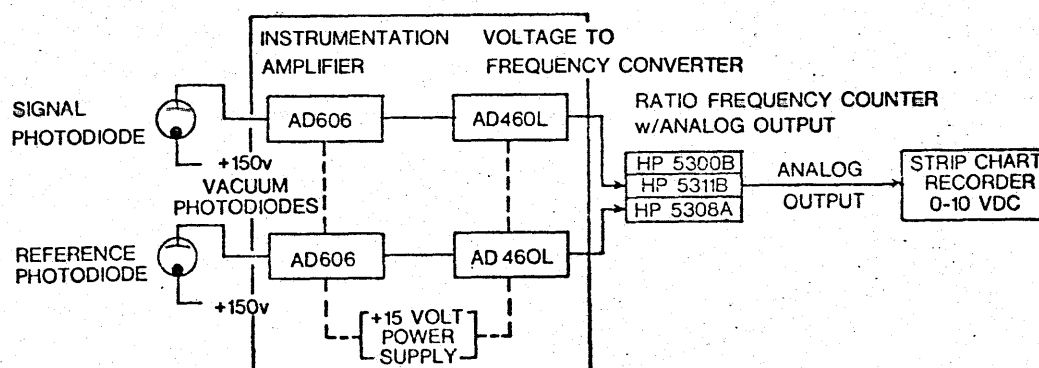


Fig. 1b. Electronic amplifier for  $H_2$  and CO analyzer.

to the photodiode by a series of 45-volt dry cell batteries. In the range of 150 to 225 volts, response of the photodiodes to a given intensity of UV light was nearly constant, so slight drift in battery potential did not affect detector sensitivity. Light striking the photodiode generated a current flow proportional to the intensity of the beam. Current flow from the photodiodes was extremely low, allowing a single set of batteries to be used for a period of six months or longer. This current was amplified and ultimately displayed on a chart recorder. A mechanically adjustable slit positioned between the light source and reference photodiode allowed the intensity of the reference signal to be varied.

The output of the Hamamatsu lamp slowly drifted through time; to compensate for drift, the signal beam was always compared to the reference beam. The output of the optical system and amplifier was somewhat noisy, so a modified amplifier was constructed. Each channel (signal and reference) was amplified separately, then converted to a frequency signal. The frequency outputs were averaged over a short interval (between 0.1 and 1 sec) via a Hewlett-Packard 5311B converter, thus eliminating much transient noise. An analog output of the ratio of the two beams was plotted on a chart recorder, or sent to a digital computer. A diagram of the electronic amplifier is shown in Figure 1b (p. 9).

#### Absorbance Cell

In the early stages of development, both the HgO and quartz absorbance cell were heated in a single large aluminum block. The cell was heated to prevent possible condensation of mercury vapor on the quartz walls and windows. Such deposition would cause a long-term shift in overall cell absorbance. The all-quartz cell design avoided the technically difficult problem of making a heat resistant seal between quartz and a dissimilar material. In this all-quartz design, carrier gas and sample entered from outside, and were preheated in a coiled tube surrounding the cell body. The gases then passed through a plug of mercuric oxide held in place by a glass frit. As mercury

vapor was produced, it was swept into the main body of the cell, and changes in the signal beam recorded. The double window design allowed the inner quartz windows, in contact with the mercury vapor, to remain at the high temperature of the heating block. The outer windows, in contact with outside air, served to insulate the inner windows from the cooler photodiode housings.

Although offering the advantages of all-quartz construction and condensation-free windows, this cell also had severe shortcomings. The most serious, especially during preliminary work in determining optimum operating conditions, was its inflexibility. Once placed in the cell, the mercuric oxide could only be changed by cooling the entire system, and cutting the quartz tubing. As a result, experiments involving changes in amount, grain size, and support of the HgO were extremely difficult and time-consuming. When the reactivity of the HgO decreased due to contamination or other causes, several weeks often passed before it could be removed and replaced.

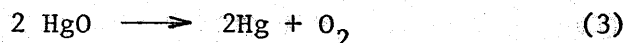
Alternate cell designs were investigated. The use of an unheated optical cell was tested, where only the HgO column was kept at high temperature. A 16-inch length of straight, thin-walled 1/4-inch diameter glass tubing was placed in an aluminum block. The block was kept at a constant temperature with 4 cartridge heaters placed symmetrically about the center glass tube. Two grams of HgO were placed about midway in the glass tube, and held in place with glass wool plugs. Quarter-inch Ultratorr(TM) fittings connected the carrier gas stream to the entrance of this heated tube. After passing across the HgO, the carrier left the heated tube and passed through a side arm connection to an unheated cell. This cell was constructed of 1-inch PVC tubing, with quartz windows held in place at both ends by soft gaskets. Carrier gas left this modified cell through a second side arm at the opposite end of the tube. Modification of this system was relatively simple. The tube containing HgO could be removed and replaced easily. The cell length and optical path length could be changed by substituting different lengths of PVC tubing. The cell could be disassembled and cleaned quickly. Most importantly, at

normal carrier gas flow rates, no deposition of mercury on the cell windows was observed. Flow characteristics of the cell, with an internal volume of about 100 ml, were similar to the all-quartz cell.

The residence time of mercury vapor in the cell following sample injection was dependent on several factors, including cell volume, flow rate of the carrier gas, and length of the HgO plug. With moderate flow rate (300 ml air/min), mercury vapor peaks generated by sample injection showed steep rises, followed by long, slowly declining tails. Accurate integration of such slowly tailing peaks by a digital integrator was difficult. A study was done to compare replicate samples using both peak height and peak area as measures of concentration (Table 1). Due to the difficulty of determining the area under the tail, peak height proved to be superior to peak area as a concentration determinant.

#### Mercuric Oxide

The baseline and sensitivity of the instrument was strongly influenced by carrier gas flow rate and HgO temperature. Table 2 shows the response of the instrument to equal amounts of H<sub>2</sub> as the operating temperature was varied. At temperatures below 200°C, the amount of Hg vapor generated by the H<sub>2</sub> injection was low. As temperature increased, the quantity of Hg generated by a given quantity of H<sub>2</sub> increased, as did the Hg vapor background due to the thermal dissociation of HgO:



This increased background absorbance was reflected in decreasing baseline numbers. A normal operating temperature of 230°C was chosen as a compromise. The percent reaction of H<sub>2</sub> with HgO was relatively high at this temperature, and the thermal dissociation of HgO did not yet dominate the signal. In contrast, the reaction of CO with HgO was less sensitive to temperature change, and showed little increase at temperatures over 200°C.

To test the completeness of the reaction of H<sub>2</sub> and CO, equal amounts (by volume) were injected into a HgO column held at 230°C.

TABLE 1. Reproducibility of Determinations

	<u>Peak Height*</u>		
	Mean	Standard Deviation	
H <sub>2</sub>	11.08	0.12	1.1%
CO	37.04	0.964	2.6%
	<u>Relative Peak Area</u>		
H <sub>2</sub>	1266	38.1	3.0%
CO	6812	287	4.2%

\* - Full Scale = 10

Data Points Used for Above

Sample #	H <sub>2</sub> Peak Ht.	H <sub>2</sub> Peak Area	CO Peak Ht.	CO Peak Area
1	11.2	1290	36.0	6890
2	11.2	1247	37.0	7050
3	11.1	1298	37.0	6860
4	11.0	1296	37.0	7310
5	11.1	1287	37.0	6350
10	10.8	1227	35.0	6530
11	11.0	1297	36.0	N.A.
12	11.0	1177	37.5	6986
13	11.2	1307	38.0	6870
14	11.2	1249	38.0	6490
15	11.1	1248	38.0	6790
16	11.1	1269	38.0	N.A.

CO generated 6.6 times more mercury vapor than did the H<sub>2</sub> at this temperature. Under these conditions, on a mole-to-mole basis, H<sub>2</sub> was about 15% as effective in releasing mercury as was CO.

Efforts were made to increase the completeness of the reaction of H<sub>2</sub> with HgO. Varying mesh sizes of HgO were introduced, and the cross sectional area of the tube holding the HgO increased. Attempts were made to deposit the normally granular HgO reagent on various surfaces. HgO is quite insoluble in water and other solvents. To precipitate this compound in the interior pore structures of supports such as Chromosorb P and Molecular Sieve 13X, the supports were soaked



TABLE 2. Sensitivity to  $H_2$  as Catalyst Temperature Varies

Temperature °C	Peak Heights (relative)	Baseline (signal/reference)
50	0.2	1.940
80	0.2	1.870
100	0.25	1.840
125	0.25	1.830
140	0.35	1.820
155	0.7	1.78
170	0.9	1.70
180	1.2	1.58
190	1.4	1.43
200	1.4	1.34
210	1.4	1.28
220	1.6	1.24
230	1.4	1.24
240	1.6	1.21
250	1.3	1.06
260	0.8	0.870
270	0.5	0.750
280	0.3	0.650
290	0.2	0.600
300	0.1	0.550

in a solution of mercuric nitrate [ $Hg(NO_3)_2$ ], a very soluble compound. Subsequent heating in air converted the  $Hg(NO_3)_2$  to  $HgO$ , thus coating the large internal surface area of the support with the active compound. These preliminary experiments failed to achieve a significantly higher conversion of  $HgO$  to  $Hg$  by  $H_2$ .

Lengthening the  $HgO$  plug did apparently increase the percentage of  $H_2$  reacting with  $HgO$ . The increase in  $HgO$  plug size also caused considerable peak broadening, however, possibly due to an impediment of the released  $Hg$  vapor as it passed through the long plug of  $HgO$ .

Optimum response to  $H_2$  was obtained using a  $HgO$  plug about 2 cm long. This path length was sufficiently long to allow a reasonable reaction efficiency (15%), yet not so long as to hinder the  $Hg$  vapor generated from being swept out quickly into the optical cell.

### Carrier Gas

After examining several candidates, compressed air was chosen as the carrier gas. Normal gas samples from the atmosphere or from air-equilibrated seawater had a composition similar to the compressed air carrier. The bulk composition and thermal conductivity did not change abruptly as the sample passed through the HgO. If helium was used as a carrier, however, a baseline shift was seen as the N<sub>2</sub> and O<sub>2</sub> components of the sample passed through. This was attributed to the large differences in thermal conductivity between helium (He) and air (O<sub>2</sub>-N<sub>2</sub>) [Weast, 1976], and the transient effects this difference caused on the rate of thermal dissociation of HgO. Injecting air samples into an air carrier gas eliminated this problem.

Catalytic reagents were used to produce a carrier gas free of any traces of CO and H<sub>2</sub> ("zero air"). This carrier gas was dried by means of a 13X molecular sieve and Drierite(TM). Silver oxide was used to oxidize CO to CO<sub>2</sub>, and Hopcalite(TM) oxidized H<sub>2</sub> to H<sub>2</sub>O. Air, after passing through this purification system, provided an extremely low, stable background. After purification, the carrier gas was directed through a Carle 6-Port Valve(TM), and past an injection port containing a rubber septum for use with syringe injections. The Carle valve was equipped with an electrically controlled actuator for automated injection. In one position, "fill," sample gas filled a stainless steel sample loop, while carrier gas flowed directly to the MS 13X column. In the other valve position, "inject," carrier gas was directed into the sample loop, sweeping the contents into the MS 13X separating column.

After the 6-port valve was purchased and installed in the system, sample injection by syringe was avoided. Skill was needed to obtain and hold uncontaminated air samples in a syringe during transfer and injection. Injection of replicate volumes of gas by hand-held syringe proved difficult.

The injection process had little effect on the baseline, due to the large reservoir volume of gas in the purification train and to

the damping effects of the 1.75 meters of MS 13X column. The slight baseline change that occurred when the sample was injected subsided well before the  $H_2$  peak came through.

Table 3 shows the retention times for  $H_2$  and CO peaks after injection of air samples. Several other gases were injected to measure their reactivity with the  $HgO$ . In these experiments, the sample loop was 46.1 ml ( $\pm 0.1$  ml); other samples were syringe injected.

TABLE 3. Retention Times

Sample	Sample Volume	Peak Arrival Time after Injection(min)	Peak Height	Gas
Purified air	loop	none observed	-	Air
Compressed air	loop	1.0	10.8	$H_2$
		4.9	35.0	CO
Outside air	loop	0.8	4.9	$H_2$
		4.9	24.5	CO
CO standard	10 ml	1.2	1.5	$H_2$
(mix of 25 ppm CO & 12 ppm $CH_4$ in He)		4.5	65.0	CO
$H_2$ test gas	10 ml	0.9	35.0	$H_2$
( $10^{-4}$ ml in air)		4.7	2.0	CO
$CH_4$	10 ml	2.7	10.2	$CH_4$
(1 ml in air)				
Ar	10 ml	1.7	1.0	Ar
(1 ml in air)				
$N_2$	10 ml	0.8	0.5	$H_2$
		4.8	4.0	CO
He	1 ml	0.3	negative	He

The small baseline rise seen after the argon (Ar) injection, at 1.7 minutes, and the baseline drop observed at about 0.3 minutes after helium injection, may reflect the high thermal conductivity of He and low conductivity of Ar as compared to  $O_2$  and  $N_2$ .

Very high concentrations of methane showed a significant reaction. The column easily separated this  $CH_4$  peak at 2.7 minutes from the  $H_2$  peak at 1.1 minutes and CO at about 4.8 minutes. The amount of  $CH_4$  injected (Table 3) was about 6 orders of magnitude higher than the

amount expected in ordinary seawater samples of 1 to 2 liters. The peaks observed in the compressed air, outside air, and compressed  $N_2$  occurred at the same time as did peaks from standards of  $H_2$  and CO, indicating the presence of trace amounts of  $H_2$  and CO in these gases.

#### Description of the Methane Instrument

Methane was measured using a Varian(TM) Series 3700 Gas Chromatograph. This instrument was equipped with dual Flame Ionization Detectors, sensitive to the C-H bonds found in  $CH_4$  and other compounds. About 10 ml of sample was normally injected through a rubber septum with a syringe, or with a sample loop and 6-port Carle(TM) Valve. Once in the He carrier gas of the instrument, the sample passed through a 1.75 meter 13X molecular sieve column held at 50°C. After separation in the column,  $CH_4$  was burned in the hydrogen-air flame of the detector. The resulting signal was amplified and sent to a digital integrator and chart recorder. An Infotronics(TM) Digital Integrator calculated peak area and recorded the result on a Digimatic(TM) Printer. A chart recorder directly plotted the peaks generated by the chromatograph. Due to frequent electronic malfunction of the integrator, peak height proved a more reliable measure of methane concentration than did peak area.

#### Atmospheric Sampling

Atmospheric samples were drawn into the instruments through a length of 1/4-inch Dekabon(TM) tubing. At the normal rate of pumping, this tubing had no measurable effect on the trace gas composition of air passing through. While sampling at sea, the tube inlet was positioned slightly ahead of the ship's bow, allowing uncontaminated marine air samples to be taken while underway. Contamination from the ship was observed occasionally while stopped on station, and when a following wind exceeded the ship's underway speed. In the laboratory at Texas A&M University in College Station, a similar air tube

was run through an opening in the building wall for sampling. At a height of approximately 30 meters, this inlet provided air samples somewhat removed from local ground level sources of trace gases, and reflected mean air composition over the Bryan-College Station metroplex.

The presence of water vapor (humidity) in air samples was easily detected. Moist air gave significantly lower values of CO, H<sub>2</sub>, and CH<sub>4</sub> concentrations than did the same air after drying. The partial pressure of water in undried samples was seen to contribute a significant and variable fraction to the total pressure and composition of the air sample. To avoid this complication, all samples were dried before injection. The drying agent used, Drierite (TM) (anhydrous CaSO<sub>4</sub>), had no discernible effect on the trace gas composition of the samples studied.

A diaphragm air pump was used for atmospheric sampling. To avoid contact of the air sample with the internal components of the pump, the pump was placed in the flow system at a point downstream of the sample loop. Air was first sucked through the Drierite and Dekabon tubing, then through the sample loop, and finally through the pump. The air initially pumped into the system was used to flush the loop and was subsequently vented. About 30 seconds before the injection of the sample, a shut-off valve was closed between the loop and pump. The reduced pressure of the loop caused outside air to continue flowing into the loop until one atmosphere of pressure was reached. After this, the sample was injected. Closing of the valve prior to injection allowed all samples to be injected at ambient pressure, and prevented backflow from the laboratory and pump into the sample loop. Since both standards and samples were dried, and injected at ambient pressure, no corrections were required for varying humidity or barometric pressure. Care was taken to insure that the regulator and sampling lines used to carry standards to the sample loop were thoroughly flushed between samples.

Partial separation of the components of a gas mixture can occur under some conditions, where flow is through a long, narrow tube. Hydrogen in a standard would be particularly susceptible to this effect due to its light weight and relatively high mean-free molecular

path. *Knudsen* [1911] examined the flow of gases through orifices and channels under conditions of low pressure (less than  $10^{-6}$  atmospheres). In this region, the mean-free path of the molecules can exceed the characteristic dimensions of the channel conducting the gases. Flow is limited by collisions between molecules and the limiting walls, not by collisions between the molecules themselves. At higher pressures, such as those used during sampling (1 atmosphere) viscous flow predominates, and separation of gases due to different mean-free paths is negligible. No differences could be detected in  $H_2$  standards bled through short or long sections of 1/8-inch diameter sample tubing under normal working conditions.

#### Water Sampling

The methods for obtaining samples in the water column will be discussed in subsequent chapters. Once collected, the Niskin bottle samples were subsampled and processed in all-glass containers. These containers were similar to 2-liter gas collecting tubes, with a 2-way stopcock placed at one end, and a 3-way stopcock at the opposite end. During water transfer, the bottles were held vertically. A short length of Tygon tubing connected the stopcock of the Niskin to the 2-way (bottom) stopcock of the glass sampler. The water in the Niskin was then siphoned into the sample bottle. The air in the glass bottle was completely displaced through the top stopcock, and the sample bottle was overflowed by approximately 1 liter. This was done to insure that the initial water transferred, in contact with air, was flushed out. The sampler stopcocks were then closed, and the sample held for further processing.

#### Gas Extraction

Several methods of removing dissolved gases from seawater were considered. The analytical methods used were considerably more sensitive to CO and  $CH_4$  than to  $H_2$ . For normal concentrations of  $H_2$  in seawater, a large sample size was required for analysis. To insure an adequate  $H_2$  signal, the dissolved gases removed from the sample

could not be diluted beyond the lower range of the instrument's sensitivity. An efficient and reproducible method for rapid removal of gases from the water sample was necessary.

One method considered was vacuum extraction [*Herr and Barger*, 1978]. Under conditions of reduced pressure, dissolved gases leave the liquid phase, and enter the head space of a container. This degassing process can be speeded by forcing the water to enter the container as a fine mist, where the high surface area exposed increases the rate of transfer. This method involves no addition of outside gases, and the resultant bubble of extracted gases is in undiluted form.

At 20°C and 35°/oo, 1 liter of seawater equilibrated with air at a total pressure of 1 atm contains 5.166 ml O<sub>2</sub>, 9.51 ml N<sub>2</sub>, and 0.258 ml Ar [*Weiss*, 1970]. Complete degassing of 1 liter of such water would place the trace components in an average volume of about 15 ml of extracted gas. The vacuum technique used by *Herr and Barger* [1978] did not produce complete degassing in their samples. An average removal of 56% of dissolved H<sub>2</sub> from seawater samples was reported. Their technique was not used in our analysis, since factors such as organic content of seawater, rates at which water enters the vacuum chamber, droplet size, etc. may affect the percentage removal for a given sample. Conditions must be carefully controlled to insure reproducibility between samples.

Another method of removing gases from seawater is the stripping technique. A purified stream of helium or other gas (stripper) is bubbled through a water sample and collected. Dissolved gases enter these bubbles, are carried to the surface, and removed from the liquid. Since the process greatly dilutes the dissolved gases originally present, a trap is often used to hold and concentrate the trace components while allowing the He to escape [*Swinerton and Linnenbom*, 1967]. Molecular Sieve 6A, at liquid nitrogen temperatures, will hold H<sub>2</sub>, CO, and CH<sub>4</sub> along with other gases, while allowing the He carrier to bleed away (Lilley, personal communication, 1979). After sample degassing is complete, the trap can

be heated, and the absorbed gases in the trap eluted into the detector. Care must be taken to insure that stripping is complete, that none of the sample bleeds through the trap during stripping, and that the carrier contains no traces of the gases to be measured. If trace contamination of the carrier occurs, a long stripping time at high flow rate will result in a very large sample blank. The stripping method has the advantage of removing essentially all dissolved gases, and, combined with a suitable trap, delivers them to the detector in concentrated form. One disadvantage of the stripping method is the relatively long time required for individual sample processing. Up to 30 minutes can be required to strip, trap, and analyze a seawater sample.

### Equilibration

Another technique used for removing dissolved gases from seawater is equilibration [McAullife, 1971]. At equilibrium, the concentration of a dissolved gas ( $C_i$ ) is proportional to its concentration (or partial pressure- $p_i$ ) in the air above the liquid and to the Bunsen solubility coefficient ( $\beta_i$ ). In seawater,  $\beta_i$  is a function of salinity and temperature.

$$C_i = \beta_i p_i \quad (4)$$

In an equilibrium system, if  $\beta_i$  and  $p_i$  are known, the concentration of a dissolved gas can be calculated.

During analysis, a small volume of "zero" air ( $V_a$ ) was introduced into a large volume of water ( $V_w$ ). The amount of a trace gas, i.e.  $H_2$ , initially present in the system is given by

$$A_H = C_w V_w + C_a V_a = C_w V_w + 0 V_a = C_w V_w \quad (5)$$

where  $C_w$  is the initial concentration of gas in water and  $C_a$  is the concentration of the gas in air. At equilibrium, the gas was distributed between the two phases

$$A_H = C'_w V_w + C'_a V_a \quad (6)$$

where



$$C'_w = \beta_1 C'_a \quad (7)$$

Therefore

$$C_w V_w = \beta_1 C'_a V_w + C'_a V'_a$$

$$C_w = C'_a (\beta_1 + V'_a / V_w) \quad (8)$$

From measurement of  $C'_a$  (the equilibrium concentration of gas in the air space above the liquid) and use of tables of  $\beta$ , the original concentration of dissolved gas in a sample can be calculated.

For a typical 2-liter sample, at 20°C and 35‰ salinity, adding 50 ml of "zero" air, then equilibrating, results in:

61% extraction for  $H_2$  ( $\beta=0.0159$ )

46% extraction for  $CH_4$  ( $\beta=0.0290$ )

56% extraction for CO ( $\beta=0.0196$ )

Hydrogen is less soluble in seawater than CO or  $CH_4$ , and is more effectively removed during equilibration. Increasing the amount of air initially added ( $V_a$ ) increases the percent of trace gases removed from the liquid, but decreases  $C'_a$ , the concentration of trace gas present in a given volume of the air phase. A compromise ratio, 50 ml air to 2000 ml seawater, was chosen.

#### Sample Processing

For processing, sample bottles were placed in a vertical holder. A burette, partially filled with water, was placed alongside the sample bottle. The burette was connected to the 2-way stopcock of the sample bottle with a section of Tygon (TM) tubing. The top arm of the 3-way stopcock was connected to a supply of "zero" air and flushed thoroughly. The water level in the burette was recorded, then the bottom stopcock was opened. The top 3-way stopcock was then turned to allow "zero" air to enter the sample bottle, and displace water into the burette. After sufficient air entered the sample bottle, the upper stopcock was returned to its original position. The water levels in the burette and sample bottle were

equalized to bring the pressure in the bottle to atmospheric pressure. The bottom stopcock was then closed and disconnected from the burette.

To speed the rate of equilibration of the samples, the bottles were first strapped in a horizontal position about the central axis of a miniature Ferris wheel. The bottles were then rotated around this axis for a fixed period of time.

A maximum of eight samples could be fitted into the device. The rotor of the equilibrator was driven by a gear-reduction motor at 27 r.p.m. for 30 minutes to insure equilibrium.

In order to check the completeness of equilibration, replicate samples were rotated for varying time periods. Thirty minutes was found adequate for the trace gases to equilibrate.

After equilibration, the sample bottles were removed and re-connected to a water-filled burette. The side arm of the 3-way stopcock was connected to a vacuum line, while the top arm was connected (via a drying tube) to the sample loop. The 3-way stopcock and sample loop were then evacuated. Next, the top and bottom stopcocks were turned to allow the equilibrated air to be displaced into the sample loop. The position of the burette was adjusted so that the water levels in the burette and sample bottle were equal. This insured a pressure of one atmosphere in the sample loop. The air sample was then injected, and peaks recorded.

The air volume held in the sample bottle ( $V_a$ ) was calculated from volume displacement of water in the burette.

As a test of equilibration efficiency, compressed air of known trace gas composition was bubbled through a volume of water. From knowledge of the air composition and solubility coefficients, dissolved content could be predicted.

Table 4 compares the results of analysis of several air equilibrated water samples to expected concentrations using Equation 8. Problems in handling and storing CO samples will be discussed later.

#### Continual Water Analysis

In addition to discrete water sampling, continual measurements of surface seawater were made while underway. Since no *in situ*

TABLE 4. Efficiency of Extraction with 30-Minute Equilibration

Gas	Measured Concentration nmole/Liter	Expected Concentration nmole/Liter
H <sub>2</sub>	0.49	0.49
	0.40	0.49
H <sub>2</sub>	0.74	0.74
	0.66	0.74
	0.82	0.74
H <sub>2</sub>	0.68	0.73
	0.69	0.73
H <sub>2</sub>	0.39	0.45
CO	0.42	0.67
	0.42	0.67
CO	0.15	0.07
CH <sub>4</sub>	1.92	2.08
	1.92	2.08
CH <sub>4</sub>	1.72	1.68

analytical equipment was available, seawater was pumped from a towed vehicle, or "fish," into the shipboard laboratory. Only part of the seawater stream was analyzed for gases. The remainder was used for chlorophyll, nutrient, and salinity analyses, and to provide a constant temperature bath for the continuous extractor. Excess output from the pump also served to flush the sampling hoses, and prevent build-up of trace gases released from the walls of the hose. The restraints of sample size, dilution, and instrument sensitivity were similar for continual and discrete measurements. A modification of the equilibration technique was used as a basis for the design and construction of the continuous extractor. In continual analysis, the goal was to rapidly extract, from a limited volume of water, a representative sample of the dissolved gases present.

The towed fish, used to supply surface seawater to the continuous extractor, was attached to a stainless steel cable and lowered into the water from a boom placed amidship. While underway, the fish was towed about 2 m away from the side of the ship, at a depth of approximately 2 to 3 m. The exact depth

was controlled by the length of cable and by the speed of the ship. A hose was run up from the forward tip of the fish along the length of cable, allowing seawater to be drawn which had not had previous contact with the ship or fish body. This hose ran to the ship's deck, where a Vanton(TM) peristaltic pump pulled seawater up to deck level, then pushed the water to the upper deck and into the laboratories. The water stream was subdivided and directed to several separate laboratories for nutrient, gas, and chlorophyll analyses. Flow rate into the  $H_2$  and CO gas extractor (Figure 2) was controlled by a Cole Palmer (TM) variable speed peristaltic pump. This rate could be varied from 0 to 2000 ml/min. Once set, water flow rates were constant ( $\pm 5\%$ ) for periods of 24 hours or longer. As the seawater entered the 1/2-inch O.D. Tygon (TM) tubing of the extractor, purified air was added to the water stream. Flow rate of the air was controlled by a standard two-stage gas regulator, and a 1-m length of M.S. 13X column. Flow rates remained within set values ( $\pm 5\%$ ) over periods of 24 hours or more. Both air and water flow were measured frequently. As the stream of air bubbles was swept along the coiled tubing by the water flow, trace gases were exchanged between the water and purified air. At the end of the spiral, about 1 m below the surface of the extractor bath, the air stream was collected and directed upward toward the sample loop of the instrument. Hydrostatic pressure at the exit of the coil forced the air through a drying column and into the sample loop. If only  $H_2$  analysis was desired, CO was selectively removed using the same catalyst as in the purification train. After passing through the sample coil, the air stream was vented to the atmosphere. Patterns of sample and standard injections were similar to those used for atmospheric sampling. Discrete gas samples could be analyzed for hydrogen content at 1-minute intervals. If CO data were desired, the time required to separate this peak in the gas chromatographic column prevented sample injections at intervals less than 5 minutes apart.

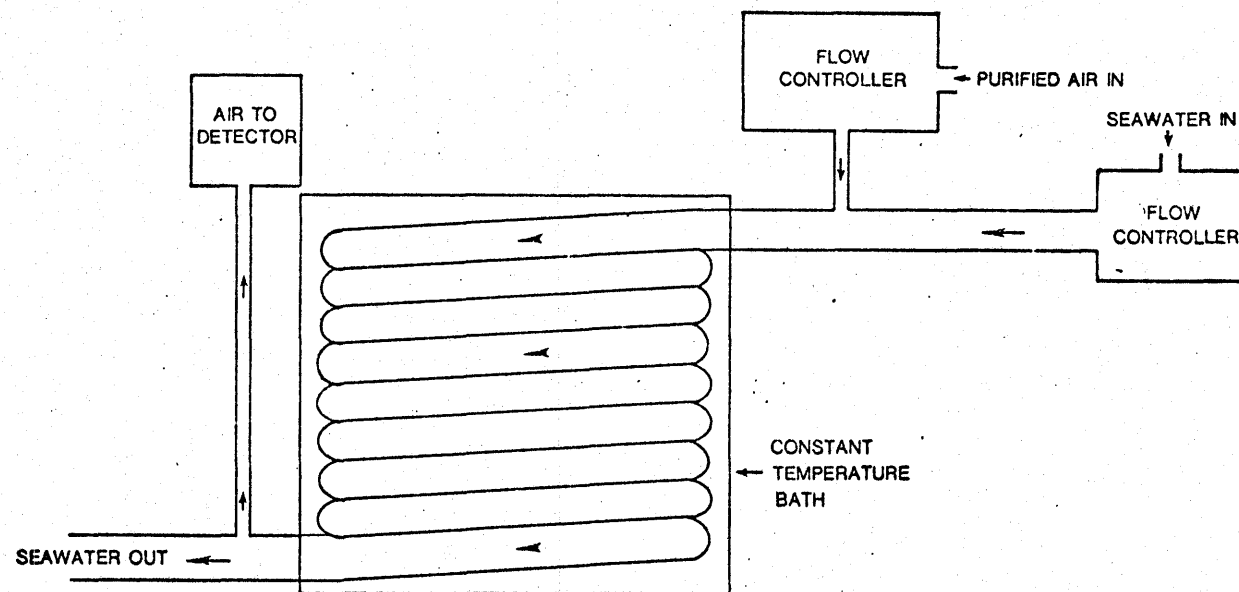


Fig. 2. Continuous extractor of dissolved gases in surface water.

With a device to precisely control flow rate, the air stream from this extractor can be used to replace the normal carrier gas stream in the  $H_2$ -CO instrument. This would allow true continuous measurements to be made, instead of the closely spaced discrete sample injections described above. Several factors prevented this from occurring on Cruise 79-G-6. Both  $H_2$  and CO measurements were desired. A continuous stream of sample would not allow the two peaks to be separated. Unless one of the gases was removed, the signal generated as the gas stream flowed through the detector would represent a sum of both  $H_2$  and CO concentrations, and would be difficult to interpret. In addition, since the  $HgO$  column was sensitive to small fluctuations in gas flow, slight changes in the air stream flow rate would cause large baseline drift. The drift in baseline would be difficult to distinguish from any real change in signal due to varying dissolved trace gas concentrations. Unless a very constant baseline could be established using a mass flow controller or other device, baseline checks would be required frequently. At regular intervals the continuous stream would need to be interrupted and switched to a carefully regulated flow of standard gas for calibration. These difficulties are not insurmountable, and adaptation of the continual sampling scheme to continuous sampling for either  $H_2$  or CO should require only careful flow control of the extractor gas stream, and devices to prevent accidental entry of water into the instrument.

In the continual method of injecting discrete samples used, each loop injected represented the gases flowing through the sample loop averaged over a short interval prior to injection. At a flow rate of 150 ml/min, the sample loop was flushed several times in the 1 minute between injections. At normal water flow rates, seawater passed from the intake of the fish to the exit of the extractor in about 2.5 minutes. An abrupt change in dissolved trace gas concentration at the fish was detectable as a peak on the chart recorder after about 3 minutes.

Figure 3 shows the response of the extractor and detector to varying concentrations of dissolved gas in a water stream drawn from

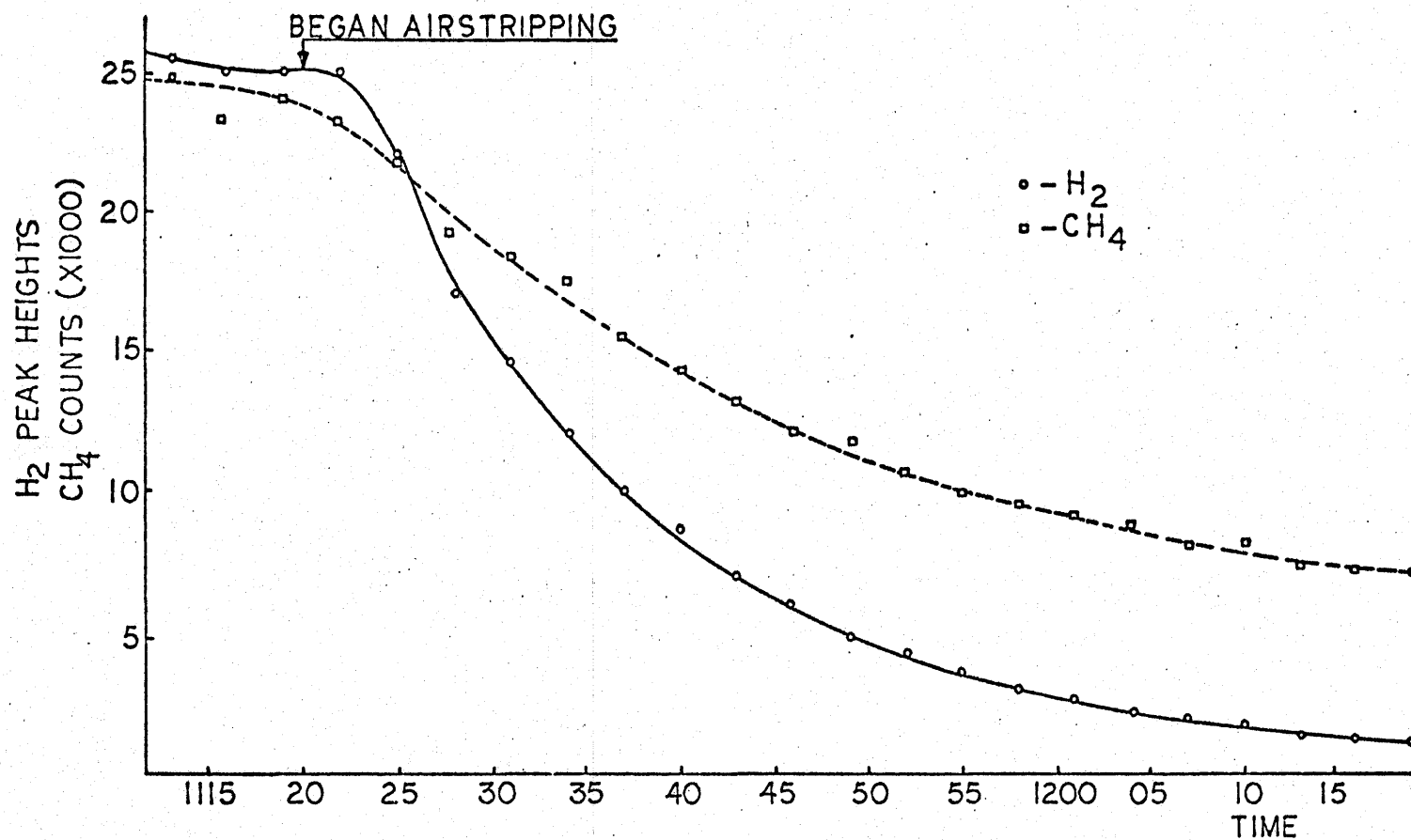


Fig. 3. Extractor response to changes in gas concentration. Air stripping of barrel began at T=1121. Most rapid changes were seen during early stages of stripping. Response leveled off as barrel water approached equilibrium with air.

a large plastic barrel. The barrel water was initially supersaturated with both  $H_2$  and  $CH_4$ . After the test run began, dissolved gas concentrations were decreased in the barrel by vigorous bubbling with air containing low concentrations of  $H_2$  and  $CH_4$ . Rapid decrease was observed at  $T = 25$  minutes, about 4 to 5 minutes after bubbling began. The decrease in dissolved gases continued for about 1 hour as concentrations approached new equilibrium values.

In Figure 3, peak height is used to indicate relative concentrations. The relationship of peak height to absolute concentration for samples passing through the extractor depended on flow rate, temperature, and coil geometry. Actual concentrations of trace gases were determined by comparing the sample peak heights to peaks produced by water containing known concentrations of dissolved gases. Two methods of calibration were used. In one, a large volume of water was equilibrated with air of known trace gas composition. This water was run through the extractor under the same conditions as normal samples. The response of the instrument to water of known trace gas content could be used to reference unknown concentrations. The other method of calibration was to draw into glass sample bottles discrete samples of water entering the extractor. These samples were later analyzed, and the concentrations compared to the peaks generated at the time the samples were drawn. Figure 4 compares extractor peak heights to measured concentrations of discrete samples taken at the same time. At high CO levels, peak height is distinctly non-linear with respect to measured CO concentration in discrete samples.

### Standards

In order to determine absolute concentration, all of the measurements of  $H_2$ , CO, and  $CH_4$  in atmospheric and water samples were referenced to standard gases held in cylinders. Several methods of calibration were examined. The linearity of the instrument's response to varying concentrations of  $H_2$ , CO, and  $CH_4$  was measured using dilutions of a standard gas with purified air. A pair of Hastings (TM)



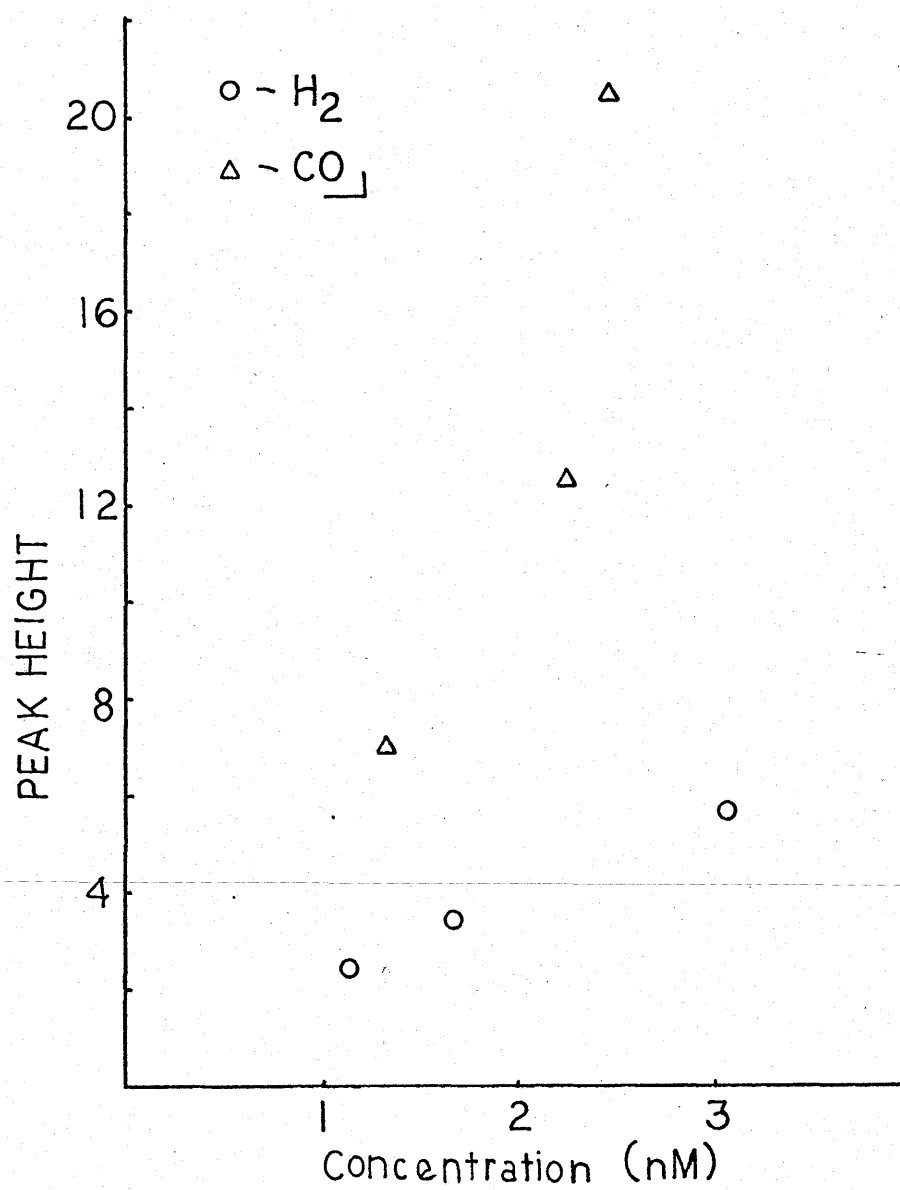


Fig. 4. Peak height response to samples of known concentration passing through the extractor.

Mass Flow Meters were used to provide a series of known ratios of standard to pure air. After each blend, the mixture flowed through the sample loop and was injected into the instrument. Figures 5 and 6 show the results from dilutions of  $H_2$  and CO standards. In the normal range of concentrations encountered in atmospheric and seawater samples (0 to 1 ppmv), the response to varying concentrations is fairly linear. Less linearity is seen at higher concentrations, especially for CO. At very high concentrations (20+ ppmv), absorbance in the optical cell reached a near constant level, indicating that absorbance of the mercury lines had reached a saturation point. Higher than normal levels of  $H_2$  and CO in samples could be accurately measured by reducing the sample size before injecting. Before mass flow meters became available, the actual amount of standard and zero air mixed together during a dilution experiment was difficult to measure accurately. Linearity of response to CO and  $H_2$  was therefore determined by indirect means. A cylinder containing a moderate concentration of  $H_2$  and CO was spiked with several cc's of pure methane. Using simple needle valves to regulate flow, a series of blends of this standard with zero air were made. For each blend, the needle valve was adjusted to give a different ratio of standard to zero air. The addition of zero air reduced the original concentrations of  $H_2$ , CO, and  $CH_4$  by equal, but unknown, factors in each blend.

The response of Flame Ionization Detectors to varying methane concentrations is linear over several orders of magnitude. This linear response to methane allowed the dilution ratio to be determined. New CO and  $H_2$  concentrations in the blended mixtures could be calculated, and concentrations of  $H_2$  and CO vs. peak height plotted. Figure 7 shows a direct comparison between CO and  $CH_4$  response for the blended samples. This gives an indication of the linearity of response of the instrument (peak height) to varying concentrations of CO.

Commercially blended standards were purchased with concentrations of  $H_2$ , CO, and  $CH_4$  in the ranges expected from normal air and water samples. Table 5 shows a comparison among standards purchased from

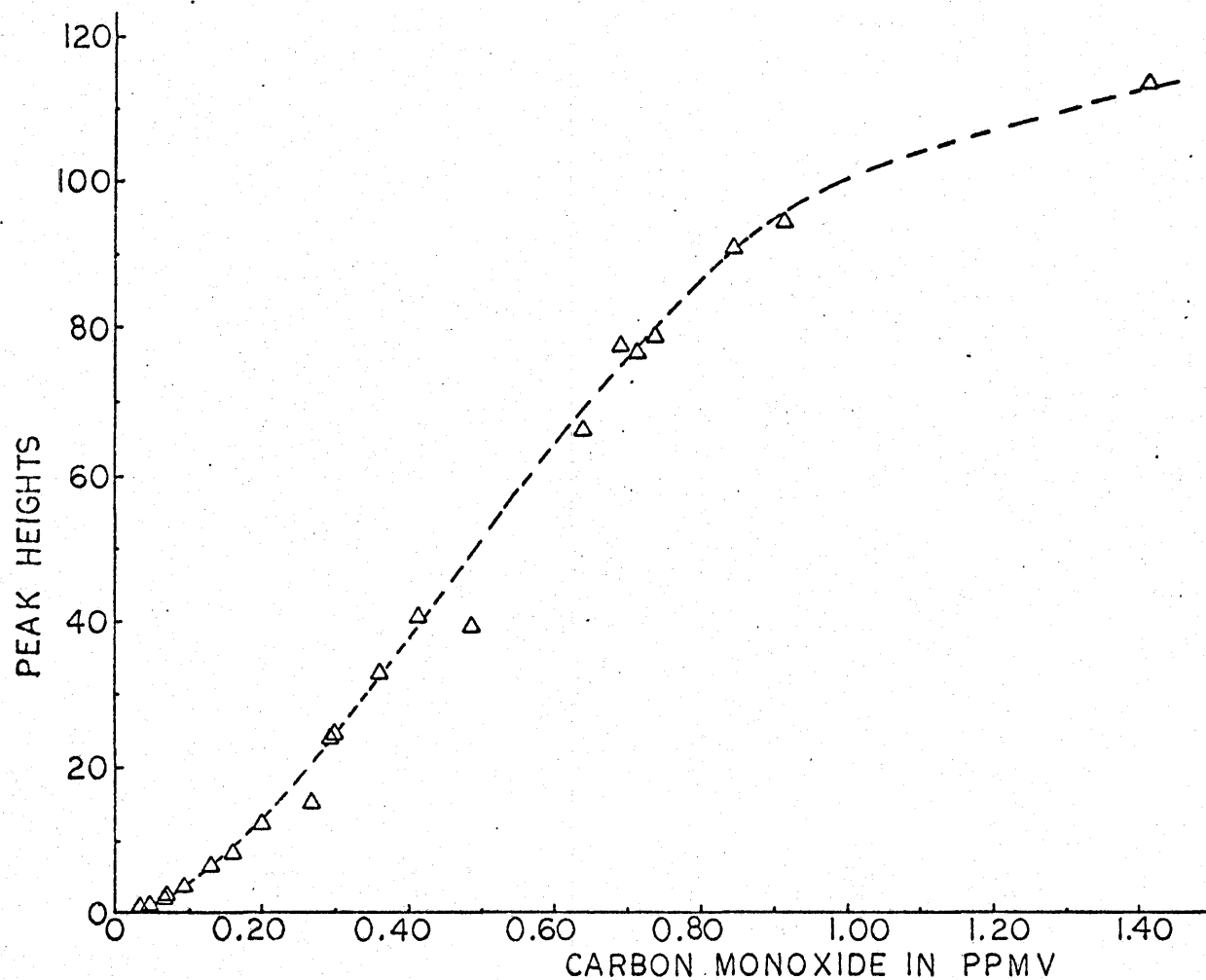


Fig. 5. Dilutions of 2.78 ppm CO standard with purified air. A pair of Hastings Mass Flowmeters were used to mix the standard with air.

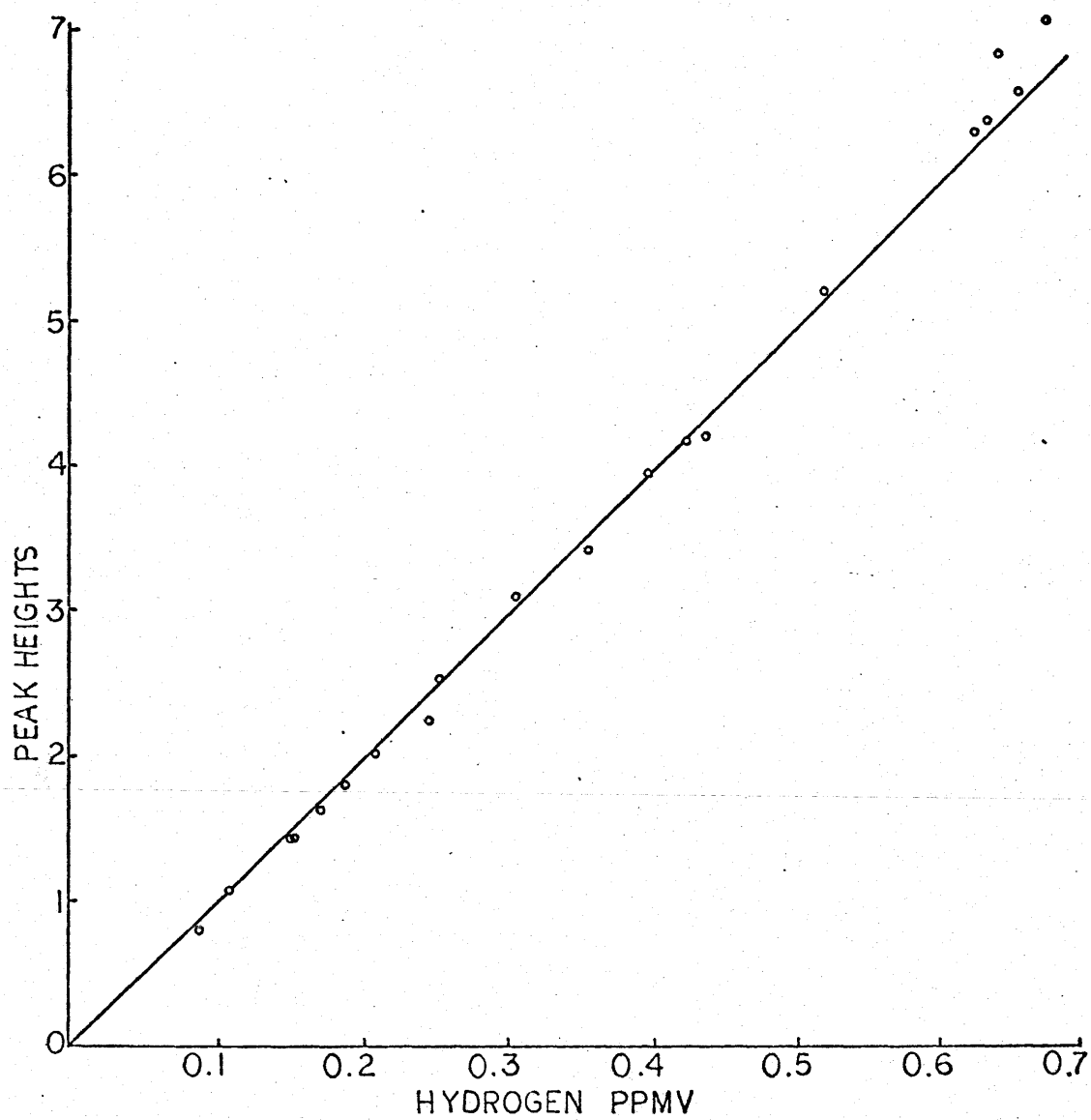


Fig. 6. Dilutions of 2.78 ppm  $H_2$  standard with purified air.

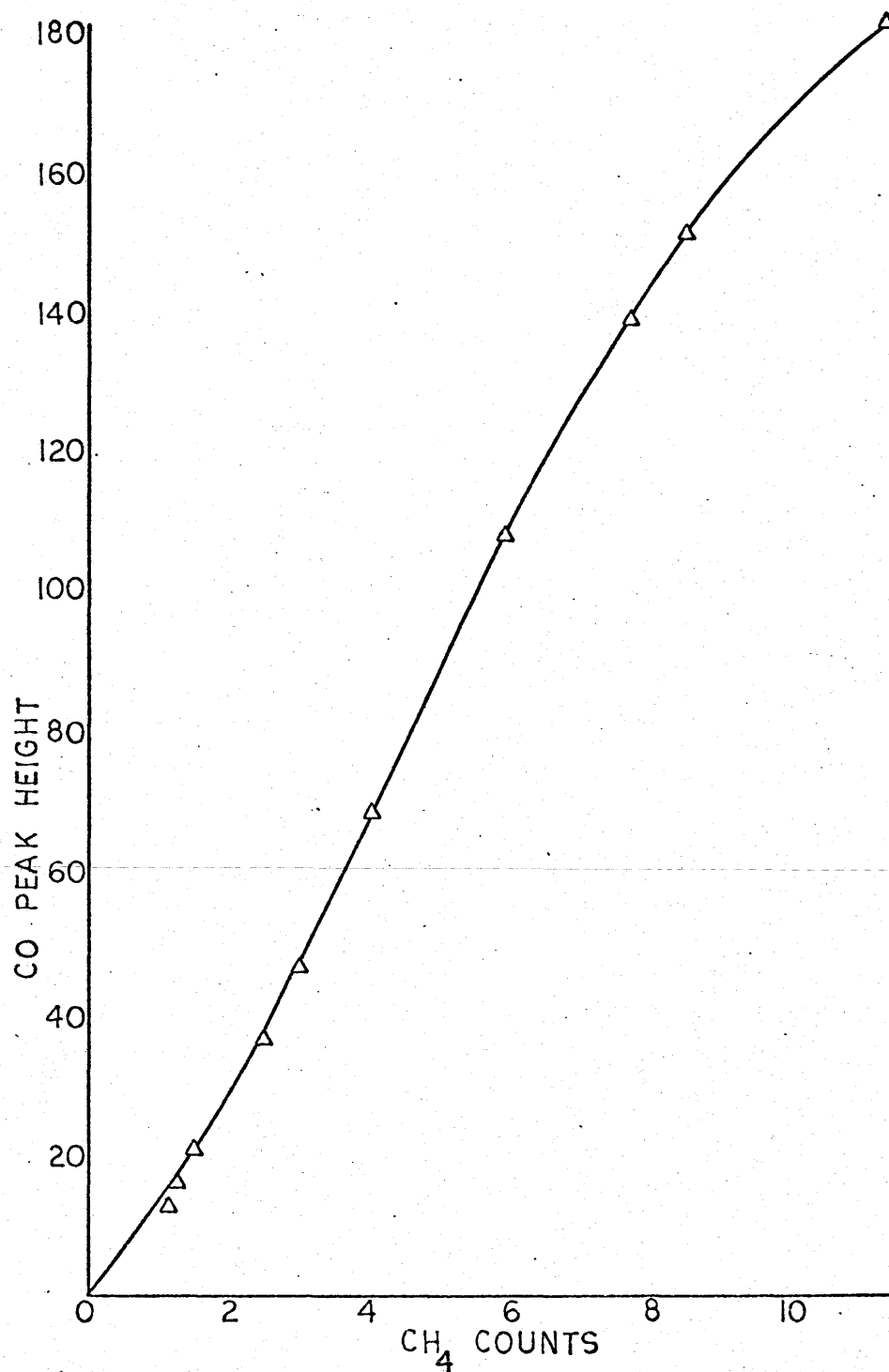


Fig. 7. Dilutions of CH<sub>4</sub>-spiked CO standard. The linear response of the flame ionization detector to CH<sub>4</sub> allows the linearity of instrument response to CO to be estimated.

TABLE 5. Comparison of Commercially Prepared Gas Standards Held in High Pressure Steel or Aluminum Cylinders

Standard	Labelled Concentration	Concentration Relative to 1 <sup>st</sup>	Difference
CO			
S1	2.67	2.67	-
A1	2.0	2.13	+6.5%
S2	10.8	10.78	-0.002%
S3	1.10	1.53	+39.0%
S4	7.7	8.18	+4.1%
S5	9.95	10.19	+2.4%
H <sub>2</sub>			
LG1	11.8	11.8	-
A2	1.5	2.61	+74.0%
S6	18.7	28.59	+53.0%
S7	18.0	11.8	-34.0%
S8	4.5	7.15	+59.0%
CH <sub>4</sub>			
M1	9.96	9.96	-
A3	5.3	5.15	+2.8%

M - Matheson, Inc., S - Scott Environmental Technology, Inc., and A - Airco, Inc. LG was a standard obtained from Dr. Louis I. Gordon, of Oregon State University. With one exception, the CO standards were consistent with the labelled concentration. Methane concentrations in cylinders from 2 suppliers also showed good agreement. Atmospheric measurements of methane concentrations were also consistent with the labelled cylinder contents.

Commercially prepared H<sub>2</sub> standards showed large inconsistencies. A standard was blended in the laboratory by diluting a microsyringe volume of pure H<sub>2</sub> in a large volume of purified air; the volume-to-volume ratios predicted a concentration of about 0.9 ppmv H<sub>2</sub>. This 0.9 standard was then compared to a commercially prepared cylinder labelled 1.5 ppm. Using 0.9 as a guide, the commercial standard actually showed a H<sub>2</sub> concentration of about 2.78 ppmv. The 0.9 standard was analyzed by Dr. Gordon, who reported a value approximately 0.91 ppmv (Figure 8). The 2.78 commercial standard was compared to a calibration curve generated with Hastings mass flow meters, and also

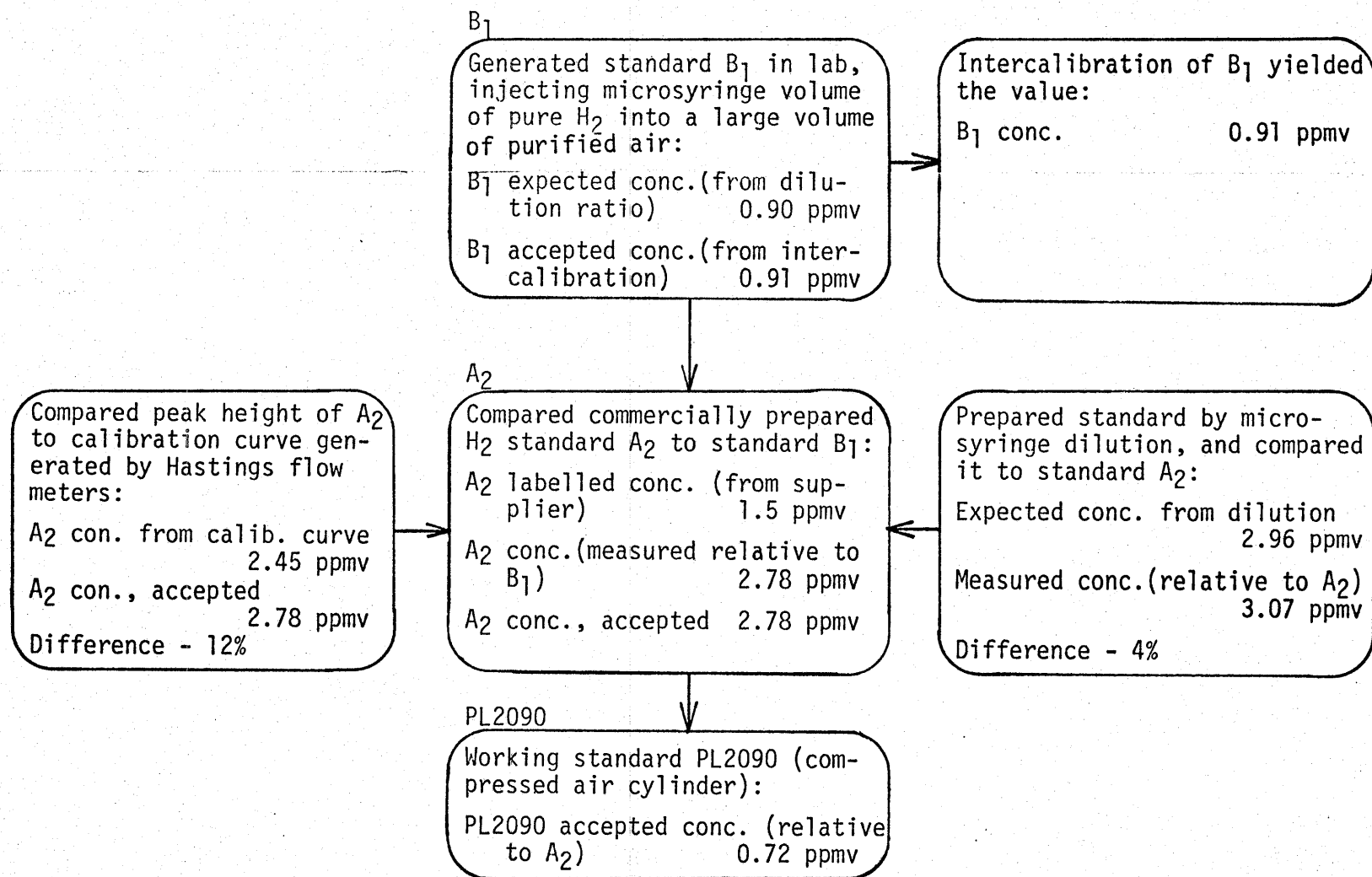


Fig. 8. Techniques used for the calibration of a working standard for H<sub>2</sub>.

to another standard prepared by microsyringe dilutions. Both techniques gave results in agreement with our accepted value of 2.78 ppmv.

The contents of a compressed air cylinder (PL2090) were analyzed as 0.72 ppmv, and this cylinder was used as a working standard for routine sample calibration.

The atmospheric values obtained at the CEPEX site and during Cruise 79-G-6 were based on the calibration scheme described above. Hydrogen concentration in marine air in the Central Pacific averaged about 0.40 ppmv; a concentration somewhat lower than reported in other regions by *Schmidt* [1978] (0.55 to 0.58 ppmv) and by *Herr and Barger* [1978], who found an average of about 0.65 ppmv. These differences may be due to real variation in atmospheric hydrogen concentration when measured at different times and locations, or to disagreement in calibration. Trace gas standards, including hydrogen, may show drift in concentration due to wall reactions (in the cylinder), or may reflect the methods used in preparation. Relying on manufacturer's claims of cylinder contents can lead to serious error. Standards prepared by microsyringe dilution or blending with mass flow meters are more prone to error than those produced in a well designed static gas dilution system. Further intercalibration with other workers should help resolve the discrepancies in reported air concentrations.

Since concentrations obtained during 79-G-6 were consistent with two independent calibration techniques (microsyringe dilution and mass flow blending), the resultant atmospheric levels for hydrogen will be used pending further calibration.

#### Microbiological Techniques

Microbiological measurements were performed by F. Azam of the Scripps Institution of Oceanography. Bacterial numbers were determined in seawater samples by staining with acridine orange, and counting under an epi-fluorescent microscope.

Aliquots of tritium-labelled thymidine were added to seawater samples. These samples were incubated, then filtered to collect the



bacterial cells. The amount of tritium-labelled thymidine taken up by these cells gives an indication of the relative bacterial activity in the sample.

## CHAPTER III

## FIELD WORK AT CEPEX

Measurements

The earliest field measurements of these gases were made during July and August, 1978, at the CEPEX site in Saanich Inlet, B.C., Canada. The study of trace gases at this location offered unique advantages. Most studies on dissolved trace gases have been made in either the natural environment, where temporal or spatial variations may obscure cause and effect relationships, or in laboratory scale experiments where important factors governing trace gas cycles (i.e. horizontal and vertical mixing, zooplankton) may be reduced or absent. *Menzel and Case* [1977] described the need for a third alternate — the mid-scale, controlled environment. The CEPEX program offered the opportunity to conduct such mid-scale experiments under circumstances where the history of the water parcel was known, horizontal advection was greatly reduced, and the biology and chemistry of the water was relatively well determined.

The CEPEX Site

Saanich Inlet, the site of the CEPEX experiments, has been the subject of considerable study, and has been described by several workers [*Herlinveaux*, 1962; *Nissenbaum et al.*, 1972; *Gucluer and Gross*, 1964 ; *Lilley et al.*, 1979]. A shallow sill partially blocks the entrance to the inlet, hindering the exchange of deeper waters. During some parts of the year, deeper waters go anoxic. They were anoxic during July-August 1978, from a depth of about 150 m to the bottom.

The CEPEX site was near the mouth of the inlet, directly under the approach pattern for the Victoria, B.C. airport. The containers were deployed in about 60 m of water. Samples were analyzed at the CEPEX shore facilities located at the Institute of Ocean Science (Canadian Department of Fisheries and the Environment), about 20 minutes by boat

from the CEPEX site. The CEPEX enclosures or "bags" have been described by *Menzel and Case* [1977]. They consist of large, flexible polyethylene containers 10 m in diameter by 26 m deep. The bags are brought up through the water column, capturing the water as they rise. Each is then attached to a large flotation ring held in place by anchors on the floor of the inlet. Waters of the inlet are somewhat stratified and the deployment does not capture exactly reproducible sections of the water column. A bag that fills early and deep will hold denser, more nutrient-rich water; then, as it comes to the surface, it may push away the lighter surface waters. Sometimes the bags are not yet completely filled when they are attached to the flotation rings; then excess surface waters must be pumped in, but this did not happen during 1978.

The CEPEX experiments were principally concerned with food web studies. The program provided routine measurements of nutrients, light, salinity, oxygen, temperature, chlorophyll, productivity, phytoplankton, zooplankton, and bacteria. This program provided an ideal base for mid-scale measurements of dissolved trace gases.

#### Sampling Methods

Water samples were collected in 5-liter Niskin bottles. These bottles were lowered by hand on a polypropylene rope kept taut by a plastic-coated hydroweight. The extent of hydrogen contamination from these bottles was measured by placing the Niskins in a 100-liter closed container of seawater. After several hours of contact, the hydrogen content of the water in the container showed an increase from 1.9 to 2.3 nanomole/liter (nM). The volume of the CEPEX containers was orders of magnitude greater than the volume of this test, and total contact time while actually sampling was shorter (generally 1 min or less). This sampling technique did not act as a significant source of H<sub>2</sub> contamination.

Early experiments at CEPEX revealed an increase of CO concentration in samples transferred to clear glass containers. This effect was seen for deep as well as shallow water samples. Table 6 compares samples collected and analyzed in clear glass bottles to those where light was excluded during handling and analysis.

TABLE 6. CO Sampling in Clear and Dark Bottles

Depth of Sample (m)	CO Concentration (nM)		Weather
	light bottle	dark bottle	
surface	3.62	3.70	rain
surface	0.67	0.45	overcast
35	2.09	1.12	sunny
108	2.10	1.03	sunny
3175*	0.76	0.02	sunny

\* - not taken at the CEPEX site

In routine sampling, the water was quickly transferred to dark all-glass 2-liter containers. The glass containers were then carried to the shore facility for analysis.

#### Atmospheric Measurements

Concentrations of these gases in the atmosphere at the CEPEX laboratory site were determined frequently. Daily averages are shown in Figure 9. The "saturation factor,"  $\Omega$ , provides a useful comparison between atmospheric and dissolved concentrations.

$$\Omega_i = C_i^{\text{obs}} / \beta_i \rho_i \quad (9)$$

where  $C_i^{\text{obs}}$  = the concentration of gas i as actually measured  
 $\beta_i$  = Bunsen solubility coefficient  
 $\rho_i$  = gas concentration in air

Saturation factors were calculated using the temperature and salinity of the water sample, and the following average concentrations ( $\rho_i$ ) in air:

$H_2$  - 0.56 ppmv  
CO - 0.19 ppmv  
 $CH_4$  - 1.55 ppmv

The air samples measured at the laboratory site occasionally showed large variations in CO content (.1 - .2 ppmv) on sampling intervals of less than 15 minutes. This may be a reflection of

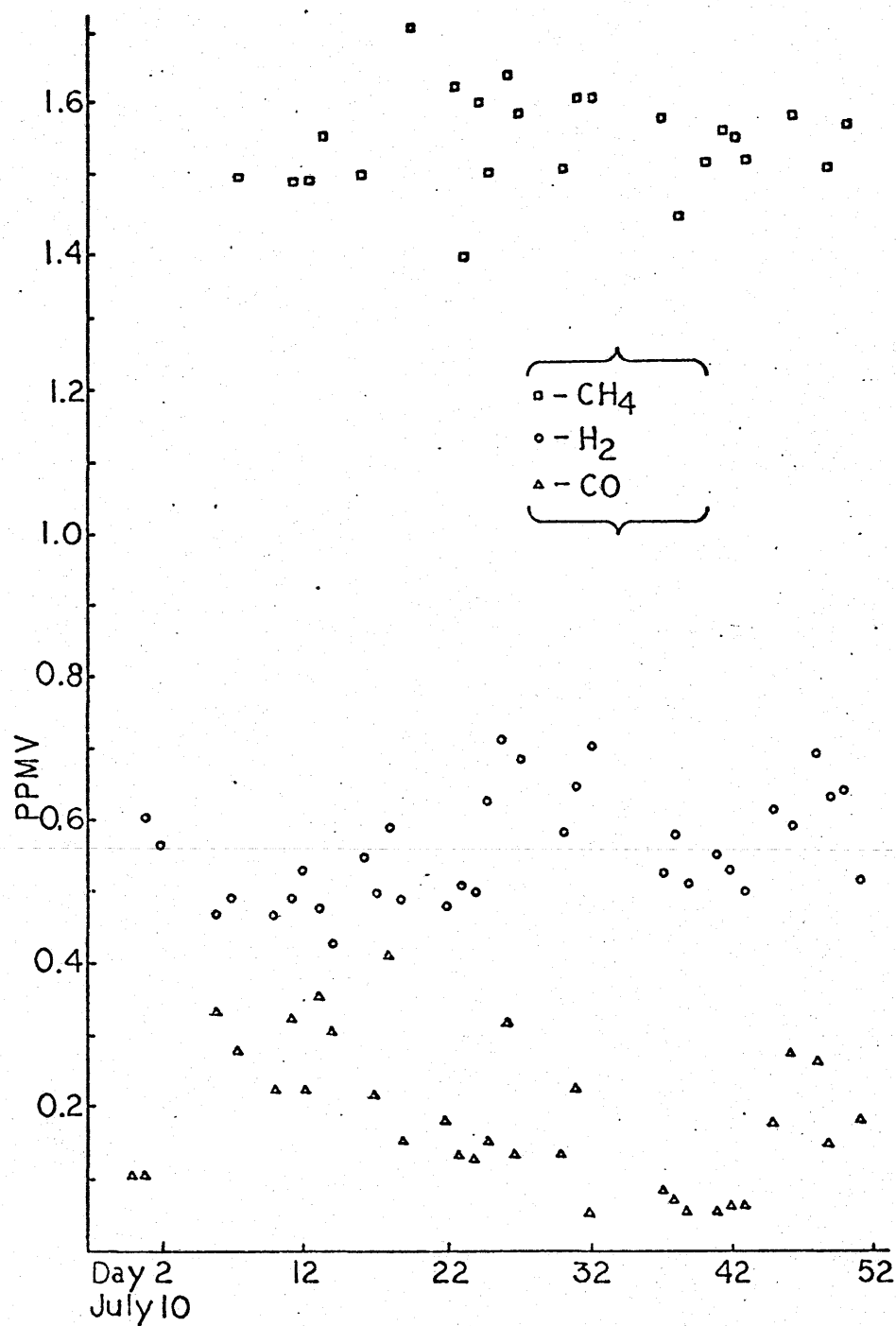


Fig. 9. Average daily atmospheric concentration of  $\text{H}_2$ ,  $\text{CO}$ , and  $\text{CH}_4$  at the CEPEX site (1978).

varying wind direction and/or anthropogenic inputs from aircraft, automobile exhaust, etc. The CEPEX enclosures were about 1 km offshore and less subject to these short-term fluctuations.

#### Water Measurements

CEPEX was designed primarily as a biological experiment. Three enclosures or "bags" were deployed during this experiment. In two of these bags physical and chemical manipulations were performed on a regular basis to examine the response of the food chain to differences in nutrient content, reduction in light levels, and artificial mixing processes. In one of these, Bag 3, only nutrient additions (nitrate and phosphate) were made after deployment. In Bag 4, the one most frequently sampled for trace gases, no physical or chemical manipulations were performed for the duration of the trace gas experiment.

After the deployment on Day 1 (July 9, 1978) a distribution pattern of  $H_2$ ,  $CO$ , and  $CH_4$  was observed in Bag 4, which underwent gradual changes in the following 6 weeks. Figure 10, from data taken on Day 12 (July 20, 1978) shows an early profile in Bag 4. All three gases are highly supersaturated relative to atmospheric concentrations.  $CO$  is highest near or at the surface. A  $CH_4$  maximum is seen at about 8 m while  $H_2$  shows lower concentrations there. These trends persisted in Bag 4 throughout the experiment.

Figure 11a shows  $H_2$ ,  $CO$ , and  $CH_4$  profiles in Bag 4 taken about 1 week later (Day 18). Highest  $CH_4$  concentrations are an order of magnitude greater than those for  $H_2$  and  $CO$ . Data on bacterial numbers and activity (provided by F. Azam) and  $O_2$  concentration are shown in Figure 11b. These bacterial measurements did not distinguish between aerobic and anaerobic forms. Although bacterial cell counts and thymidine uptake by bacteria show little correlation in these samples, highest cell counts are found at the depth of the  $CH_4$  maximum. Oxygen is present throughout the water column, although concentrations are somewhat lower at deeper depths. These profiles indicate that if anaerobic bacteria cause the observed  $CH_4$  maximum by production and

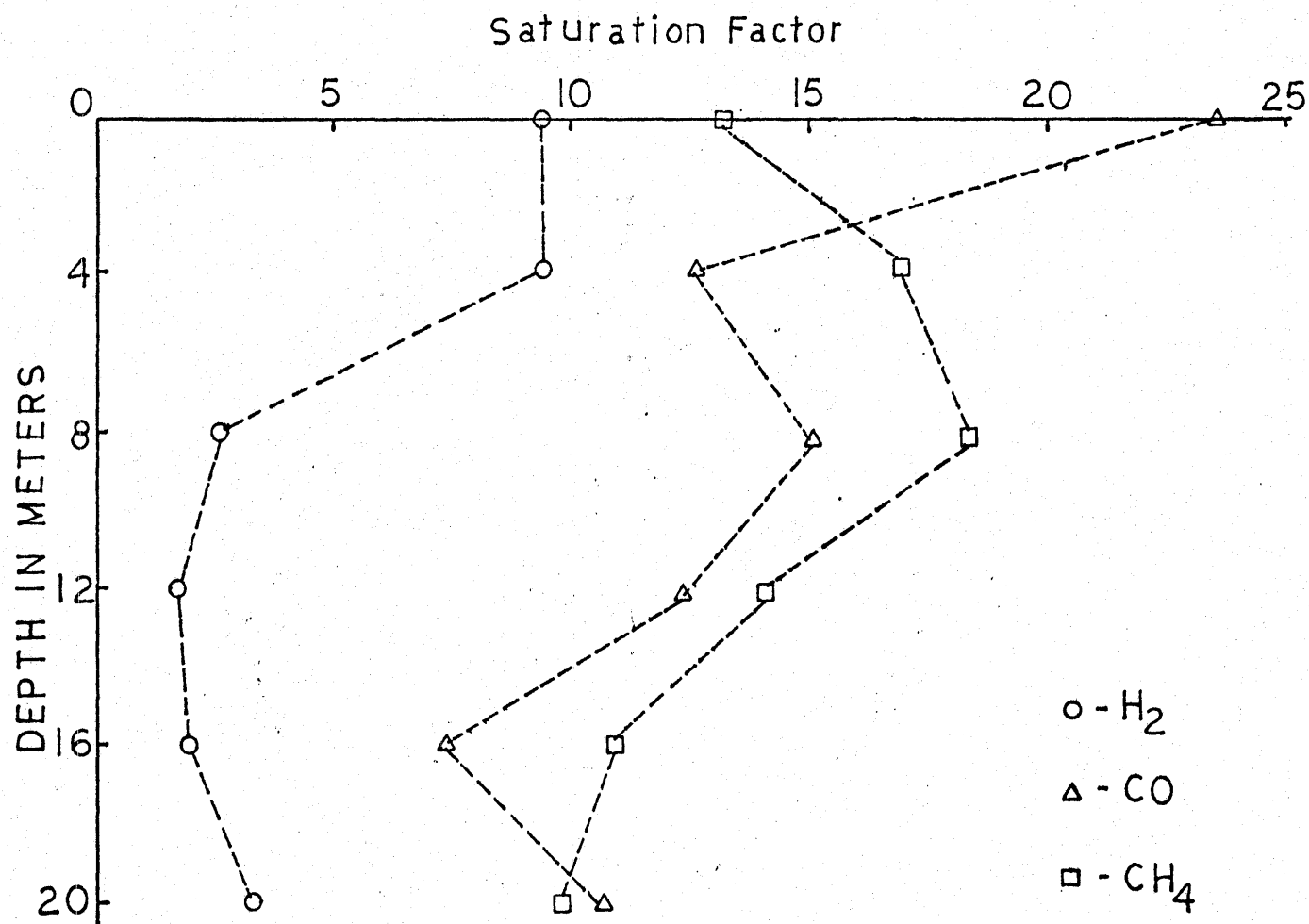


Fig. 10. Vertical profiles of gases in Bag 4 at 11 AM on Day 12 (July 20, 1978). Saturation factors are calculated using the following atmospheric concentrations:  $H_2$  - 0.56,  $CO$  - 0.19, and  $CH_4$  - 1.55 ppmv.

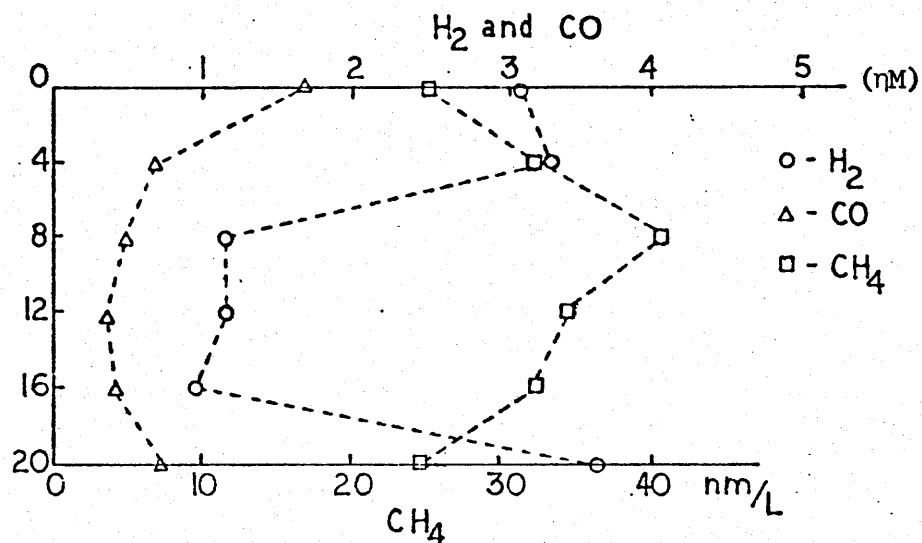


Fig. 11a. Dissolved gases in Bag 4 on Day 18 (July 26, 1978). CO was unusually low on this day, which was very dark and overcast.

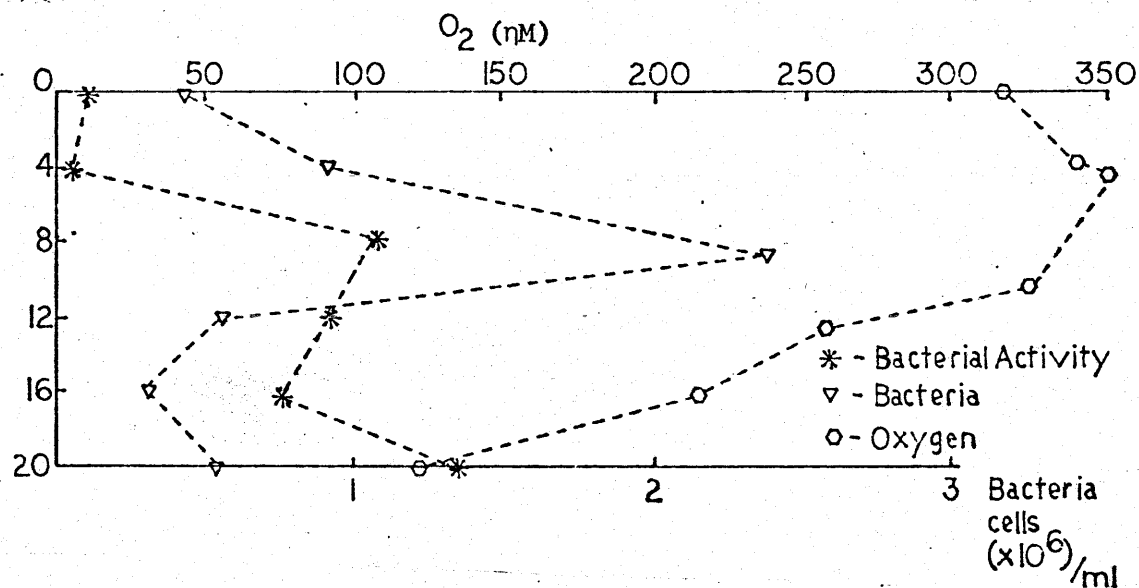


Fig. 11b. Dissolved  $O_2$ , bacteria numbers, and bacterial activity in Bag 4 on Day 18 (July 26, 1978). Bacterial activity (uptake of labelled thymidine) is plotted on a relative scale.



release of the gas, then they accomplish this in water containing significant amounts of dissolved  $O_2$ .

The gradual depletion of nutrients from the surface layer in Bag 4 is illustrated by the trend in silica concentration (Figure 12). As the experiment progressed, chlorophyll concentrations decreased in the upper half of the bag. During the same period, the depth of the chlorophyll maximum moved lower down into the water column (Figure 13). This deepening may reflect both the decline in total numbers and the sinking of phytoplankton cells out of the upper layer.

Paralleling this is a decline in the concentration of  $H_2$  at the surface after Day 12 (July 20), and a subsequent rise of  $H_2$  concentration at the depth of 20 m. After Day 18 (July 26), until the termination of the experiment, all depths sampled in Bag 4 showed decreasing concentrations of dissolved  $H_2$  (Figure 14). Methane (Figure 15) showed less variability, with perhaps a slight rise in concentration at 20 m after Day 18 (July 26).

Bag 3, with nutrient additions, showed quite a different evolution. Figures 16a and 16b show  $CH_4$ ,  $H_2$ , and bacteria cell count profiles taken on Day 13 (July 21) and Day 45 (Aug. 22). The distribution on Day 13 is similar to that in Bag 4—a  $CH_4$  maximum and  $H_2$  minimum at 8 m. By Day 45 (Aug. 22)  $CH_4$  had risen dramatically at depths below 8 m, while  $H_2$  was low throughout the bag. Higher productivity, stimulated by nutrient additions, may play a role in methane production deeper in the bag. No relationship between  $CH_4$  and cell numbers is evident from the profiles. Overall, bacterial cell numbers were much higher on Day 45 than Day 13. Divers inspecting the outside of the enclosures (at a depth of about 24 m) observed significant accumulation of sediment in the narrow cone-shaped tips of the bags. The amount seen in Bag 3 was greater than that in Bag 4, perhaps reflecting nutrient additions in Bag 3. Although dissolved  $O_2$  was present in significant amounts in Bag 3 at 10 and 16 m depth, anoxic conditions could have developed deeper in the bag as the sediment layer accumulated.

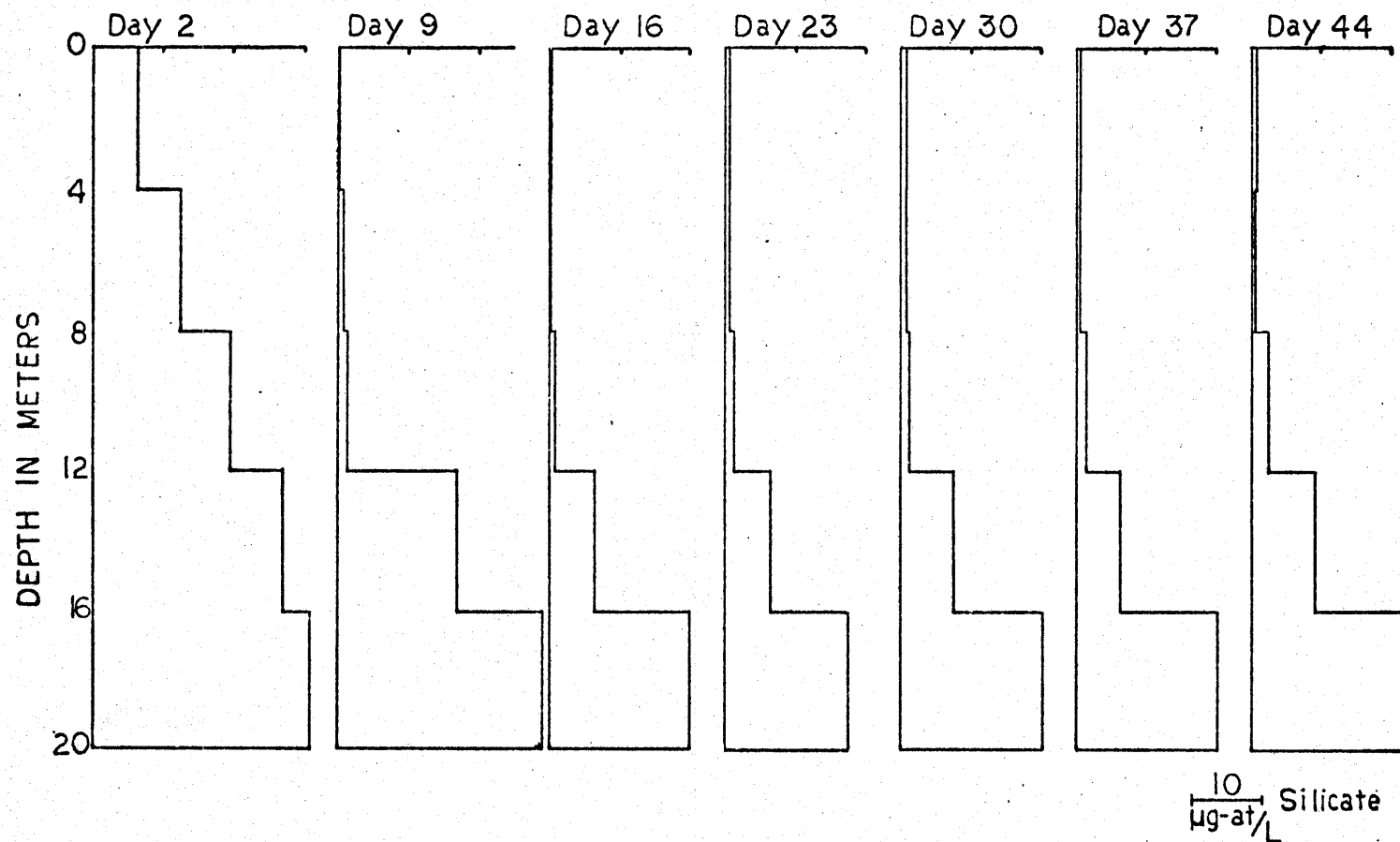


Fig. 12. Silicate profiles from Bag 4. Samples were collected by pump with the inlet drawn at a relatively constant rate thru the 4 m sampling interval.

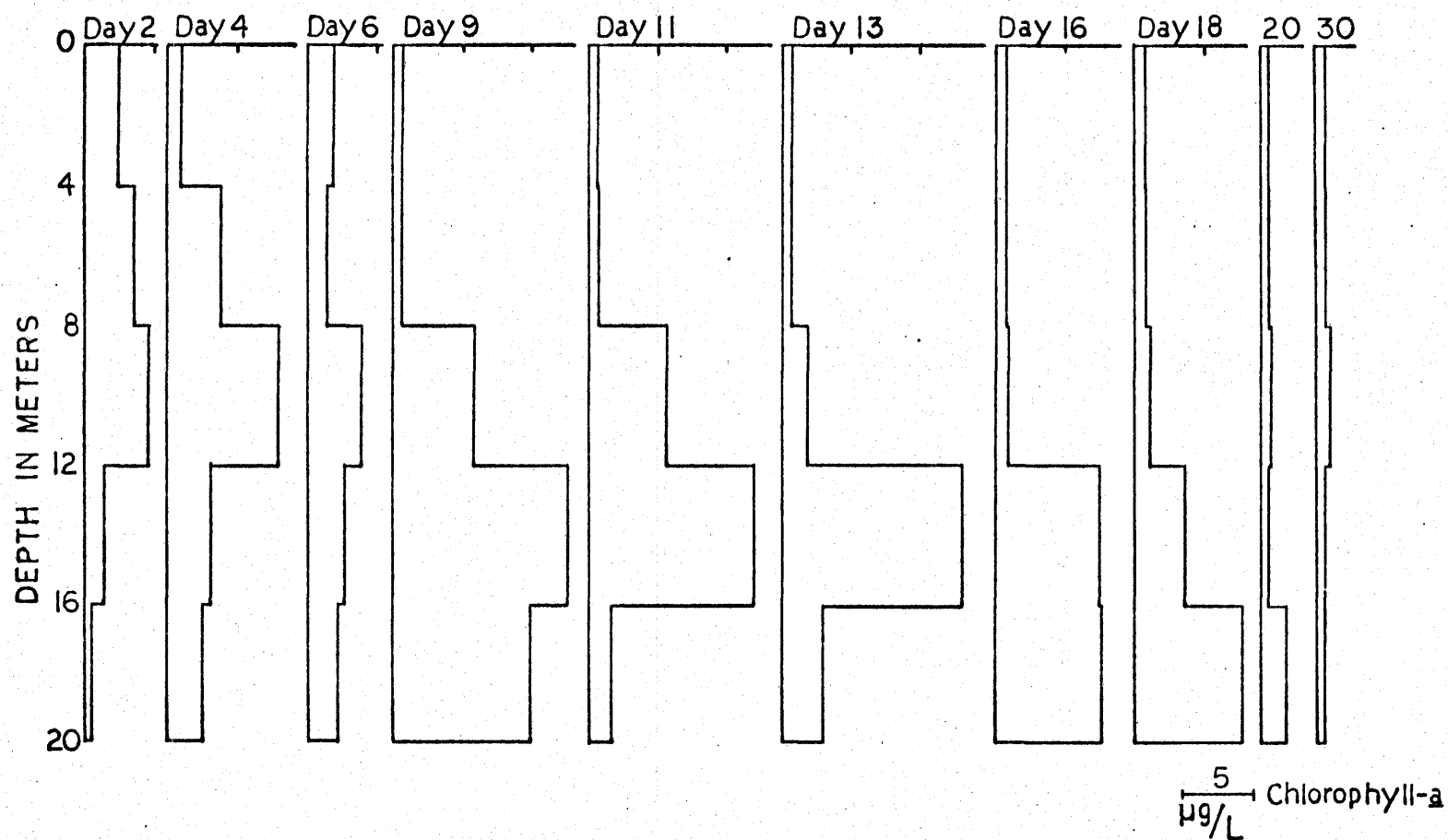


Fig. 13. Chlorophyll-a concentrations in Bag 4. Samples were collected and integrated over 4-m intervals.

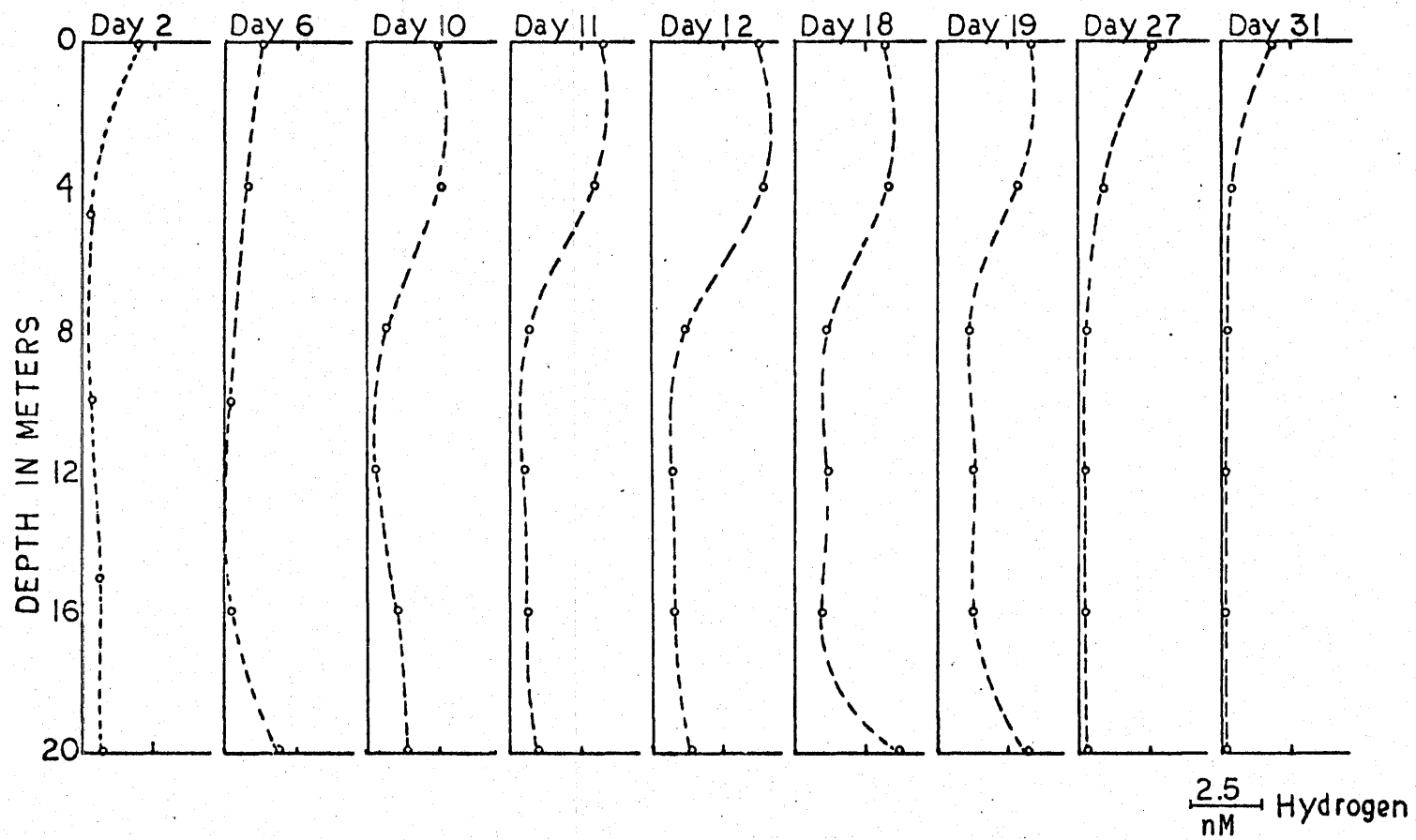


Fig. 14. Hydrogen concentrations in Bag 4.

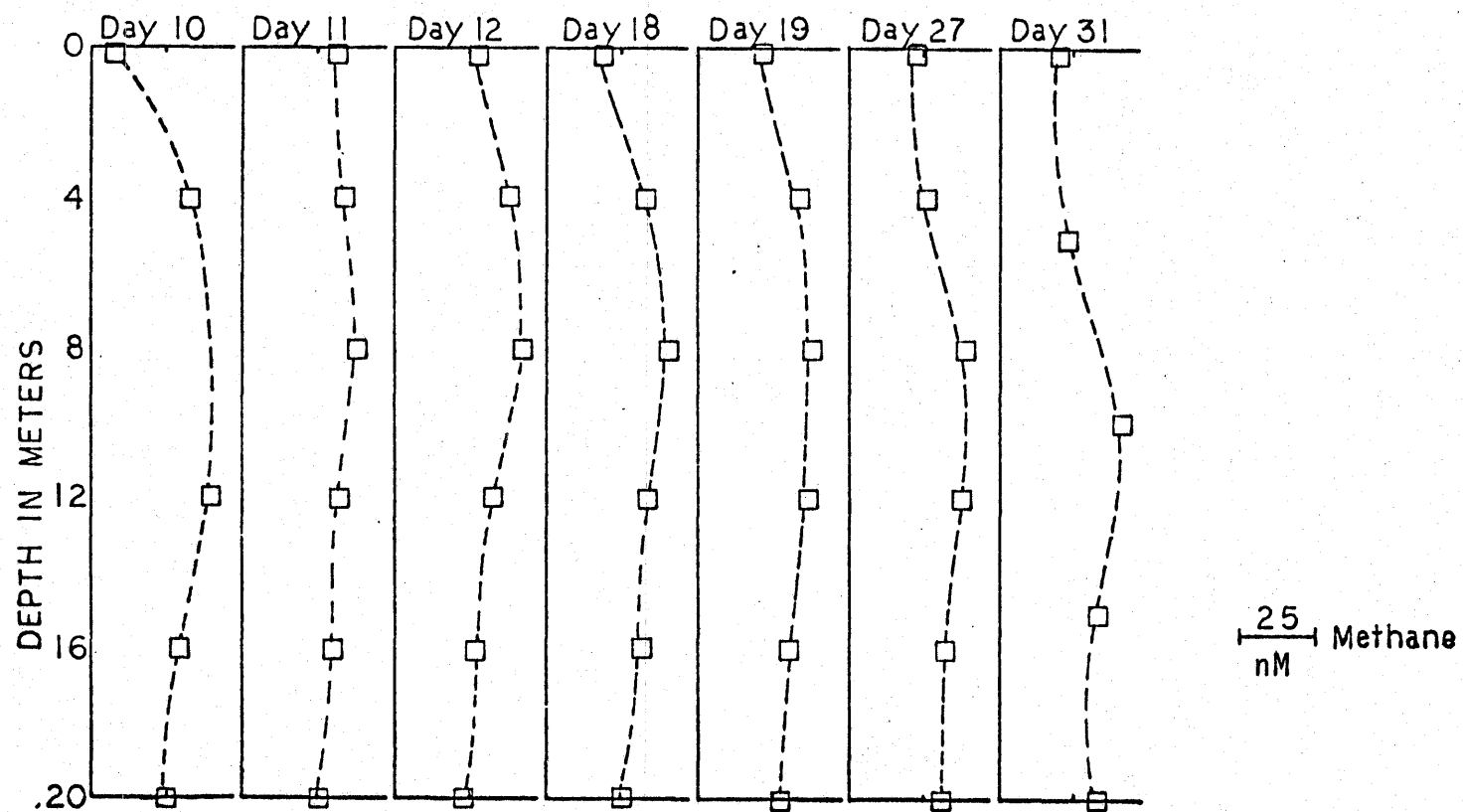


Fig. 15. Methane concentrations in Bag 4.

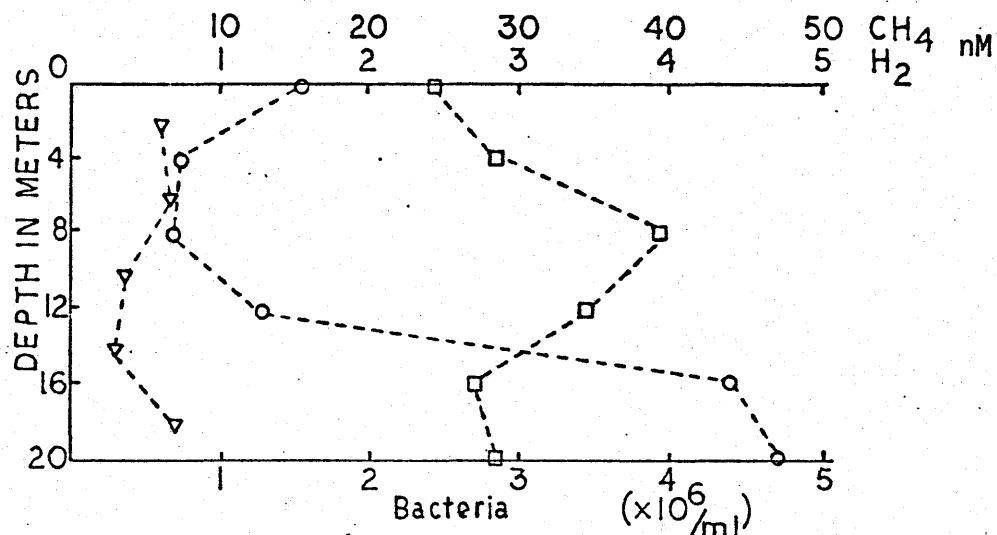


Fig. 16a. H<sub>2</sub>, CH<sub>4</sub>, and bacteria cell numbers in Bag 3 on Day 13.

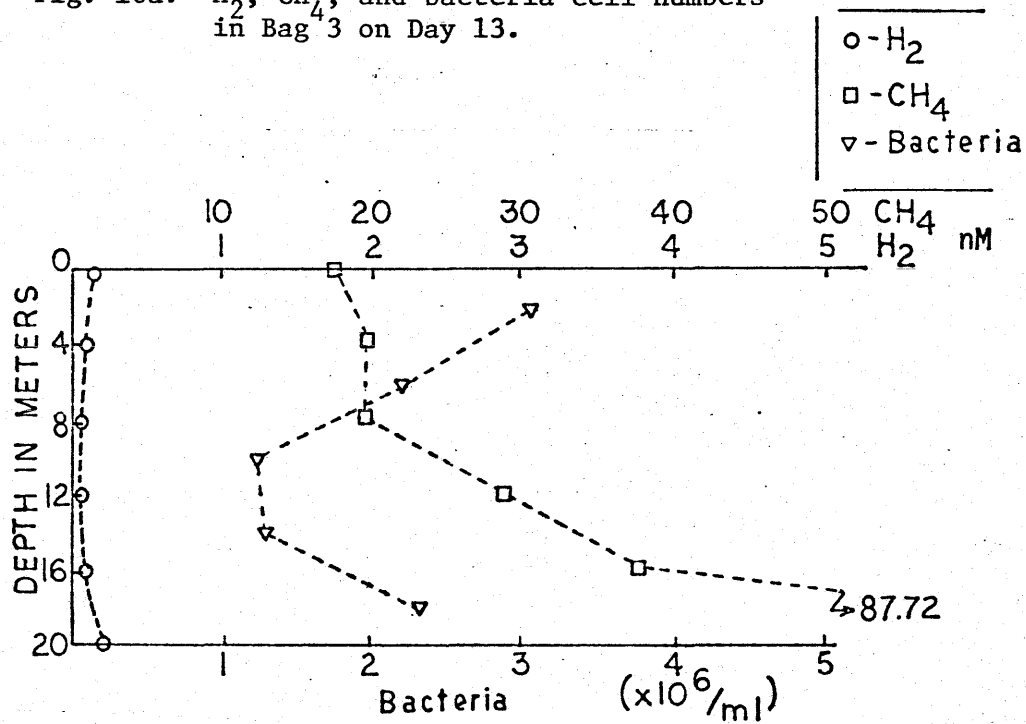


Fig. 16b. H<sub>2</sub>, CH<sub>4</sub>, and bacteria cell numbers in Bag 3 on Day 45.

Several hydrocasts were made outside the bags in Saanich Inlet. Figure 17 shows a shallow cast on Day 16 (July 24). At this time, at similar depths, dissolved  $\text{CH}_4$ ,  $\text{H}_2$ , and  $\text{CO}$  concentrations were higher outside than inside Bag 4. A hydrocast extending to near the bottom (approximately 170 m) of the inlet is shown in Table 7. A slight maximum is seen for  $\text{CH}_4$  and nitrite ( $\text{NO}_2^-$ ), and a minimum of  $\text{O}_2$  is seen at 50 m. Both  $\text{H}_2$  and  $\text{CO}$  are undersaturated below 25 m. Methane shows extremely high concentrations at or below 150 m.

Lilley *et al.* [unpublished manuscript, 1979] have made measurements of dissolved  $\text{H}_2$  and  $\text{CH}_4$  in Saanich Inlet and report similar distributions.

Diurnal studies were carried out both inside the bags and in the surface water of Saanich Inlet. Figure 18 shows the increase of  $\text{CO}$  and  $\text{H}_2$  during the daylight hours in Bag 4.  $\text{CO}$  reached maximum concentration at about 3 PM. The increase in  $\text{H}_2$  is smaller and the maximum lags somewhat behind that of  $\text{CO}$ . Both gases showed decreases after

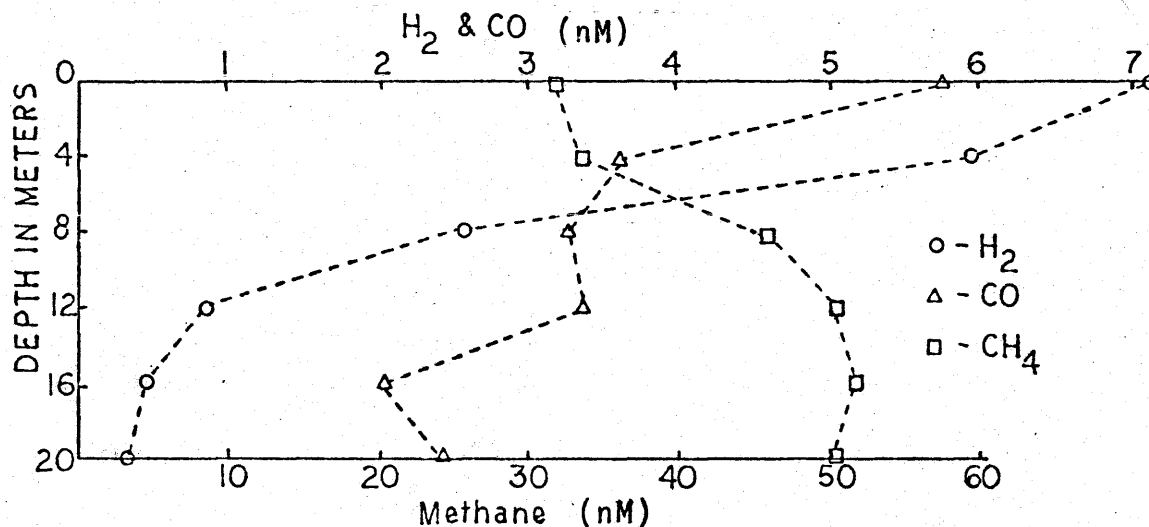


Fig. 17. Shallow hydrocast in Saanich Inlet on Day 16.

TABLE 7. Vertical Cast, Saanich Inlet 16 Aug. (Day 39)

Depth (m)	H <sub>2</sub> (nM)	CO (nM)	CH <sub>4</sub> (nM)	O <sub>2</sub> (μM)	Relative Bacterial Activity	Chlorophyll (μg/l)	PO <sub>4</sub> <sup>-3</sup> (μM)	NO <sub>2</sub> <sup>-</sup> (μM)
0	16.07	7.81	26.8	332	5.8	2.65	0.70	0.08
25	0.36	0.04	42.7	166	0.6	0.44	1.91	0.39
50	0.13	0.04	50.4	114	1.0	0.17	2.41	0.51
75	0.13	0.04	41.6	124	0.3	0.24	2.50	0.36
125	0.09	0.04	33.1	67	1.2	0.84	3.31	0.27
150	0.13	0.04	250.9	8	0.4	0.24	4.92	0.13
165	0.27	0.22	1292.0	nil*	0.2	0.17	4.93	0.12

\* Absence of O<sub>2</sub> at this level was established on 14 Aug. by the Coastal Zone Oceanography Program at the Institute of Ocean Sciences. The above profile was at the same location as their Station 5.

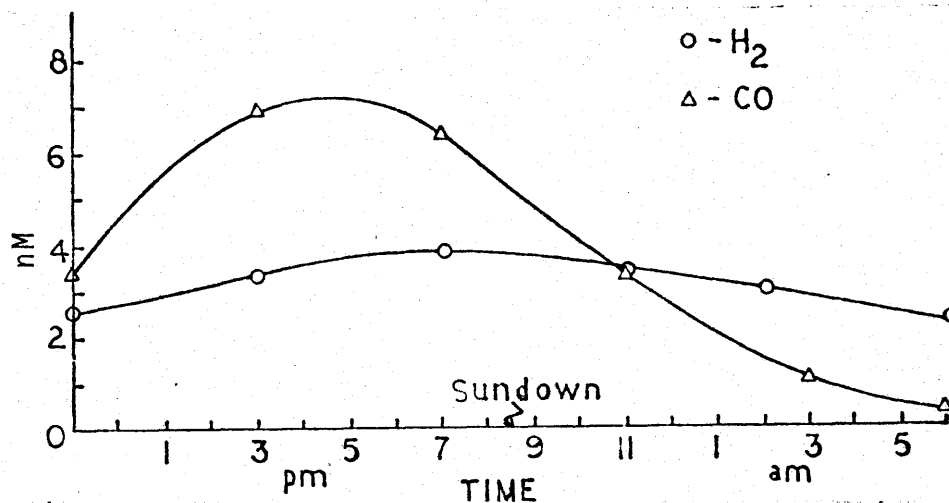


Fig. 18. Diurnal variations in H<sub>2</sub> and CO in surface waters of Bag 4 on Days 32 and 33.



sunset. Similar studies were undertaken in Saanich Inlet (Table 8). CO concentrations showed dramatic decreases at night, while the values for  $H_2$  and  $CH_4$  showed no apparent trend. This may reflect surface patchiness and the difficulty of returning to the same water mass for repetitive sampling.

TABLE 8. Open Water Surface Values

Date		$H_2$ (nM)	CO (nM)	$CH_4$ (nM)
Aug. 20	1 PM	2.19	5.09	25.98
	8 PM	6.70	6.07	26.07
Aug. 21	1 AM	2.90	1.21	23.39
	5 AM	5.89	0.89	27.99
(sunset at 8:30 PM)				

Surface water measurements made by *Lilley et al.* [unpublished manuscript, 1979] also reflect the variability of  $H_2$  and  $CH_4$  near the surface in Saanich Inlet.

#### Incubation Experiments

Surface water taken from the bags was placed in clear and in darkened sample bottles, and incubated in a water bath at 19°C. Table 9a shows the rapid build-up of CO in clear bottles exposed to sunlight. These increases also occurred in illuminated samples that had been poisoned with a 500  $\mu$ M sodium azide solution. CO concentrations showed some increases when samples poisoned with both sodium azide and mercuric chloride were illuminated.

No systematic changes in  $H_2$  or  $CH_4$  were observed over the time span of these illumination experiments. However,  $H_2$  and CO concentrations decreased in water samples held in dark containers for an extended period of time (Table 9b).

TABLE 9a. Effect of Light on Trace Gases in Seawater

Sample	CO (nM)	H <sub>2</sub> (nM)	CH <sub>4</sub> (nM)
No poisons added			
Sample A (120 min incubation in sun)			
initial*	1.44 $\pm$ .16	0.28 $\pm$ .02	30.01 $\pm$ 1.30
final	3.35	0.31	30.13
Sample B (90 min incubation)			
sun	4.73	4.82	10.36
shade	0.58	4.15	11.83
Sample C (90 min incubation)			
sun	4.51	0.67	12.63
shade	0.63	0.80	12.37
Sample D (90 min incubation)			
sun	4.82	0.85	12.54
shade	0.71	0.89	11.16
(Samples B, C, D were all the same water, but were given various initial gas concentrations; not measured.)			
* - 4 replicates analyzed			
Poisoned with sodium azide (500 $\mu$ M)			
Sample A (120 min incubation in sun)			
initial (duplicates)	1.52	0.27	29.20
	1.74	0.22	30.45
final	3.62	0.27	29.02
Poisoned with sodium azide and mercuric chloride (500 $\mu$ M NaN <sub>3</sub> , 0.25 $\mu$ M HgCl <sub>2</sub> )			
Sample E† (360 min incubation in sun)			
no poison	3.96	0.41	
poisoned	4.83	0.41	
† - water from open ocean, Central Pacific			

TABLE 9b. Effect of Dark Storage on Trace Gas Concentration  
in Seawater

Time Held	CO (nM)	H <sub>2</sub> (nM)	CH <sub>4</sub> (nM)
No poisons added			
Sample F			
3 hrs	1.43	0.22	15.98
	1.29	0.18	16.43
21 hrs	0.04	0.13	16.34
	0.04	0.09	16.03
93 hrs	0.22	0	18.62
	0.22	0.09	19.06
Sample G			
0 hrs	0.49	1.92	22.37
24 hrs	0	0.45	22.05
Poisoned with sodium azide (500 $\mu$ M)			
Sample G			
0 hrs	0.45	1.79	21.70
	0.49	1.79	18.48
24 hrs	0.04	0.45	20.58
Poisoned with sodium azide and mercuric chloride (500 $\mu$ M NaN <sub>3</sub> , 0.5 $\mu$ M HgCl <sub>2</sub> )			
Sample E			
6 hrs no poison	3.45	0.39	
poisoned	3.38	0.40	

The initial rate of decrease of CO was more rapid than that of hydrogen. After 93 hrs., a slight rise in CH<sub>4</sub> was observed. A decrease in H<sub>2</sub> and CO can also be observed in samples poisoned with sodium azide and held in dark containers. No significant change in CH<sub>4</sub> was noted. Laboratory cultures of phytoplankton were isolated and placed in gas-tight sample bottles. Trace gas concentrations were monitored over an 8-day period. In all samples, dark bottles showed significantly lower concentrations of CO than bottles illuminated with artificial light. H<sub>2</sub> content was slightly higher in the illuminated bottles (Figure 19). The darkened phytoplankton cultures did not show the rapid decline to near zero levels of H<sub>2</sub> and CO that was observed with natural seawater samples from the CEPEX containers. After about 1 week, CH<sub>4</sub> concentrations increased rapidly in both light and dark bottles.

#### Discussion-CEPEX

Properties are distributed within a water mass in response to advection, diffusion, production, consumption, and boundary effects. The CEPEX containers offer some unique departures from the normal array of such influences. Advection in the bags may be considered negligible since the bag walls isolate the system from currents of the inlet. Diffusion too was almost entirely negligible. The walls of the bag preclude mixing with outside waters and damp-out any large-scale vertical eddies so that vertical diffusion was very slow. These rates were measured using spikes of tritium-labeled water, or dye, injected at mid-depths in the bag (Bacon and Mercier, unpublished). Measurements of the tracer distributions during the following weeks allowed estimates to be made of the vertical eddy diffusion coefficients ( $K_z$ ). In Bag 4, Bacon and Mercier found the value of  $K_z$  to decrease with depth, according to the relation  $K_z = 0.093 \exp -z/7.8$  where  $z$  is in meters and  $K_z$  in  $\text{cm}^2 \text{sec}^{-1}$ . This relation gives coefficients of  $0.007 \text{ cm}^2 \text{sec}^{-1}$  at the bottom to  $0.09 \text{ cm}^2 \text{sec}^{-1}$  at the top. These are much lower than values typical for upper ocean layers - so low, in fact, that the vertical eddy diffusion process was

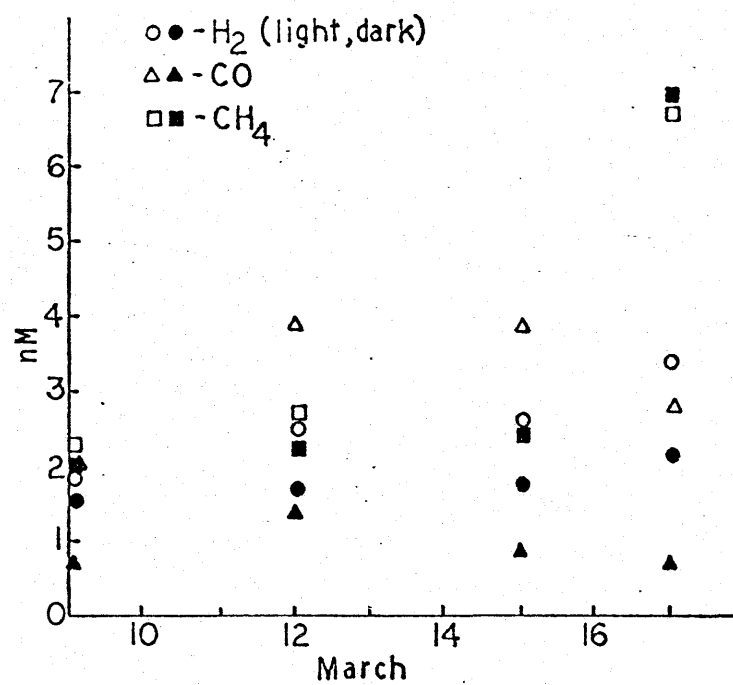


Fig. 19. Incubations of phytoplankton cultures in light and dark bottles (March, 1979).

practically negligible. One may estimate the effective scale length ( $L$ ) of vertical diffusion processes over various mixing intervals ( $t$ ) from the approximate relation  $L^2 = K_z t$ . This relation suggests an effective mixing length per day of 90 cm at the top of the container and 25 cm near the bottom, or 5 m and 1.5 m, respectively, per month.

The flux of a gas across the air-sea interface can be modelled by

$$\text{Flux} = F = D_i (C_s - \beta_i \rho_i) / z \quad (10)$$

where:  $z$  - is the "stagnant film thickness" - (inversely proportional to wind and wave motion) (cm)

$D_i$  - is the molecular diffusion coefficient of the gas ( $\text{cm}^2 \text{sec}^{-1}$ )

$(C_s - \beta_i \rho_i)$  - is the difference in aqueous concentration of dissolved gas between the bulk of the water ( $C_s$ ) and the air-water interface ( $\beta_i \rho_i$ ) (moles/ $\text{cm}^3$ )

The quantity  $D_i/z$  is known as the "piston velocity," and indicates the speed by which a gas can cross the air-sea interface.

Exchange across the air-water boundary would be severely constrained by the lack of vertical mixing. Any gas exchanged across the air-water interface would be replenished or redistributed very slowly into the adjacent water levels. Boundary layer impedance must further slow the exchange. The non-turbulent regime should permit rather thick "stagnant-film" layers of perhaps 200  $\mu\text{m}$  or more. These would imply gas-exchange piston velocities of no more than 90 cm/day. Since the gases studied were generally supersaturated ( $\Omega > 1$ ), the boundary effect would be one of gas escape. The expected result would be a decline in dissolved gas concentration toward the interface with a scale length of a meter or so; such a decline was not observed. The typical  $\text{H}_2$  and CO profiles showed the opposite: highest levels at the surface. Therefore, gas exchange and vertical mixing were not major factors controlling the distribution of gases, but must have contributed to the daily loss of excess gas from the upper meter or so.

Gases might exchange through container walls since polyethylene is somewhat permeable. The double walls were reported [Menzel and Case, 1977] to be 12 mil thick (0.030 cm). The assumption that

molecular diffusion of gases through the polyethylene film was as fast as through water yields a piston velocity of 50 cm/day for lateral penetration. Since the container diameter is 9.5 m and chemical differences inside and out are not great, any such exchange must have had only a slight influence on the contents of the container.

These considerations lead to an interesting conclusion: that redistribution processes inside the bag are almost totally ineffective on dissolved substances. Materials in solution will pretty much stay where they are produced until they are consumed.

Obviously some things do move inside the container. Phytoplankton, detritus, and fecal pellets are settling through the waters. Zooplankton and small fish may move through the waters in all directions. Their effect on the distribution processes must be considered. Still, few areas in the ocean can be found which have such an unambiguous set of circumstances for studying chemical distributions.

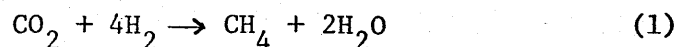
The surface concentrations of all three of these gases and of chlorophyll were higher at the CEPEX site, both inside and outside the containers, than surface concentrations observed in normal open ocean waters. But no direct simple relationship is evident among the various parameters measured here. Each gas has its own distribution pattern which seems to reflect the complexity of biological, chemical, and physical factors operating in the water column. Microorganisms must be important, but neither total cell counts nor activity (by thymidine uptake) showed a clear relation to observed gas distributions. Quite possibly the actions of specific bacterial types dominate the gas distributions, but their role may be completely obscured within the gross level measurements which were performed.

Of the three gases,  $\text{CH}_4$  was clearly the most abundant and, over the course of the experiment, showed the most stable distribution pattern. The persistent mid-depth maximum in the container was shallower than the analogous maxima in outside waters of the inlet or in the open ocean; but as in open waters, the maximum seemed to sit on the pycnocline. At the very low diffusivities in the bag, the  $\text{CH}_4$  gradient shown in Figure 11a (p. 45) implies an upward flux of about

$0.10 \text{ nmol cm}^{-2} \text{ day}^{-1}$ ; by comparison  $25 \text{ nmol/cm}^2$  represents the standing crop of  $\text{CH}_4$  in the upper 8 m. A production mechanism may be acting to replenish the diffusive losses, but it need not be too vigorous. The upward diffusive flux could be entirely accommodated by loss through the interface. If a quiet water, boundary-layer thickness of  $200 \text{ }\mu\text{m}$  and a concentration of  $2 \text{ nM}$  at the interface is assumed, the flux through the boundary film can be about  $1.5 \text{ nmol cm}^{-2} \text{ day}^{-1}$  when the surface water  $\text{CH}_4$  concentration is  $25 \text{ nM}$ . Some sink is required to absorb diffusive transfer below the  $\text{CH}_4$  maximum, but the eddy diffusion coefficients are even less there than above the maximum, so loss rates must be correspondingly less, perhaps by a factor of 2.

*Mechalas* [1974] and others have suggested that rapid oxidation of  $\text{CH}_4$  must occur in oxic waters. Conceivably both production and consumption reactions could be occurring simultaneously; the CEPEX measurements could not show such a rapid turnover of the  $\text{CH}_4$  inventory and no other evidence is available to indicate that such a turnover occurs.

Many of the microbial studies recorded in the literature link  $\text{CH}_4$  production with  $\text{H}_2$  consumption. The association of the  $\text{CH}_4$  maximum and the  $\text{H}_2$  minimum might be taken as evidence of such linkage here. But the bacterially mediated reaction



requires four  $\text{H}_2$  molecules for each  $\text{CH}_4$  produced. The  $15 \text{ nM}$   $\text{CH}_4$  maximum cannot be derived from the small  $\text{H}_2$  deficits observed here, unless some more complex  $\text{H}_2$  supply system is operating, unseen.

It seems equally possible that the only  $\text{CH}_4$  consumption mechanisms were those necessary to accommodate the slight downward diffusive flux; then we have there a very stable methane reservoir, with a residence time of perhaps a year. The initial  $\text{CH}_4$  content of the captured inlet waters might account for the profiles observed in Bag 4 if we take into account the artificial upwelling associated with the launching.



Methane production clearly did occur in oxic waters of Bags 2 and 3. On Aug. 22 (Day 45) the  $\text{CH}_4$  content in the deepest samples from Bag 3 went to high values. Nothing in the available data would explain these values directly. Possibly the increase was an indirect result of anoxic conditions occurring in waters below the depth of sampling. Nutrient additions to Bag 3 did raise the productivity in the bag substantially, and although sludge was pumped out of the cone each time nutrients were added, the build-up of materials in the bottom of the cone may well have caused some anoxia and associated  $\text{CH}_4$  production. Even higher  $\text{CH}_4$  values were found at even shallower depths in Bag 2. No oxygen measurements were made on these waters.

The high  $\text{CH}_4$  values up around the 20 m depth level in Bags 2 and 3 might be explained by any of several mechanisms. Possibly eddy diffusion brought the  $\text{CH}_4$  up from the nadir of the bag; mixing processes might be more rapid in the cone-shaped portion because it is less well secured, and might be tossed in the passing currents. Or perhaps bubbles of  $\text{CH}_4$  form in the sludge, then rise slowly, dissolving in the supernatant waters. Methane bubbles do form in estuarine sediments at depths even greater than those in the bag. The observed distribution of dissolved  $\text{CH}_4$  requires that these bubbles dissolve completely at or below the 20 m depth, but such behavior is natural for small bubbles [Guinasso and Schink, 1973]. Eddy diffusion at the rates measured in the bags would normally not bring any significant amount of material up from 9 m below. But if  $\text{CH}_4$  bubbles are possible, it must also be recognized that dissolved  $\text{CH}_4$  concentrations — to form bubbles at that depth — must be 5 orders of magnitude greater than any we measured. Thus the observed traces may represent only the leading edge of a vast  $\text{CH}_4$  concentration below the zone of measurement.

Exchange of  $\text{H}_2$  out of the surface waters of Bag 4, to the atmosphere, must have been less than  $0.2 \text{ nmol cm}^{-2} \text{ day}^{-1}$ . Diffusive fluxes ranged about  $0.01 - 0.05 \text{ nmol/cm}^2 \text{ day}^{-1}$  downward. These were quite small compared to an inventory of  $2 \text{ nmol/cm}^2$  in the upper 8 m of water. Near the surface the  $\text{H}_2$  inventory doubled between July 14

and July 18 — an increase of  $0.3 \text{ nM day}^{-1}$ . From July 18 to 19 the increase was  $0.8 \text{ nM day}^{-1}$ . These changes in inventory substantially exceed the transport fluxes, again demonstrating that *in situ* production and consumption dominate.

The pattern of  $\text{H}_2$  distribution seems related to the biological activity (Figures 13 and 14, pp. 48, 49). High chlorophyll inventories are associated with high hydrogen inventories, although the  $\text{H}_2$  increase lags by a few days. The most notable feature of this relationship though is that the vertical distributions do not correspond. The surplus of  $\text{H}_2$  occurs largely in the upper 8 m while the chlorophyll maximum is near the bottom, and sinking. The elevated levels of dissolved  $\text{H}_2$  and the elevated levels of chlorophyll may be related, but the nature of the relationship is not obvious and probably not all the  $\text{H}_2$  inventory is so related. A number of hypotheses might be offered to explain the  $\text{H}_2$  production; these need not be mutually exclusive:

- a. hydrogen is a by-product of certain photosynthetic reactions within reducing micro-environments;
- b. hydrogen production is permitted in the presence of oxygen and nitrogen when CO is also present;
- c. hydrogen is produced within micro-environments as a fermentation or decomposition process;
- d. hydrogen may be produced at these concentration levels even in oxic waters, reactions may involve extra-cellular organic material;
- e. hydrogen is produced in the guts of zooplankton and released in some pattern dependent upon their feeding or excretion habits.

The disparity between the depth of the chlorophyll and the rise in  $\text{H}_2$  concentrations strongly suggests a zooplankton source. Grazing near the bottom of the bag may be followed by upward migration and subsequent release of  $\text{H}_2$  in the upper waters. However, this is probably not the only source. The zooplankton migration does not seem a good explanation for the daily cycling of  $\text{H}_2$  shown in Figure 18 (p. 53). This cycle was observed after the chlorophyll bloom had disappeared completely from the zone of measurements. The fact that

the maximum in the cycle occurred in surface water during daylight hours certainly does not point towards a zooplankton source. Light-induced production of  $H_2$  appears to be occurring in the uppermost layers, perhaps supported by the presence of CO. This mechanism could cause the initial and final depth profiles of  $H_2$ , but its influence would be obscured in the open sea where vertical mixing and exchange with the atmosphere should push the surface maximum of  $H_2$  downward in the water column. Distinct, sometimes rapid, decreases in dissolved  $H_2$  from one profile to the next at all levels in the container indicate that  $H_2$  is being consumed in oxic as well as anoxic environments. The *in vitro* experiments suggest that these consumption reactions occur with rate constants of  $\sim 0.05 \text{ hr}^{-1}$ .

The reducing conditions that produced high  $CH_4$  content in the deep Inlet waters caused no marked increase in  $H_2$  or CO. The high  $CH_4$  values in Bags 2 and 3 were associated with quite low values of dissolved  $H_2$ .

Carbon monoxide appears to be as active as  $H_2$ , but marches to a different drummer. Like the other gases, CO was high in these rich coastal waters. However, CO levels did not drop as the bloom subsided. This persistence was not the result of chemical stability or the absence of a CO consumption mechanism. On July 26 the CO inventory dropped by a factor of 4 from previous measurements. On July 27 it was up by 3x from the previous day. These striking rates of production and consumption were related to variations in the intensity of incident sunlight. It has already been established that CO levels are related to biological activity and to illumination levels [Seiler and Schmidt, 1974]. Purely photochemical reactions cannot be ruled out as an important source of CO; the relationship to overall productivity in water and the persistence of high CO levels after the bloom suggest photochemical reactions on dissolved organics may be the major component of the CO production, but involvement of the inorganic, carbonate system should also be considered.

The losses in CO observed from one profile to the next in the CEPEX containers clearly do not result from losses to the atmosphere.

*In vitro* CO consumption rates range in the neighborhood of  $0.1 \text{ hr}^{-1}$ , so CO should soon disappear without continuing production. Such production may exceed consumption only in illuminated waters. Probably several production methods are operating with different priorities under differing conditions.

## CHAPTER IV

## MEASUREMENTS IN OPEN OCEAN ENVIRONMENTS

Observations Made Aboard USNS Desteiguer

The analytical instruments and extractor were first tested at sea in March of 1979 aboard the *USNS Desteiguer* in the Eastern Tropical Pacific. Water samples on this cruise were obtained from 30-liter Niskin bottles. A metal rosette capable of supporting 12 of these bottles was used to raise and lower the Niskin samplers. The bottles could be tripped individually at depth by an electric signal sent by way of the supporting cable. A compilation of hydrocast data from this cruise is listed in the Appendix.

Unfortunately, the use of the rosette sampler created a serious problem in obtaining reliable measurements of dissolved hydrogen. In addition to the metal frame and instruments lowered with the rosette (nephelometer, STD, fluorometer), a sacrificial anode attached to the rosette was a potential source of contamination. The actual degree of contamination was variable, since the motion of the rosette in the water column prior to tripping a sample bottle could not be determined accurately. Several experiments were performed to measure the effect of the rosette sampler on  $H_2$  concentration in water samples. In one experiment, the rosette was held at about 10 m depth for several minutes. A sample bottle was then tripped and the unit returned to the deck. A Niskin lowered to 10 m on a stainless steel cable was tripped a short time later. The following results were obtained:

TABLE 10. Samples from 10 m

	$H_2$ (nM)	CO(nM)	$CH_4$ (nM)
Rosette	1.16	2.99	1.79
Niskin on wire	0.22	3.35	2.01

A significantly higher  $H_2$  concentration was seen in the sample obtained using the rosette.

In another experiment, three samples were taken by the rosette sampler at a depth of 100 m. The first was obtained while the rosette was descending into the water column. The second was taken while ascending. The final sample was taken after the rosette had been held at 100 m depth for 10 min. Again,  $H_2$  concentrations differed in the three samples.

TABLE 11. Samples from 100 m

Sample Position	$H_2$ (nM)
Descending	0.36
Ascending	0.49
Held for 10 min	0.67

The difference between descending and ascending samples may have been due to the position of the anode near the top of the rosette. The ascending sample contained water that had briefly passed over the anode, and perhaps been contaminated with  $H_2$  generated there.

In spite of these difficulties, several generalizations can be made using the cruise data:

- 1) Highest dissolved  $CH_4$  concentrations were found between 100 and 200 m depth, with values there about 2 times higher than those at the surface.
- 2) Hydrogen and CO were highest and most variable in the upper 200 m.
- 3) Hydrogen concentrations as measured were lower and more uniform at greater depths, especially at the earlier stations. In deep water, all 3 gases were generally undersaturated with respect to present atmospheric concentrations.
- 4) No maxima comparable to that for  $CH_4$  were consistently observed for  $H_2$  or CO.
- 5) The greater scatter in data on  $H_2$  concentration at Stations 7, 8, and 9 may be due to deterioration of the painted metal surfaces of the rosette, or other sources of contamination.

## Cruise 79-G-6

### Atmospheric Measurements

Further measurements of atmospheric and dissolved hydrogen and carbon monoxide were made during Cruise 79-G-6 in the Central Pacific. This cruise, aboard the *R/V Gyre*, began at Hawaii, crossed the equator to Papeete, Tahiti, moved eastward to the Marquesas Islands, and terminated in San Diego, California (see Figure 20). Atmospheric samples were taken frequently. Averages along sections of the cruise track are shown in Figure 20. Contrary to the gradients reported by *Herr and Barger* [1978] in the Atlantic, near-surface  $H_2$  measurements in the atmosphere were very uniform over long stretches of the cruise track. Carbon monoxide levels showed little fluctuation on a day-to-day basis, but did show lower values south of  $10^\circ N$ . Similar latitudinal gradients for CO are reported by *Seiler* [1974]. Higher and more variable concentrations of  $H_2$  and CO were observed on the approach to Papeete (Figure 21) and off the coast of Baja, California. The increase in CO concentration while approaching the North American coast was detected much farther offshore than any significant rise in  $H_2$ . CO concentrations in Papeete harbor and San Diego increased by an order of magnitude over average open ocean levels.

### Water Profiles

Typical profiles in the upper 200 m of the water column are shown in Figure 22. CO showed highest values in the top 50 m, often exceeding by 50 times the atmospheric equilibrium concentration.  $H_2$  concentrations averaged about 1.5 times atmospheric equilibrium in the upper 100 m. Maximum values for  $H_2$  were usually observed about 10 m below the surface. Full water column profiles are shown in Figure 23. In these hydrocasts, concentrations of dissolved  $H_2$  and CO varied most in near-surface regions. Below 1000 m, both gases were undersaturated with respect to present atmospheric levels of  $H_2$  and CO. Most deep Pacific  $H_2$  concentrations were lower than values reported in the Atlantic by *Herr and Barger* [1978].

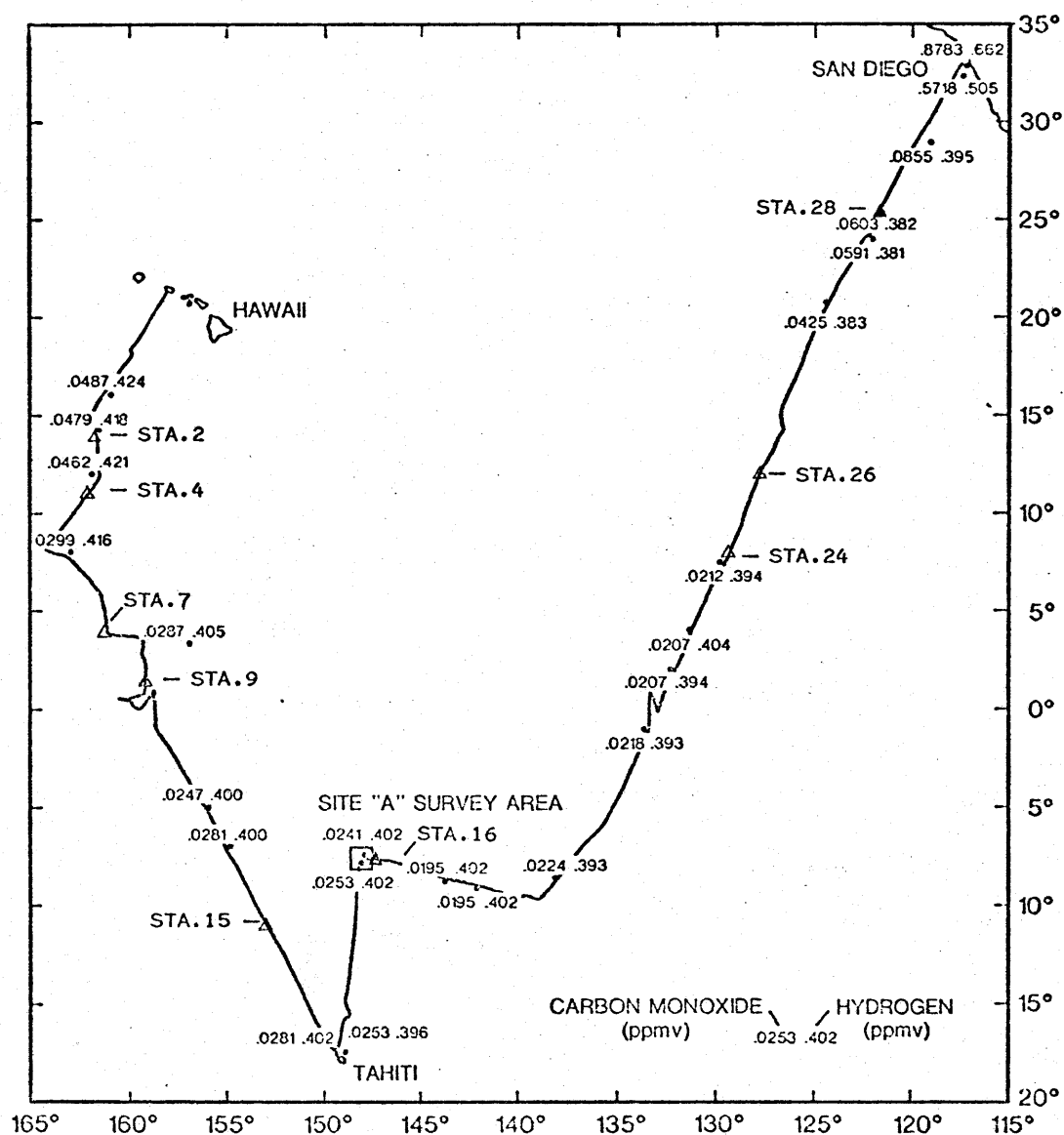


Fig. 20. Daily averages of atmospheric  $H_2$  and CO along cruise track 79-G-6.



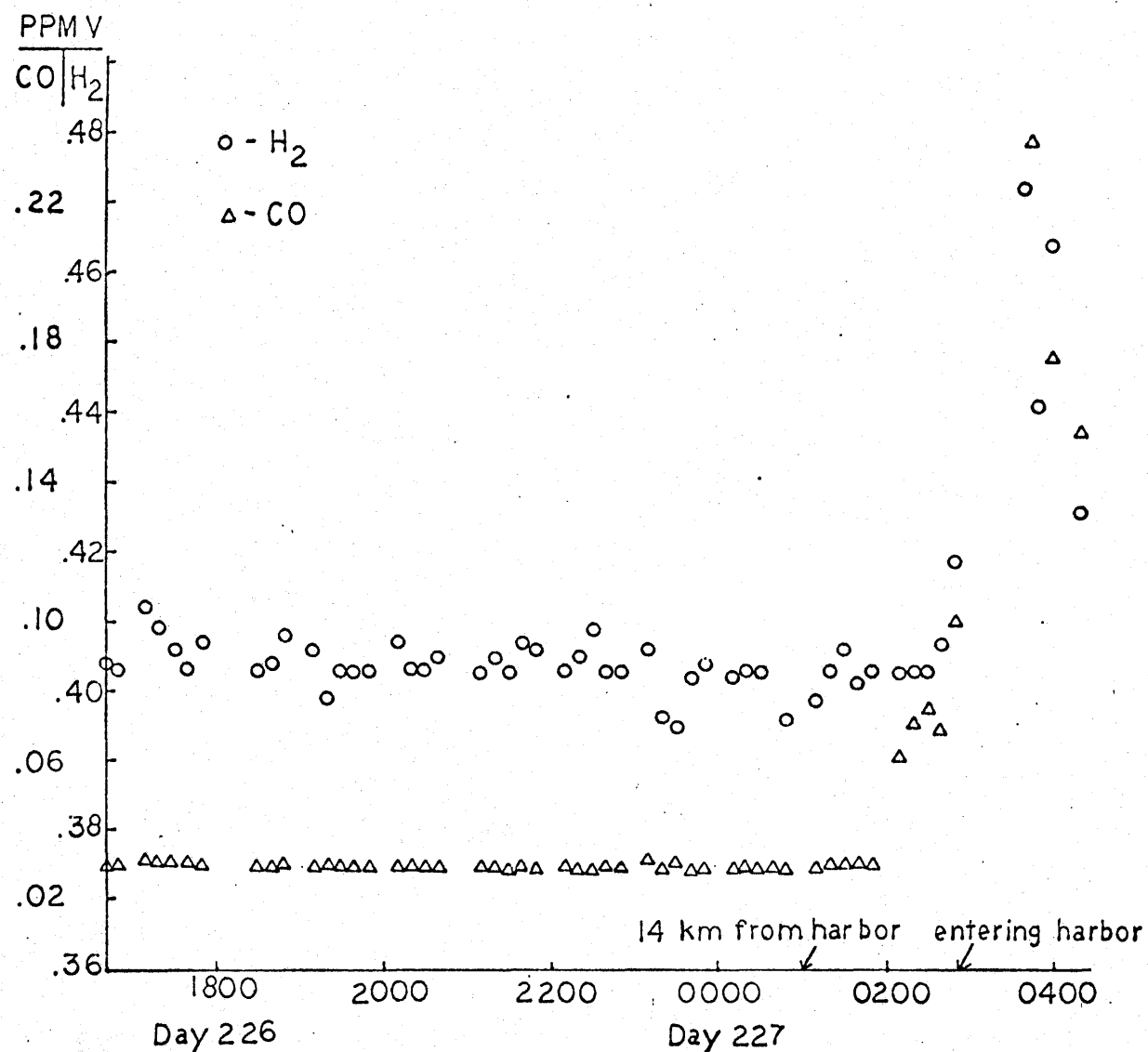


Fig. 21. Measurements of atmospheric  $H_2$  and CO while approaching Papeete, Tahiti, Day 226J 1979.

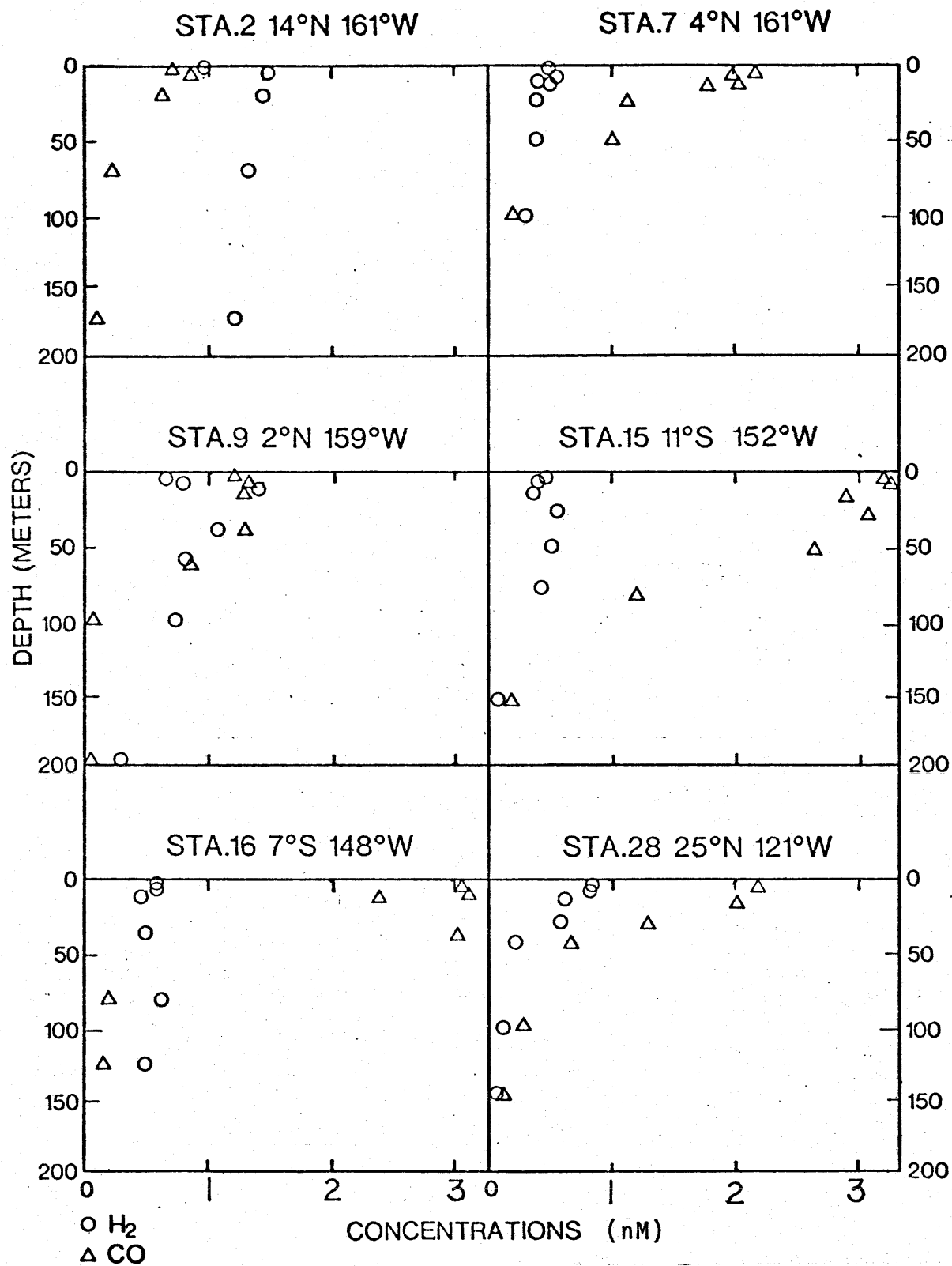


Fig. 22. Typical  $H_2$  and  $CO$  concentrations in the upper 200 m. Stations 2 and 9 occurred at night.

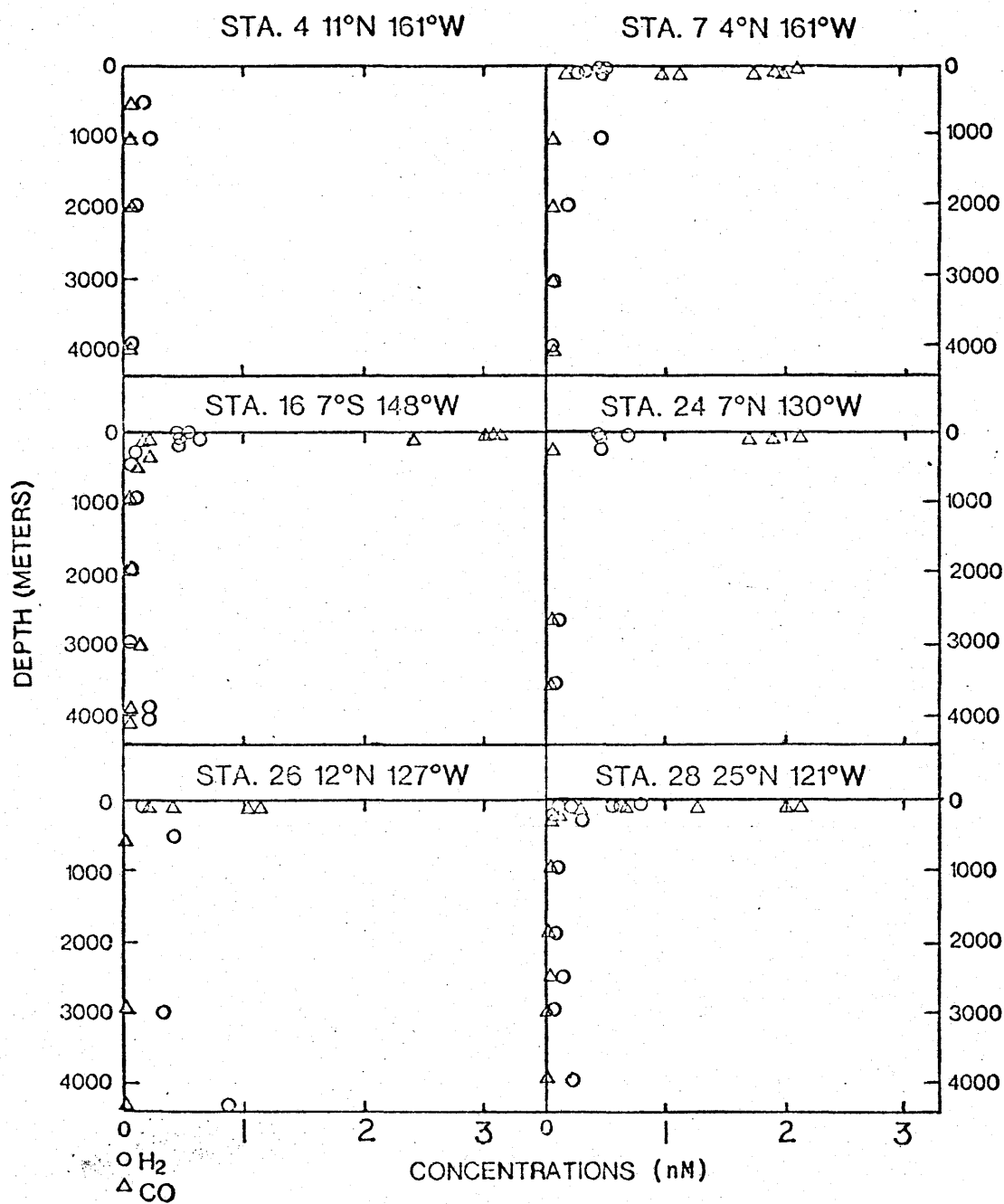


Fig. 23. H<sub>2</sub> and CO concentration profiles in full water column hydrocasts.

However, Stations 26 and 28, near the eastern end of the cruise, showed elevated concentrations of  $H_2$  in samples taken below 3000 m.

#### Underway Measurements

While underway between hydrostations, a continuous pumped stream of surface water was analyzed. Figure 24 shows CO concentration in water samples run at 10-minute intervals. The gradual decline in CO concentrations after sunset was paralleled by an increase in relative fluorescence in the water stream (P. Setser, personal communication, 1979). Dissolved  $H_2$  concentrations in surface water were relatively uniform for long intervals; no clear diurnal cycle was seen in the open ocean.

Contamination checks were run on the seawater stream after passing through the fish, pump, and hoses. A portion of seawater held in a large plastic barrel was pumped through the sampling system. Concentrations of  $H_2$  and CO in discrete samples drawn from the pumped stream were compared to samples drawn directly from the barrel. Table 12 compares concentrations of  $H_2$  and CO in the barrel to concentrations in the pumped water stream. In pumped water, a slight increase in  $H_2$  concentration was observed, while a larger increase in CO occurred. After pumping was halted, the water remaining in the barrel was sampled.

TABLE 12. Comparison of Direct and Pumped Samples

Type of Sample	$H_2$ (nM)	CO (nM)
From Barrel at Start	0.45	1.88
	0.40	2.23
Through Pump and Hose	0.40	3.34
	0.49	2.88
From Barrel at Termination of Pumping	0.45	2.28
From Barrel 30 Minutes after Termination	0.49	2.95

Thirty minutes after the pumping experiment was ended, higher CO concentrations were found in the barrel. The cause of this rise is unclear, but may be due to contamination from the container walls,

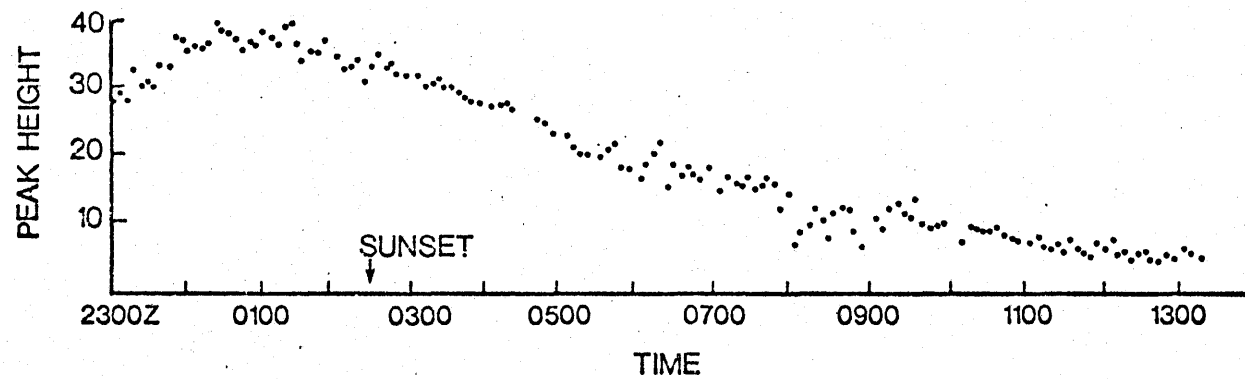


Fig. 24. Decrease of CO at sunset in surface water, Day 253J 1979.

or from the effect of sunlight on the water held in the barrel. The increased CO in pumped samples was probably due to the addition of this gas from the hose walls. The limited volume of seawater contained in the barrel prevented a thorough flushing of the hoses before samples were drawn. The seawater present in the hose at the start of the experiment had been in contact with the hose walls for a period of several hours. In continual sampling, it was assumed that the constant flushing of the hose reduced CO contamination to lower and more constant levels.

After passing through the pumping system, only a slight change in dissolved  $H_2$  concentration was observed.

While underway, discrete samples were routinely drawn from the pumped stream. These were compared to surface samples obtained in a plastic bucket thrown overboard and retrieved with a length of plastic rope. Water from the pumped stream came from a depth of about 2 to 3 m, while bucket samples skimmed seawater from the top 0 to 10 cm. In open ocean areas, little difference was seen between the  $H_2$  content of the two sample types (Table 13).

TABLE 13. Comparison of Two Types of Surface Samples

Day(1979)	Time	Position	Sample Type	$H_2$ (nM)	CO (nM)
250 J	0640Z	2°N 132°W	Stream	0.45	2.32
			Bucket	0.42	2.32
255 J	0140Z	12°N 127°W	Stream	0.42	2.92
			Bucket	0.34	2.48
255 J	0750Z	12°N 127°W	Stream	0.33	2.33
			Bucket	0.33	1.55

As the ship approached the coastal waters off California, the differences between the bucket and pumped samples increased (Table 14). This indicated the presence of a sharp gradient in  $H_2$  and CO concentrations within the upper few meters of surface water in near-shore locations.

TABLE 14. Comparison of Near-Shore Surface Samples

Day(1979)	Time	Position	Sample	H <sub>2</sub> (nM)	CO(nM)
258 J	1600Z	25°N 121°W	Stream	2.47	0.94
			Bucket	0.39	0.61
	1700Z	25°N 121°W	Stream	1.24	1.41
			Bucket	0.42	0.85
260 J	1600Z	(Approach- ing San	Stream	13.40	5.14
			Bucket	10.28	5.21
	1730Z	Diego)	Stream	14.07	5.20
			Bucket	8.38	5.53

A run of continual measurements of H<sub>2</sub> and CO in the water stream is shown in Figures 25 and 26. Variability of H<sub>2</sub> and CO concentrations increased dramatically in surface waters as the ship approached the coast of California. Large fluctuations were seen in samples injected 10 minutes apart. Data on fluorescence and water temperature also revealed high spatial heterogeneity in the surface water of this region.

#### Discussion - Cruise 79-G-6

##### Air Measurements

Measurements of the concentration of H<sub>2</sub> in the atmosphere made during 79-G-6 indicate that the distribution of this gas in near-surface air is quite uniform over this region of the Central Pacific. Away from land areas, little short-term variability was found among the hundreds of air samples taken along the cruise track. A gradient of about 0.02 ppmv was observed between Hawaii and Tahiti. Lowest concentrations occurred between the Marquesas Islands and San Diego. These small gradients may reflect spatial and temporal variability in tropospheric H<sub>2</sub> concentration in these regions. It is also possible that a slight drift in the H<sub>2</sub> concentration of air held in the standard cylinders could cause the variation in reported values.

*Schmidt* [1978] studied the variation in atmospheric concentration of H<sub>2</sub>. Very high concentrations were reported in the North Sea,

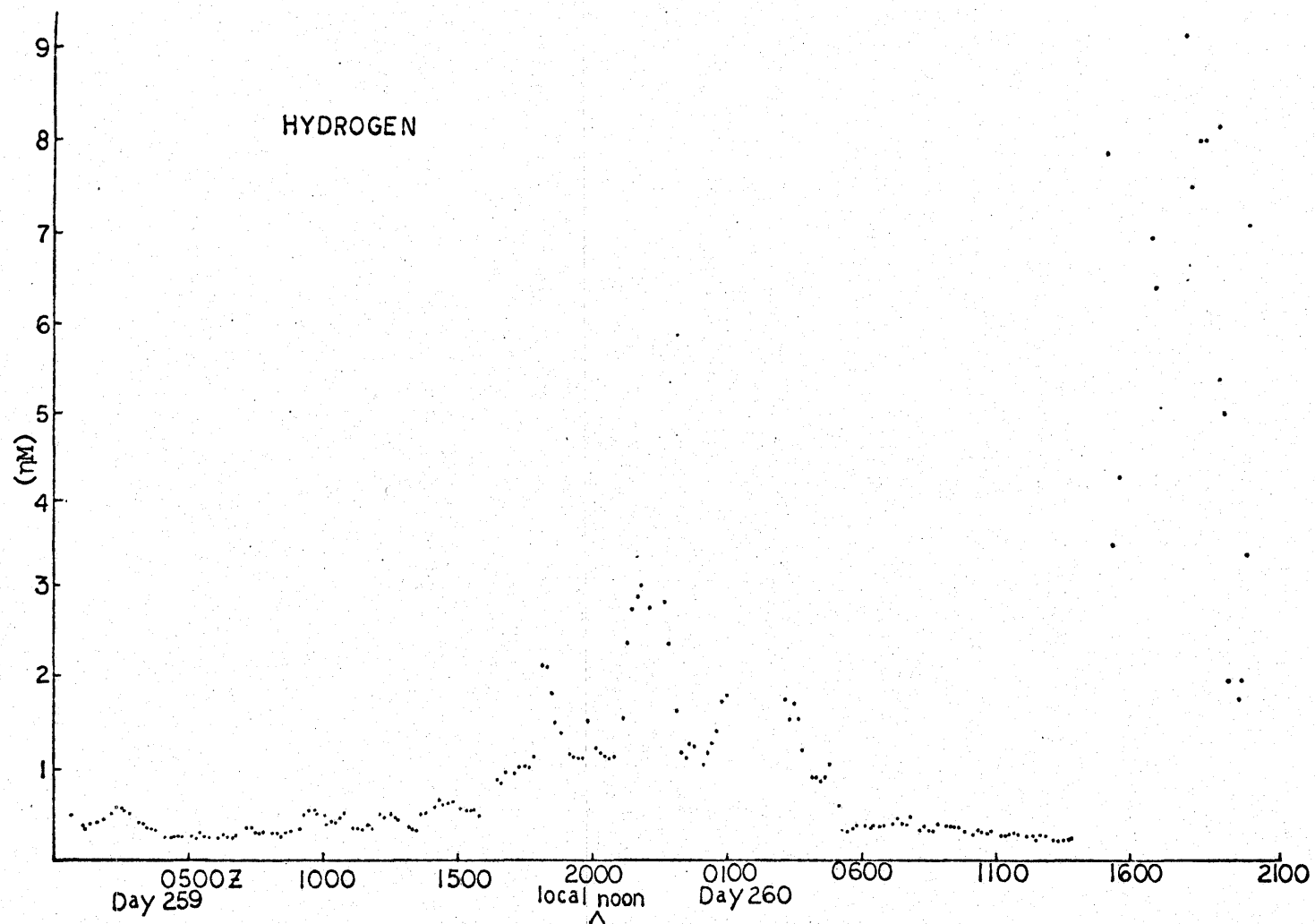


Fig. 25. H<sub>2</sub> concentrations approaching the coast of California. Fish retrieved at approximately 2200Z (before entering San Diego Bay).



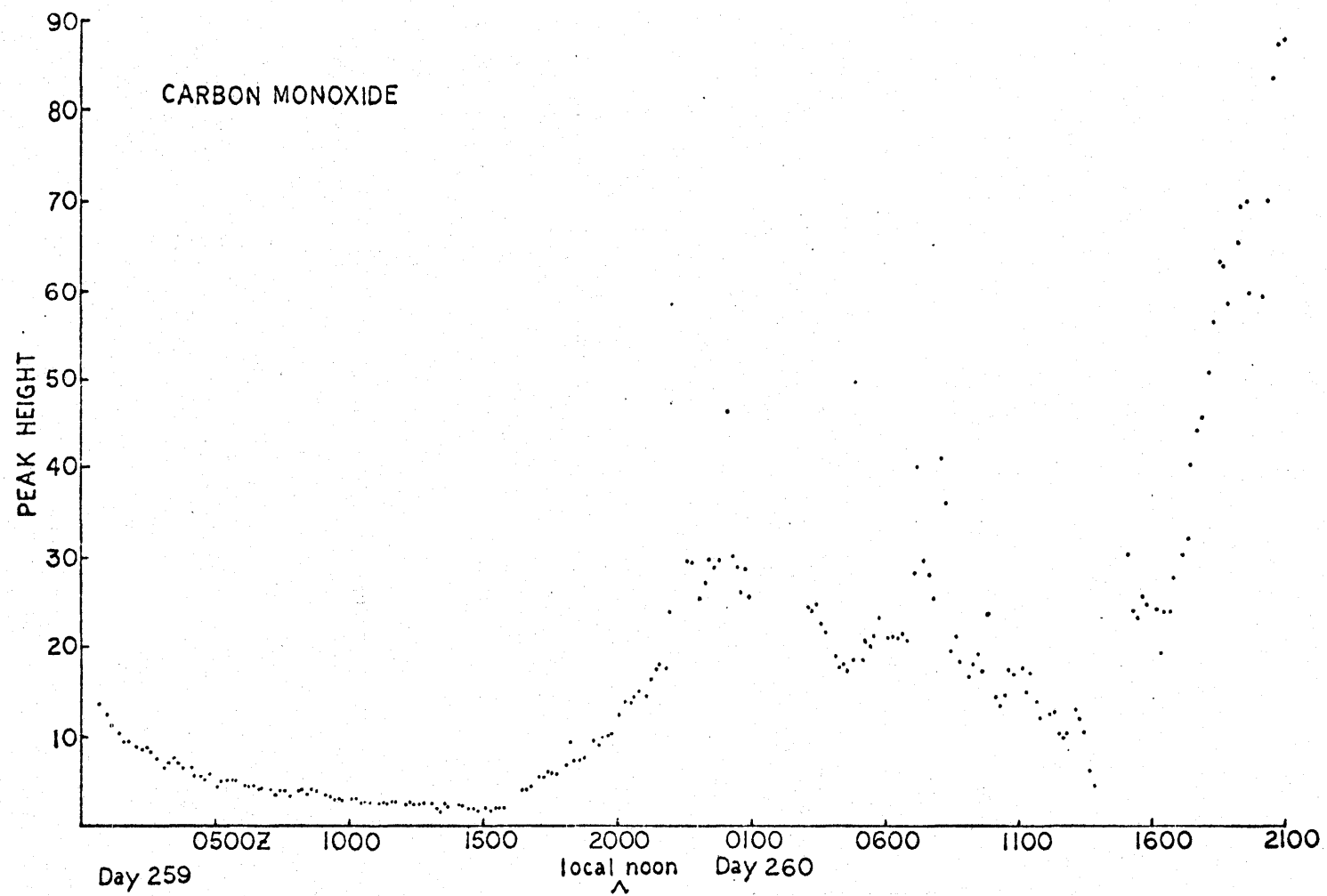


Fig. 26. Surface water CO concentrations approaching the coast of California.

probably due to anthropogenic inputs. A difference of about 5.8% was reported between the near-surface air of the Northern and Southern hemispheres (0.584 vs. 0.552 ppmv). In the upper troposphere Schmidt reported Northern Hemisphere air averaged 1.5% higher than Southern Hemisphere air. Measurements made during an extended aircraft flight showed slightly higher  $H_2$  concentrations over the east coast of North America as compared to the west coast. Concentrations as low as 0.51 ppmv were reported between  $5^\circ$  and  $10^\circ$  S latitude over the west coast of South America. Concentrations below 0.50 ppmv were observed over a rural region of Canada. These low values were hypothesized to be the result of strong biological sinks at the surface. *Ehhalt et al.* [1977] reported variations in the  $H_2$  content in the troposphere on the order of 10% in a period of one year. An average concentration in the troposphere of 0.50 ppmv was given. A systematic gradient of  $H_2$  in the lower troposphere was observed over the Pacific. This gradient, although present during all seasons, could not be attributed to known sources. Profiles taken over the Everglades in Florida, and Death Valley, California, revealed  $H_2$  concentrations of approximately 0.40 ppmv at ground level.

The differences in average  $H_2$  concentrations in the atmosphere reported by *Schmidt* [1978], *Ehhalt et. al.* [1977], and *Herr and Barger* [1978], as well as the observed spatial inhomogeneities, indicate a relatively short residence time for this gas in the atmosphere. Differences in average concentration between the hemispheres suggest higher input (perhaps from anthropogenic sources) into the northern hemisphere.

The strong north-south gradient in CO concentration observed during 79-G-6 indicates both a short residence time for this gas in the atmosphere, as well as a significant input of CO into the Northern Hemisphere. All CO concentrations measured between  $10^\circ$  and  $35^\circ$  N were greater than 0.040 ppmv. Concentrations south of the equator fell between 0.028 and 0.0195 ppmv. Increasing CO concentrations were observed from a distance of at least 1500 km offshore while approaching the coast of California. These higher concentrations may be a result of wind transport of CO from sources on the North American continent. The relatively

high CO levels south of Hawaii (between 10° and 15° N may also be the result of transport from a distant source.

#### Dissolved Gas Measurements

From the more limited set of water samples, no distinct latitudinal pattern of dissolved H<sub>2</sub> or CO distribution can be given for near-surface water. Diurnal variation in dissolved CO concentration, together with short-term variation due to changing cloud cover, etc., obscured any overall differences in CO concentrations at the stations sampled.

No diurnal cycle in atmospheric CO was observed paralleling the dissolved CO cycle. Increased CO flux to the atmosphere during the day-time could not be detected in near-surface air samples.

Net flux (F) of H<sub>2</sub> and CO from the water to atmosphere can be calculated using Equation 10 (p. 59)

$$F = D_i (C_s - \beta_i \rho_i) / z$$

*Broecker and Peng* [1974] give data for average stagnant film thickness (z), and for the diffusion coefficients of H<sub>2</sub> and CO. From their measurements of C<sup>14</sup> and Rn<sup>222</sup> a world average of  $z = 40 \pm 30$  microns was derived. At 28°C (the average water temperature along much of the cruise track),

$$D_H = 4.97 \times 10^{-5} \text{ cm}^2/\text{sec}$$

$$D_{CO} = 2.14 \times 10^{-5} \text{ cm}^2/\text{sec}$$

*Wiesenburg and Guinasso* [1979] give solubilities of H<sub>2</sub> and CO in seawater at 28°C and 35‰ of:

$$H_2 = 0.0148 \text{ mlH}_2/\text{ml-atm} = 0.0006607 \text{ moleH}_2/\text{l-atm}$$

$$CO = 0.0176 \text{ mlCO}/\text{ml-atm} = 0.0007857 \text{ moleCO}/\text{l-atm}$$

From average atmospheric concentrations of H<sub>2</sub> and CO measured along the cruise of

$$H_2 = 0.40 \times 10^{-6} \text{ atm}$$

$$CO = 0.034 \times 10^{-6} \text{ atm}$$

predicted dissolved concentrations of these gases at the interface are

$$\beta_{H_2} \rho_{H_2} = 5.92 \times 10^{-9} \text{ L/L} = 0.264 \text{ nM } H_2$$

$$\beta_{CO} \rho_{CO} = 5.98 \times 10^{-10} \text{ L/L} = 0.027 \text{ nM } CO$$

Average concentrations measured in the near-surface water using bucket samples are

$$C_{H_2} = 8.96 \times 10^{-9} \text{ L/L} = 0.40 \text{ nM } H_2$$

$$C_{CO} = 4.50 \times 10^{-8} \text{ L/L} = 2.00 \text{ nM } CO$$

(Average CO is obtained from equal numbers of day and night samples.) These numbers yield an average  $H_2$  supersaturation factor of 1.5x, and average CO supersaturation of 74x. Net flux to the atmosphere is calculated as:

$$F_{H_2} = 5.33 \times 10^{-4} \text{ mole/m}^2\text{-yr} = 1.07 \times 10^{-7} \text{ g/cm}^2\text{-yr}$$

$$F_{CO} = 3.33 \times 10^{-3} \text{ mole/m}^2\text{-yr} = 9.32 \times 10^{-6} \text{ g/cm}^2\text{-yr}$$

In their calculations, *Herr and Barger* [1978] used dissolved  $H_2$  concentrations averaged over the entire mixed layer to obtain an annual transfer rate of  $H_2$  to the atmosphere. They calculated a flux of  $0.33 \times 10^{12}$  g $H_2$ /yr from the northern hemisphere oceans (area =  $1.44 \times 10^{18}$  cm<sup>2</sup>). This yields an average flux of  $2.29 \times 10^{-7}$  g/cm<sup>2</sup>-yr, about twice that calculated from data taken in the Pacific during 79-G-6.

*Linnenbom et al.* [1973] calculated an upper limit of CO flux from ocean to atmosphere of  $6 \times 10^{-5}$  g/cm<sup>2</sup>-yr. This estimate was based on the assumption that the entire difference in concentration seen between day and night profiles was due to gas exchange with the atmosphere. This result gives an upper limit, since atmospheric exchange is not rapid enough over a time scale of one day to account for the depletion seen in the upper 50 to 100 m.

*Seiler* [1974] estimated net flux of  $1 \times 10^{14}$  gCO/yr for the world ocean. This yields a flux of about  $2.8 \times 10^{-5}$  gCO/cm<sup>2</sup>-yr, which is close to my estimate from 79-G-6 data.

### Water Profiles

In the upper 150 meters of the water column both  $H_2$  and CO were usually above atmospheric solubility levels. The variability in

profiles (Figure 22, p. 71) may reflect both geographical and temporal variation in production and consumption rates. Enhanced gas exchange at some stations due to local conditions may also have contributed to the net concentrations observed. Stations 7,9,15, and 16 show  $H_2$  maxima slightly below the surface, indicating that gas exchange may have reduced dissolved  $H_2$  concentration in the upper meters. During daylight hours the extremely rapid production of CO by the action of sunlight on surface water may overwhelm the loss of CO from the surface layer by atmospheric exchange. The slight minima in CO concentration at the surface during night-time sampling (Stations 2 and 9) may result from a combination of *in situ* consumption along with gas exchange with the atmosphere.

Below 1000 m, both dissolved  $H_2$  and CO were generally present in concentrations below present atmospheric saturation levels. Dissolved  $H_2$  concentration of 0.05  $\eta$ M (1  $\eta$ l/l) were measured in many deep water samples. These concentrations are significantly lower than those reported by Herr and Barger [1978]. These workers reported that most  $H_2$  concentrations in samples from the North Atlantic below 1500 m clustered around 8  $\eta$ l/l.

The low dissolved  $H_2$  concentration measured in the Pacific may be a result of the greater age of deep water found there. Deep Pacific water was formed and equilibrated with the atmosphere at an earlier time than deep Northern Atlantic water. Fluctuations in atmospheric  $H_2$  concentration during the period between the formation of the two water masses could contribute to the difference in reported dissolved concentrations. In light of the rapid production and consumption rates seen in surface water at CEPEX, however, it is likely that *in situ* processes are the dominant factor in controlling dissolved  $H_2$  concentration in deep water. The low concentration of  $H_2$  in Pacific Ocean samples below 1000 m may reflect slow *in situ* biological and chemical processes occurring in the water column. Net concentrations observed at depth may be relatively independent of atmospheric saturation levels at the time of water mass formation.

At Stations 26 and 28, along the eastern end of the cruise track, the water samples taken below 3000 m had anomalously high dissolved  $H_2$  concentrations. Too few data points are available to characterize this region as being enriched in dissolved  $H_2$ . Further intensive sampling is necessary to confirm these measurements, and to locate a possible deep water source for excess dissolved  $H_2$ . Potential sources include transport from areas of intense biological activity, and input of  $H_2$  from geologically active regions on the deep-sea floor.

More complete understanding of the rates of  $H_2$  (as well as  $CH_4$ ,  $CO$ ,  $N_2O$ , etc.) production and consumption processes in deep water is important in determining the usefulness of these gases as tracers of water mass movement.

## CHAPTER V

## SUMMARY AND CONCLUSIONS

$H_2$  and CO concentrations measured in the atmosphere over the Central Pacific differed from measurements made near populated areas. When monitoring ambient air over land areas, the  $H_2$  and CO concentrations often were observed to change rapidly. The variations suggest that human activities can cause rapid local fluctuations in the trace gas composition of the atmosphere. During 79-G-6, in areas far removed from major population centers, short-term fluctuations in air composition were not observed.

The concentration of  $H_2$  measured in the atmosphere normally exceeded that of CO. In the Central Pacific the ratio of  $H_2$ /CO in air was greater than 10:1 (0.40 ppm/.03 ppm). This ratio decreased in the air samples taken on the near-land areas. Average CO concentrations measured during July-August, 1978, on Vancouver Island, B. C., were about 5x higher than the average concentration of CO measured in the Central Pacific one year later.

A gradient in atmospheric CO concentration was observed between the Northern and Southern Hemispheres in the Central Pacific region. The presence of such a gradient indicates a short residence time for CO in the atmosphere, and may reflect the higher level of industrial activity in the Northern Hemisphere.

In spite of the large amount of CO that has been released by man during the last 100 years, average concentrations measured in the Central Pacific (an area comprising a sizable fraction of the earth's surface) was less than 0.05 ppmv. Apparently, the CO released into the troposphere has not accumulated there. Any direct threat to health that CO poses may be significant only in localized urban areas where dispersal and removal processes in the atmosphere cannot keep up with input from manufacturing, automobiles, etc. Outside these areas, natural processes seem able to reduce CO concentration to much lower levels.

Latitudinal gradients in atmospheric  $H_2$  concentration over the Pacific were smaller than those observed for  $CO$ . Overall,  $H_2$  levels in air changed by less than 5% between  $25^\circ N$  and  $20^\circ S$ . In the open ocean over 24-hour (or longer) periods, little variability in either  $H_2$  or  $CO$  concentrations was detected.

As with  $CO$ , distinct increases in atmospheric  $H_2$  were observed near land areas.  $H_2$  concentration in air increased by 25% off the coast of California, and by a factor of 2 or more in Papeete Harbor and San Diego Bay.

$H_2$  has been measured in the near-surface atmosphere by other workers. Some results have indicated that  $H_2$  concentration can be quite variable, even in areas such as the mid-Atlantic. Further studies are needed to clarify the distribution pattern of  $H_2$  in the atmosphere.

In near-shore and open ocean surface waters, dissolved  $CO$ ,  $H_2$ , and  $CH_4$  normally exceeded atmospheric solubility levels. This implies that the oceans act as a source of these gases to the atmosphere. The total flux of oceanic  $CO$  ( $1.2 \times 10^{11}$  mol/yr, calculated from Pacific cruise data), is small relative to the total amount of  $CO$  present in the atmosphere. In light of the short residence time of  $CO$  in the atmosphere, the contribution made by oceanically derived  $CO$  is probably less than 10% of the total atmospheric flux.  $H_2$  is only slightly supersaturated in Central Pacific surface water. The calculated flux of  $H_2$  ( $1.9 \times 10^{11}$  mol/yr) from the oceans probably represents a very small fraction of the total  $H_2$  budget of the atmosphere.

Concentrations of dissolved  $H_2$ ,  $CO$ , and  $CH_4$  were higher and more variable in biologically productive coastal areas than in the open ocean environment. The experiments performed at CEPEX were designed to study the inter-relationships of trace gases with a variety of chemical and biological parameters. Average concentrations of dissolved  $H_2$ ,  $CO$ , and  $CH_4$  in the surface water of Saanich Inlet and in the CEPEX bags were higher than levels measured in the Pacific. The ratio of hydrogen was about 5:1, methane 10:1, and  $CO$  (maximum day-time values) 3:1. The concentrations observed in coastal waters may



be related to higher overall rates of biological activity there (both production and decomposition).

In Saanich Inlet, higher concentrations of methane were found in the deeper water. Dissolved  $H_2$  concentrations in deep water samples there were quite low, however. If  $H_2$  production rates are high in such an anoxic area, consumption of  $H_2$  must also be rapid.

Water in the CEPEX enclosures was prevented from mixing with the water of the inlet. Measurements in the bag over the course of the experiment indicated that production of these 3 reduced gases can occur in water containing significant amounts of dissolved  $O_2$ .

In both Saanich Inlet and the Central Pacific, dissolved  $H_2$  and CO concentrations decreased rapidly with depth. In Saanich Inlet, sub-equilibrium concentrations were observed at depths below about 25 m; in the Pacific, sub-equilibrium concentrations of  $H_2$  and CO were found below about 200 m. The  $H_2$ , CO, and  $CH_4$  concentrations measured in most deep Pacific water samples were significantly below present atmospheric saturation levels. It is possible that the partial pressure of these gases in the atmosphere has varied through time. The deep water in the Pacific may have been formed at the sea surface during a period when the atmospheric concentrations were lower than present. It is more likely, however, that the original dissolved concentrations have been altered by *in situ* processes. The concentration observed in deep Pacific water may not simply reflect past atmospheric concentrations, but instead may be the net result of production and consumption processes occurring in the deep water column. The rate at which these processes can occur in deep water is unknown at present. In the shallow water at CEPEX, the trace gas distribution observed clearly demonstrates that rapid *in situ* processes are possible.

Diurnal cycles of dissolved CO were observed in the CEPEX containers at Saanich Inlet, and in the Central Pacific. A similar diurnal cycle of dissolved  $H_2$  was seen in a CEPEX enclosure. Continuous surface sampling data indicate that a  $H_2$  diurnal cycle may occur in the surface waters off the coast of California. These cycles seem to follow light intensity.

*In vitro* experiments were performed at the CEPEX site. Production and consumption of dissolved  $H_2$  and CO were observed in seawater samples stored in gas-tight containers. CO production occurred in the presence of light, even in samples poisoned with sodium azide.

The production and consumption rates obtained from incubation experiments are rapid enough to explain the gains and losses observed in surface seawater.

*In situ* sources and sinks of  $H_2$ , CO, and  $CH_4$  are present in the water column. The distribution of these trace gases in seawater result from a combination of biological, chemical, and physical processes.

## REFERENCES

- Atkinson, L. P., and F. A. Richards, The occurrence and distribution of methane in the marine environment, *Deep Sea Res.*, 14, 673-684, 1967.
- Barnes, R. O., and E. D. Goldberg, Methane production and consumption in anoxic marine sediments, *Geology*, 4, 297-300, 1976.
- Bernard, B. B., Light hydrocarbons in marine sediments, Ph.D. dissertation, Texas A & M University, College Station, Tx, 1978.
- Borgerson, M. J., An analytical method for the determination of molecular hydrogen in seawater, Master's thesis, Oregon State University, Corvallis, Ore., 1978.
- Broecker, W. S., and T. H. Peng, Gas exchange rates between air and sea, *Tellus*, 26, 21-35, 1974.
- Brooks, J. M., Deep methane maxima in the Northwest Caribbean Sea: Possible seepage along the Jamaica Ridge, *Science*, 206, 1069-1071, 1979.
- Brooks, J. M., and W. M. Sackett, Sources, sinks, and concentrations of light hydrocarbons in the Gulf of Mexico, *J. Geophys. Res.*, 78, 5248-5258, 1973.
- Cappenberg, T. E., Interrelations between sulfate-reducing and methane-producing bacteria in bottom deposits of a freshwater lake. 1) Field observations, *Antonie van Leeuwenhoek*, 40, 285-295, 1974.
- Chapman, D. J., and R. D. Tocher, Occurrence and production of carbon monoxide in some brown algae, *Canadian J. of Botany*, 44, 1428-1442, 1966.
- Crozier, T. E., and S. Yamamoto, Solubility of hydrogen in water, seawater, and NaCl solutions, *J. Chem. Eng. Data*, 19, 242-244, 1974.
- Deuser, W. G., E. T. Degens, G. R. Harvey, and M. Rubins, Methane in Lake Kivu: New data bearing on its origin, *Science*, 181, 51-54, 1973.
- Douglas, E., Carbon monoxide solubilities in sea water, *J. Phys. Chem.*, 71, 1931-1933, 1967.
- Ehhalt, D. H., U. Schmidt, and L. E. Heidt, Vertical profile of molecular hydrogen in the troposphere and stratosphere, *J. Geophys. Res.*, 82, 5907-5911, 1977.
- Fink, U., D. H. Rank, and T. Q. Wiggins, Abundance of methane in the earth's atmosphere, *ONR Tech. Rep. NONR-656 (12) NRO14-401*, 1965.

- Glueckauf, E., and G. P. Kitt, The hydrogen content of atmospheric air at ground level, *Quart. J. Roy. Meteorol. Soc.*, **83**, 522-528, 1957.
- Gordon, L. I., Y. Cohen, and D. R. Standley, The solubility of molecular hydrogen in seawater, *Deep Sea Res.*, **24**, 937-941, 1977.
- Gray, C. T., and H. Gest, Biological formation of molecular hydrogen, *Science*, **148**, 186-192, 1965.
- Gucluer, S. M., and M. G. Gross, Recent marine sediments in Saanich Inlet, a stagnant marine basin, *Limnol. Oceanogr.*, **9**, 359-376, 1964.
- Guinasso, N. L., Jr. and D. R. Schink, A simple physicochemical acoustic model of methane bubbles rising in the sea, *Tech. Rep 73-15-T*, Texas A&M University, 1973.
- Herlinveaux, R. H., Oceanography of Saanich Inlet in Vancouver Island, British Columbia, *J. Fish. Res. Bull. Canada*, **19**, 1-37, 1962.
- Herr, F. L., and W. R. Barger, Molecular hydrogen in the near-surface atmosphere and dissolved in waters of the Tropical North Atlantic, *J. Geophys. Res.*, **83**, 6199-6205, 1978.
- Ingersoll, R. B., R. E. Inman, and W. R. Fisher, Soil's potential as a sink for atmospheric carbon monoxide, *Tellus*, **26**, 151-158, 1974.
- Jaffe, L. S., Carbon monoxide in the biosphere: Sources, distribution and concentrations, *J. Geophys. Res.*, **78**, 5293-5305, 1973.
- Jones, J. H., J. T. Kummer, K. Otto, M. Shelef, and E. E. Weaver, Selective catalytic reaction of hydrogen with nitric oxide in the presence of oxygen, *Environ. Sci. Technol.*, **5**, 790, 1971.
- Junge, C., W. Seiler, U. Schmidt, R. Boch, K. D. Greese, F. Radler, and H. J. Ruger, Kohlenmonoxid- und Wasserstoff produktion mariner Mikroorganismen Nahrmedium mit synthetischem Seewasser, *Die. Naturwiss*, **59**, 514-515, 1972.
- Kluyver, A. J., and G. T. P. Schnellen, On the fermentation of CO by pure cultures of methane bacteria, *Arch. Biochem.*, **14**, 57-70, 1947.
- Knudsen, M. V., Die molekulare Wärmeleitung der Gase und der Akkommodation skoeffizient, *Annalen der Physik*, **34**(4), 593-656, 1911.
- Lamontagne, R. A., J. W. Swinnerton, V. J. Linnenbom, and W. D. Smith, Methane concentrations in various marine environments, *J. Geophys. Res.*, **78**, 5317-5324, 1973.
- Levy, H., Photochemistry of the lower troposphere, *Planet. Space Sci.*, **20**, 919-935, 1972.
- Lilley, M. D., J. A. Baross, and L. I. Gordon, Dissolved hydrogen and methane in Saanich Inlet, British Columbia, unpublished manuscript, Oregon State University, Corvallis, Ore., 1979.

- Linnenbom, V. J., J. W. Swinnerton, and R. A. Lamontagne, The ocean as a source for atmospheric carbon monoxide, *J. Geophys. Res.*, **78**, 5333-5340, 1973.
- Loewus, M. W., and C. C. Delwiche, Carbon monoxide production by algae, *Plant Physiol.*, **38**, 371-374, 1963.
- Martens, C. S., and R. A. Berner, Methane production in the interstitial waters of sulfate-depleted marine sediments, *Science*, **185**, 1167-1169, 1974.
- Martens, C. S., and R. A. Berner, Interstitial water chemistry of anoxic Long Island Sound sediments. 1) Dissolved gases, *Limnol. Oceanogr.*, **22**(1), 10-25, 1977.
- McAullife, C., Gas chromatographic determination of solutes by multiple phase equilibration, *Chem. Technol.*, **1**, 46-51, 1971.
- McConnell, J. C., M. B. McElroy, and S. C. Wofsy, Natural sources of atmospheric carbon monoxide, *Nature*, **233**, 187-188, 1971.
- McCullough, J. D., R. A. Crane, and A. O. Beckman, Determination of carbon monoxide in air by use of red mercuric oxide, *Indust. Engin. Chem. Analy. Ed.*, **19**, 999-1002, 1947.
- Mechalas, B. J., Pathways and environmental requirements for biogenic gas production in the ocean, in *Natural Gases in Marine Sediments*, edited by I. R. Kaplan, pp. 11-25, Plenum Press, New York, 1974.
- Menzel, D. W., and J. Case, Concept and design: Controlled ecosystem pollution experiment, *Bull. Mar. Sci.*, **27**(1), 1-7, 1977.
- Migeotte, M. V., Spectroscopic evidence of methane in the earth's atmosphere, *Phys. Rev.*, **73**(5), 519-520, 1948.
- Migeotte, M. V., The fundamental band of carbon monoxide at  $4.7\mu$  in the solar spectrum, *Phys. Rev.*, **75**, 1108-1109, 1949.
- Mitsui, A., and S. Kumazawa, Hydrogen production by marine photosynthetic organisms as a potential energy resource, in *Biological Solar Energy Conversion*, edited by A. Mitsui, S. Miyachi, A. San Pietro, and S. Tamura, pp. 23-51, Academic Press, New York, 1977.
- Nissenbaum, A., B. J. Presley, and I. R. Kaplan, Early diagenesis in a reducing fjord, Saanich Inlet, British Columbia - I. Chemical and isotopic changes in major components of interstitial water, *Geochim. Cosmochim. Acta*, **36**, 1007-1027, 1972.
- Pickwell, G. V., E. G. Barham, and J. W. Wilton, Carbon monoxide production by a bathypelagic siphonophore, *Science*, **144**, 860-862, 1964.
- Reeburgh, W. S., Methane consumption in Cariaco Trench waters and sediments, *Earth Plant. Sci. Lett.*, **28**, 337-344, 1976.
- Robbins, R. C., K. M. Borg, and E. Robinson, Carbon monoxide in the atmosphere, *J. Air Pollut. Contr. Assoc.*, **18**, 106-110, 1968.

- Schlegel, H. G., Production, modification, and consumption of atmospheric trace gases by microorganisms, *Tellus*, 26, 11-20, 1974.
- Schmidt, U., The latitudinal and vertical distribution of molecular hydrogen in the troposphere, *J. Geophys. Res.*, 83, 941-946, 1978.
- Schmidt, U., and W. Seiler, A new method for recording molecular hydrogen in atmospheric air, *J. Geophys. Res.*, 75, 1713-1716, 1970.
- Scranton, M. I., and P. G. Brewer, Occurrence of methane in the near-surface waters of the western subtropical North-Atlantic, *Deep Sea Res.*, 24, 127-138, 1977.
- Seiler, W., The cycle of atmospheric carbon monoxide, *Tellus*, 26, 116-135, 1974.
- Seiler, W., and C. Junge, Carbon monoxide in the atmosphere, *J. Geophys. Res.*, 75, 2217-2226, 1970.
- Seiler, W., and U. Schmidt, Dissolved nonconservative gases in seawater, in *The Sea*, vol. 5, edited by E. D. Goldberg, pp.219-243, Wiley-Interscience, New York, 1974.
- Swinerton, J. W., R. A. Lamontagne, and V. J. Linnenbom, Carbon monoxide in rainwater, *Science*, 172, 943-945, 1971.
- Swinerton, J. W., and V. J. Linnenbom, Determination of the C<sub>1</sub> to C<sub>4</sub> hydrocarbons in sea water by gas chromatography, *J. of Gas Chromatography*, 5, 570-573, 1967.
- Swinerton, J. W., V. J. Linnenbom, and C. H. Cheek, A sensitive gas chromatographic method for determining carbon monoxide in seawater, *Limnol. Oceanogr.*, 13, 193-195, 1968.
- Swinerton, J. W., V. J. Linnenbom, and C. H. Cheek, Distribution of methane and carbon monoxide between the atmosphere and natural waters, *Environ. Sci. Technol.*, 3, 836-838, 1969.
- Weast, R. C., editor, Thermal conductivity of gases, in *Handbook of Chemistry and Physics*, p. E-2, CRC Press, Cleveland, 1976.
- Weiss, R. F., The solubility of nitrogen, oxygen, and argon in water and seawater, *Deep Sea Res.*, 17, 721-735, 1970.
- Wiesenburg, D. A., and N. L. Guinasso, Jr., Equilibrium solubilities of methane, carbon monoxide, and hydrogen in water and sea water, *J. Chem. Engin. Data*, 24, 356-360, 1979.
- Williams, R. T., and A. E. Bainbridge, Dissolved carbon monoxide, methane, and hydrogen in the Southern Ocean, *J. Geophys. Res.*, 78, 2691-2694, 1973.
- Wilson, D. F., J. W. Swinerton, and R. A. Lamontagne, Production of carbon monoxide and gaseous hydrocarbons in seawater: Relation to dissolved organic carbon, *Science*, 168, 1577-1579, 1970.
- Wittenburg, J. B., The source of carbon monoxide in the floats of the Portuguese man-of-war, *Physalia physalis* L., *J. Exper. Bio.*, 37, 698-705, 1960.

Wolfe, R. S., Microbial formation of methane, *Adv. Microb. Physiol.*,  
6, 107-146, 1971.

## APPENDIX

Dissolved Gases in Vertical Profiles from  
Cruise #1207-79 of the *USNS Desteiguer*

Depth (m)	CH <sub>4</sub> (nM)	H <sub>2</sub> (nM)	CO (nM)	Depth (m)	CH <sub>4</sub> (nM)	H <sub>2</sub> (nM)	CO (nM)
Station 1 - 17 April 1979 24° 59.5' N 117° 59.1' W				Station 3 - 20 April 1979 17° 44.1' N 118° 18.8' W			
100	1.96	0.60	0.36	1	1.83	1.79	2.95
109	3.04	0.45	0.22		1.61	1.52	2.72
110	2.32	1.65		139	4.20	0.27	0.09
119	1.88	0.45	0.18		4.69	0.45	0.09
160	2.14	0.42	0.13	302	3.62	0.36	0.04
	3.35	0.27	0.13	502	0.94	0.54	0.09
250	2.81	0.63	0.04	Station 4 - 21 April 1979 14° 43.9' N 115° 02.7' W			
	2.63	0.80	0.09	1	1.83	3.13	5.00
	1.92	0.71	0.04	31	2.01	1.25	2.90
400	2.05	0.63	0.04	55	1.83	1.52	3.66
600	0.67	0.03	0.04	78	3.35	0.80	2.19
800	0.89	0.54	0.04		3.30	0.71	1.16
1000	1.07	0.45	0.04	130	3.79	0.45	2.10
1300	1.74	0.36	0.09	137	2.99	0.45	1.70
Station 2 - 18 April 1979 21° 23.2' N 118° 19.0' W				161	2.28	0.63	0.31
0	1.96	0.71	2.68	186	2.23	0.80	1.79
40	1.96	0.63	2.68	222	2.14	0.63	1.56
	1.88	0.71	2.10	273	1.96	0.54	2.01
110	2.19	0.45	1.03	326	2.37	0.63	0.98
	2.37	0.54	2.10	Station 5 - 23 April 1979 12° 30.6' N 111° 15.1' W			
140	3.04	0.45	0.89	1	1.70	5.45	1.12
180	2.95	0.80	0.54	15	1.74	3.84	1.21
200	2.63	0.36	1.16	47	1.56	3.75	0.36
250	1.43	0.45	0.67	64	2.63	4.29	1.12
	1.61	0.45	1.16		2.68	2.59	0.76
	1.03	0.27	0.09	94	3.97	0.89	0.58
	1.07	0.36	0.09	103	3.48	0.71	0.09
400	0.40	1.25	0.27	119	3.17	0.54	0.13
	0.36	0.63	0.09	140	2.41	0.71	0.13
500	0.40	0.36	0.31	174	1.74	0.80	0.09
600	0.22	0.36	0.09	250	1.83	0.36	0.09
	0.40	0.45	0.31	325	1.74	0.80	0.09
	0.31	0.18	0.04	401	2.01	0.54	0.27
		0.27	0.13		1.88	0.54	0.13
800	0.27	0.27	0.09		1.92	0.45	0.31
	0.31	0.36	0.09	600	0.67	0.71	0.36
	0.45	0.54	0.27		0.67	0.71	0.36
					0.67	0.71	0.31



## APPENDIX (continued)

Depth (m)	CH <sub>4</sub> (nM)	H <sub>2</sub> (nM)	CO (nM)	Depth (m)	CH <sub>4</sub> (nM)	H <sub>2</sub> (nM)	CO (nM)
Station 5 - continued				Station 7 - continued			
800	0.36	0.63	0.27	800	0.27	0.71	0.09
1249	0.18	0.71	0.13		0.31	0.81	0.09
	0.18	0.71	0.13	1000	0.13	0.36	0.09
1750	0.13	0.18	0.09		1.16	0.36	0.09
Station 6 - 23 April 1979				1200	0.18	0.27	0.09
9° 40.2' N 106° 54.9' W					0.18	0.36	0.18
1	1.88	8.75	1.47	Station 8 - 27 April 1979			
10	2.05	11.07	1.61	7° 00.0' N 97° 12.1' W			
	2.14	10.71	1.43	1.5	1.65	3.04	0.85
	1.61	11.25	1.21	15	1.70	4.82	0.89
19	1.92	10.89	0.98	50	1.88	1.52	0.31
29	2.05	10.89	0.94	75	3.44	1.96	0.18
54	2.90	2.14	0.67	125	2.72	0.89	0.13
99	2.90	0.89	0.13	150	1.83	0.89	0.13
125	2.10	2.50	0.22	250	1.61	2.23	0.13
201	1.52	3.30	0.13	386	1.38	2.23	0.04
299	1.25	3.75	0.22	400	1.38	1.61	0.13
400	1.07	1.43	0.13	450	3.93	1.96	0.31
	1.07	1.34	0.31	574	0.40	1.16	0.45
800	0.18	1.25	0.31	1000	0.13	1.61	0.36
	0.40	1.25	0.13	1300	0.18	1.52	0.18
1600	0.22	1.96	0.22	1400		1.25	0.40
	0.18	1.88	0.18	2000	0.18	0.71	0.31
2500	0.27	1.61	0.63	Station 9 - 29 April 1979			
	0.22	1.52	0.63	7° 07.7' N 91° 31.5' W			
Station 7 - 25 April 1979				15	2.32	4.11	0.80
7° 00.0' N 102° 23.3' W				50	2.41	3.39	0.54
0	2.77	2.23	0.22	75	1.65	2.14	0.22
1	1.96	0.98	4.60	125	1.88	0.63	0.18
	1.88	0.98	4.55		1.70	0.98	0.18
15	1.38	1.25	0.09		1.38	0.63	0.13
30	2.14	1.07	0.13	150	1.65	1.70	0.13
42	2.23	1.07	0.09	200	1.34	0.45	0.18
60	1.56	1.25	0.09	400	1.21	1.07	0.13
80	2.68	0.89	0.09		0.98	4.38	0.22
100	2.63	1.07	0.09	500	0.80	1.25	0.31
125	1.21	1.25	0.04		0.89	1.43	0.40
150	0.89	1.79	0.09	600	0.67	1.16	0.13
300	1.47	2.95	0.09	1000	0.18	0.89	0.31
500	0.89	0.45	0.18	1500	0.09	0.80	0.31
	0.98	0.54	0.18	2000	0.13		
600	0.40	1.07	0.13	2500	0.18	1.43	0.18

## VITA

John Logan Bullister was born to John Logan and Thelma Ruth Bullister on January 3, 1952 in Pittsburgh, Pennsylvania. He graduated from Central Catholic High School in June, 1969. He graduated from the University of Pittsburgh with a Bachelor of Science Degree in Biology and Mathematics in June, 1973.

From 1973 to 1975 he taught secondary school and adult education on the West Indian island of Antigua. He enrolled as a graduate student at Texas A&M University in September, 1976.

He currently resides at 4880 Cole Street, San Diego, California.

The typist for this thesis was Chunok K. Lee.